TRPV4-TRPC1 Heteromeric Channel: its Property and Function

MA, Xin

A Thesis Submitted in Partial Fulfilment

of the Requirements for the Degree of

Doctor of Philosophy

in

Physiology

The Chinese University of Hong Kong

May 2010

Thesis/Assessment Committee

Professor Yung Wing Ho (Chair)

Professor Yao Xiaoqiang (Thesis Supervisor)

Professor Tsang Suk Ying Faye (Committee Member)

Professor Yang Jian (External Examiner)

Declaration of Originality

The work contained in this thesis is original research carried out by the author in the Department of Physiology, Faculty of Medicine, the Chinese University of Hong Kong, starting from August 2007 to March 2010. No part of the work described in this thesis has already been or is being submitted to any other degree, diploma or other qualification at this or any other institutions.

Abstract of the thesis entitled:

TRPV4-TRPC1 heteromeric channel: its property and function

Submitted by MA Xin

For the degree of Doctor of Philosophy

at The Chinese University of Hong Kong in March 2010

Hemodynamic blood flow is one of most important physiological factors that control vascular tone. Flow shear stress acts on the endothelium to stimulate the release of vasodilators such as nitric oxide (NO), prostacyclin and endothelium-derived hyperpolarizing factors, causing endothelium-dependent vascular relaxation. In many cases, a key early signal in this flow-induced vascular dilation is Ca^{2+} influx in endothelial cells in response to flow. There is intense interest in searching for the molecular identity of the channels that mediate flow-induced Ca^{2+} influx. The present study aimed at identifying an interaction of TRPV4 with TRPC1, and investigating functional role of such a complex in flow-induced Ca^{2+} influx.

With the use of fluorescence resonance energy transfer (FRET), co-immunoprecipitation and subcellular colocalization methods, it was found that TRPC1 interacts physically with TRPV4 to form a heteromeric channel complex. In addition, our experimental results indicate that C-terminal and N-terminal domains of both channels are required for their interaction.

Attempts were made to determine the pore properties, such as permeability, rectification and voltage-dependent block, of the putative TRPV4-TRPC1 channel.

We demonstrated that this putative TRPV4-TRPC1 heterotetrameric channels displays distinct property different (although not drastically different) from TRPV4 homotetrameric channel with regard to I-V relation, kinetics of cation current, cations permeability and rectification properties. Together, the data from FRET and functional studies both suggest that heterologous expression of TRPV4 and TRPC1 can produce functional TRPV4-TRPC1 heterotetrameric channel.

Ion channels are delivered to the plasma membrane via vesicle trafficking. Thus the vesicle trafficking is a key mechanism to control the amount of TRP channel proteins in the plasma membrane, where they perform their function. TRP channels *in vivo* are often composed of heteromeric subunits. However, up to the present, there is lack of knowledge on trafficking of heteromeric TRP channels via vesicular translocation. In the present study, we examined the effect of Ca^{2+} store depletion on the translocation of TRPV4-TRPC1 heteromeric channels to the plasma membrane. Experiments using total internal fluorescence reflection microscopy (TIRFM) and biotin surface labeling showed that depletion of intracellular Ca^{2+} stores triggered a rapid translocation of TRPV4-TRPC1 channel proteins into the plasma membrane. Fluorescent Ca^{2+} measurement and patch clamp studies demonstrated that store Ca^{2+} depletion augmented several TRPV4-TRPC1 complex-related functions, which include store-operated Ca^{2+} influx and cation current as well as 4α-PDD-stimulated Ca^{2+} influx and cation current. The translocation required stromal interacting molecule 1 (STIM1). Furthermore, TRPV4-TRPC1 complex is more favorably translocated to the plasma membrane than TRPC1 or TRPV4 homomers. Similar mechanisms were identified in native endothelial cells, where the TRPV4-TRPC1 complex is a key component mediating flow-induced Ca^{2+} influx and subsequent vascular relaxation.

In functional study, flow elicited a $[Ca^{2+}]_i$ rise in TRPV4-expressing HEK cells. Co-expression of TRPC1 with TRPV4 markedly prolonged this $[Ca^{2+}]_i$ transient, and it also enabled this $[Ca^{2+}]_i$ transient to be negatively modulated by protein kinase G (PKG). Furthermore, this $[Ca^{2+}]_i$ rise was inhibited by an anti-TRPC1 blocking antibody T1E3 and a dominant negative construct TRPC1Δ567-793. Physical

interaction of TRPV4 with TRPC1 and functional role of such a complex were also found in the primary cultured rat mesenteric artery endothelial cells (MAECs) and human umbilical vein endothelial cells (HUVECs). A TRPC1-specific siRNA was used to knock-down TRPC1 protein levels in HUVECs. Interestingly, this siRNA not only reduced the magnitude of flow-induced $[Ca^{2+}]_i$ rise, but also accelerated the decay of flow-induced $[Ca^{2+}]_i$ transient. Pressure myograph was used to investigate the functional role of such a complex in flow-induced vascular dilation. T1E3 also decreased flow-induced vascular dilation. Thogether, the data from endothelial cells are consistent with those in overexpressed HEK cells, supporting the notion that TRPC1 interacts with TRPV4 to prolong the flow-induced $[Ca^{2+}]_i$ transient, and that TRPV4-TRPC1 complex plays an important role in flow-induced vascular dilation.

In summary, my study demonstrated that TRPV4 is capable of assembling with TRPC1 to form a functional TRPV4-TRPC1 heteromeric channel. TRPV4-TRPC1 heteromeric channel can rapidly translocate to the plasma membrane after Ca^{2+} depletion in intracellular stores. This TRPV4-TRPC1 heteromeric channel plays an important role in flow-induced endothelial Ca^{2+} influx and its associated vascular relaxation.

論文摘要

血流是重要的血管張力調節因數之一，血流剪切力作用于血管內皮細胞引起多種血管擴張素的生成，包括一氧化氮（NO）、前列腺素（PGI_2）、和內皮依賴性超級化因數（EDHF）。一般而言，在血流剪切力引起的血管擴張的過程中，內皮細胞鈣內流是關鍵的早期信號之一。在血流引起的鈣內流的研究中，研究者努力探討參與這個過程的分子受體或通道。本研究旨在探究瞬时感受器电位通道 V 型成员 4 (TRPV4)和瞬时感受器电位通道 C 型成员 1(TRPC1)之間的異聚體通道組裝、異聚體通道離子通透孔的電生理特性、異聚體上膜以及該異聚體通道在血流剪切力引起的細胞鈣內流、血管擴張中的重要作用。

本研究以鐳射共振能量轉移、免疫共沉澱和亞細胞共定位爲手段探究 TRPV4 和 TRPC1 異聚體通道的組裝情況。研究結果發現 TRPV4 和 TRPC1 存在物理上的連接，這預示著 TRPV4 和 TRPC1 通過物理上的連接形成 TRPV4-TRPC1 異聚體通道複合體。此外，研究結果也證明 TRPV4 和 TRPC1 通道 C-末端和 N-末端是形成 TRPV4-TRPC1 通道複合體所必需的分子結構域。

在生物化學和分子螢光的研究結果基礎上，在本研究中，我們進一步研究了 TRPV4-TRPC1 異聚體通道離子通透孔特性的三個方面：離子通透性、整流和電壓依賴性抑制。研究結果表明 TRPV4-TRPC1 通道複合體的電流-電壓關係、電流的特點、離子通透性以及整流特性和 TRPV4 同聚體通道均有所不同，儘管這個區別不是十分巨大；同時在本研究中，我們利用鐳射共振能量轉移研究了 TRPV4-TRPC1 通道複合體的亞基組合情況；總之，本研究結果表明 TRPV4 和 TRPC1 共表達可以形成新的 TRPV4-TRPC1 異聚體離子通道。

離子通道通過囊泡運輸到達細胞膜表面。因此囊泡運輸是控制暫態感受器電位通道(TRP)家族在細胞膜數量的關鍵因素。TRP 通道家族在體內常以異聚體形式存在。但是，到目前爲止，尚未有關於異聚體 TRP 通道囊泡轉運上膜的報導。本研究旨在用全內反射螢光顯微鏡、細胞膜蛋白提取、細胞內鈣濃度測量以及膜片鉗的方法探究細胞內鈣庫操縱的鈣內流誘導 TRPV4-TRPC1 通道複合體的快速上膜情況。研究結果表明細胞內鈣庫操縱的鈣內流誘導 TRPV4-TRPC1 通道複合體的快速上膜，並且該過程是 STIM1 參與介導的。此外，TRPV4-TRPC1 通道複合體較 TRPV4 或者 TRPC1 同聚體而言，更加易於上膜。同樣本研究的結果也在原代內皮細胞上得到證明。研究結果表明了細胞內鈣庫操縱的鈣內流也誘導 TRPV4-TRPC1 通道複合體的快速上膜在血流剪切力引起的鈣內流和血管舒張的過程中擁有極其重要的生理意義。

本研究進一步探究 TRPV4-TRPC1 通道複合體在血流剪切力引起的細胞鈣內流、血管擴張中的作用。研究結果表明，在 TRPV4 單獨表達的人胚腎(HEK293)細胞上，血流剪切力可以引起細胞鈣內流。TRPC1 和 TRPV4 共表達可以顯著延長血流剪切力引起的細胞鈣內流，並且與 TRPC1 的共表達可以使 TRPV4-TRPC1 異聚體通道被磷酸激酶 G 負反饋調節。血流剪切力引起的細胞鈣內流可以被 TRPC1 的抑制性抗體(T1E3)和 TRPC1 的顯性抑制質粒(TRPC1Δ567-793)所抑制。重要的是，TRPV4-TRPC1 通道複合體在過量表達系統中的功能同樣可以在原代內皮細胞上體現；一是在急性分離的大鼠腸阻力血管內皮細胞上；二是在人臍靜脈內皮細胞上，二者均共同表達 TRPV4 和 TRPC1。在人臍靜脈內皮細胞上，血流剪切力引起的細胞鈣內流可以被 T1E3 和 TRPC1Δ567-793 所抑制；TRPC1 特異性小干擾 RNA 可以有效地抑制 TRPC1 蛋白的表達水準。有趣的是，TRPC1

特異性小干擾 RNA 不僅顯著減少血流剪切力引起的細胞鈣內流的幅度，而且顯著減少血流剪切力引起的細胞鈣內流的持續性。這個結果和 TRPC1 與 TRPV4 共表達可以顯著延長血流剪切力引起的細胞鈣內流相一致。進一步，在阻力血管上，我們使用鈣敏感螢光染料和壓力血管機動描記器來探究 TRPV4-TRPC1 異聚體通道在血流剪切力引起的細胞鈣內流和血管舒張的作用。血流剪切力引起的血管段上內皮細胞鈣內流和血管舒張可以被 T1E3 顯著抑制。這些研究結果充分表明 TRPV4-TRPC1 異聚體通道在血流剪切力引起的細胞鈣內流和血管舒張所起的重要作用。

總而言之，我們的研究證明了 TRPV4 和 TRPC1 共表達可以形成功能性 TRPV4-TRPC1 異聚體離子通道；細胞內鈣庫操縱的鈣內流誘導 TRPV4-TRPC1 異聚體離子通道的快速上膜，可以使與 TRPV4-TRPC1 異聚體離子通道相關的兩個方面的功能均有顯著增加；重要的是，TRPV4-TRPC1 異聚體離子通道在血流剪切力引起的細胞鈣內流和血管舒張發揮了重要作用。

Acknowledgements

I owe my deepest gratitude to my supervisor, Prof. Xiaoqiang Yao for his guidance, inspiration and care from the initial to the final level, and for his expert, careful and efficient reading and revision of this thesis and papers arising from this thesis.

I would like to show my gratitude to Prof. Yu Huang for his support and valuable advice during my Ph.D study.

I gratefully acknowledge Prof. Jianhong Luo, Prof. Qiang Xia, Dr. Shuang Qiu and Dr. Jingyuan Cao for their advice and help on the FRET and TIRF experiment at Zhejiang University.

I gratefully acknowledge Prof. Bernd Nilius and Prof. Indu S. Ambudkar for their expert, careful reading and revision of papers arising from this thesis.

This thesis would not have been possible unless there was help and assistance from my labmates in Prof. Yao's lab throughout the course of this project.

I gratefully acknowledge help from Ms. Fung Ping Leung and Mr. Chi-Wai Lau.

I am indebted to many of my colleagues and staffs in the Department of Physiology for their care and support these years.

Last but not least, I owe special thanks to my family for their generous support and encouragement throughout my study.

Table of content

Table of figures

Chapter 1

General introduction

Protein-protein interactions involving TRP channels and functional roles of such interaction in signal transduction

1.1. Introduction

Protein-protein interactions play an important role in cellular signal transduction process. Such interactions are intrinsic to every cellular process including DNA replication, transcription, translation, splicing, secretion, cell cycle control and signal transduction. The physical association between two proteins allows one protein-mediated response to be modulated by signaling transduction pathways that usually act on its coupling partner.

Transient receptor potential (TRP) channels are a superfamily of ion channels that consist of at least 30 members. These channels can be into 7 subfamilies including TRPC, TRPV, TRPM, TRPP, TRPML, TRPA and TRPN. All TRP channels are cation channels, though the permeability for different mono- and divalent cations varies greatly among isoforms. A typical TRP subunit is composed of six membrane-spanning domains and a hydrophobic segment between the fifth and sixth trans-membrane domains that forms the putative pore region loop. Cytosolic N-terminus and C-terminus tails flank the six trans-membrane domains. Functional TRP complexes are presumed to be homo- as well as heterotetramers. Homotetramers consist of four identical subunits while heterotetramers are composed of different subunits. Heteromeric TRP channels have electrophysiological and/or pharmacological properties different from those of homomeric TRP channels.

Heteromeric assembly of TRP channels also allows the channels activity to be regulated by more diverse array of cellular signaling.

In this chapter, I intend to summarize the current knowledge on protein-protein interaction involving TRP channels. The following subjects will be discussed: (i) Heteromeric coaasembly of different TRP subunit with the same TRP subfamily; (ii) Heteromeric coaasembly of different TRP subunit across different TRP subfamilies. (iii) Interaction of TRP channels with Ca^{2+}-activated K^+ channels; (iv) Intereaction of TRP channels with several other auxiliary proteins.

1.2. Heteromeric coaasembly of TRP subunits within the same TRP subfamily and their functional roles in signal transduction

In TRP channel family, heteromeric coaasembly of different TRP subunits within the same TRP subfamily occurs frequently.

1.2.1 TRPC subfamily

TRPC subfamily is involved in Ca^{2+} entry and is composed of seven members (TRPC1-TRPC7), all of which are Ca^{2+}-permeable cation channels. Based on their sequence homology and the functional similarities, TRPC subfamily can be further subdivided into three subgroups: C1/C4/C5, C3/C6/C7, and C2 (Clapham *et al.*, 2005).

1.2.1.1 TRPC1 and TRPC5

TRPC1 and TRPC5 each can co-assemble to form homotetrameric channels, They can also co-assemble together to form a new heterotetramic channel which has significantly different electrophysiological characters from homotetrameric TRPC1, TRPC5 or any other TRPCs: (1). The current-voltage relationship for TRPC1/TRPC5 heterotetramer was clearly distinct from the inwardly rectifying current-voltage relationship of the TRPC5 homotetramers; (2) The single channel conductance for TRPC5 homotetramers and TRPC1/TRPC5 heterotetramers were about 38 pS and 5 pS, respectively; (3) TRPC1/TRPC5 heterotetramers exhibits altered permeation

properties from TPRC5 homotetramers; (4) TRPC1/TRPC5 forms a functional non-selective cation channel gated by G_q-coupled receptors (Zhang *et al.*, 2005) not by the store depletion. It was clearly demonstrated that different activation between TRPC5 homotetramer and TRPC1/TRPC5 heterotetramer is due to the difference in subunits assembly.

1.2.1.2 TRPC1/TRPC3, TRPC1/TRPC4, TRPC6/TRPC7

Physical interaction between TRPC1 and TRPC3 has been demonstrated using co-immunoprecipitation method (Liu *et al.*, 2005). Related to this are findings that TRPC1/TRPC3 functions as a novel thapsigargin- and OAG (2-acetyl-sn-glycerol)-sensitive, store-operated non-selective cation channels in human parotid gland ductal cells (Liu *et al.*, 2005). Additional recent evidence showed that NO/cGMP/PKG-mediated inhibition of TRPC1/TRPC3 channels occurred in native vascular smooth muscle cells. They suggested that a feedback system involving NO and TRPC1/TRPC3 channels in the control of vascular tone (Chen *et al.*, 2009). In fact, similar heteromeric assembly across the same TRPC subfamily has been previously reported. For example, TRPC1 and TRPC4 form a novel cation channel in mammalian brain (Strubing *et al.*, 2001), and TRPC6 and TRPC7 contributes to heteromultimeric channels in vascular smooth muscle cells (Maruyama *et al.*, 2006). However, physical interaction of TRPC1/TRPC4 generates whole-cell currents that is indistinguishable from currents through TRPC1/TRPC5 heteromers (Strubing *et al.*, 2001). Heteromeric assembly of TRPC6/TRPC7 has been suggested in-synaptosomes derived from adult rat brain (Goel *et al.*, 2002) and A7r5 vascular smooth muscle cells (Maruyama *et al.*, 2006). Furthermore, a study by Maruyama *et al.* reported biochemical evidence of TRPC6/TRPC7 coassembly. They demonstrated that anti-TRPC7 immunoreactive protein could be coimmunoprecipitated from vascular smooth muscle cells lysates using anti-TRPC6 protein. They also suggested that TRPC6/TRPC7 heteromer plays an important role in arginine vasopressin-induced cation current of vascular smooth muscle cells (Maruyama *et al.*, 2006).

1.2.1.3 TRPC1/TRPC4/TRPC5, TRPC3/TRPC6/TRPC7

Multiple combinations of heteromeric TRPC channel complexes have been explored by a systematic approach based on co-targeting assays, fluorescence resonance energy transfer (FRET) determination, co-immunoprecipitation and functional tests (Hofmann *et al.*, 2002). Heteromerization of mammalian TRPC channels has been clearly demonstrated among the most closely related phylogenetic subgroups TRPC1/TRPC4/TRPC5 and TRPC3/TRPC6/TRPC7 which feature a promiscuity of heteromeric assembly. Also, it is interesting to note that TRPC2 did not interact with any other TRPC subunit, and members of TRPC1/TRPC4/TRPC5- and TRPC3/TRPC6/TRPC7-subgroups were unable to interact across the borders of their respective subgroup (Hofmann *et al.*, 2002). Native TRPC1/TRPC4/TRPC5 and TRPC3/TRPC6/TRPC7 heteromers were found in rat cortex and cerebellum, respectively (Goel *et al.*, 2002), although physiological role of these tri-complexes is yet to be defined.

1.2.2 TRPV subfamily

TRPV subfamily consists of six members (TRPV1-TRPV6) according to the common functional and biophysical properties of gene products. Based on the phylogenesis, it can be further subdivided into two subgroups: TRPV1-V4 and TRPV5-V6 (Clapham *et al.*, 2005).

1.2.2.1 TRPV1/TRPV2

Interaction between TRPV1 and TRPV2 has been demonstrated by FRET, co-immunoprecipitation and confocal laser scanning microscopy (Hellwig *et al.*, 2005). When TRPV1-YFP was coexpressed with TRPV2-CFP with different ratio, there was a partial overlapping of the fluorescence both in the plasma membrane region and in intracellular compartments. In cells co-expressed with TRPV2-FLAG and similar amounts of YFP-tagged TRPV1 and TRPV2, TRPV2-FLAG preferentially coimmunoprecipitated with TRPV2-YFP, suggesting that the

homomeric configuration was favored by TRPV2. Although homomultimers of TRPV1 and TRPV2 was favored, the heteromeric assembly of TRPV1/TRPV2 does occur. The physiological significance of such a TRPV1-V2 hetertetramer remain unclear, because co-expression of both channel subunits is seen only in few specialized sensory neurons (Greffrath *et al.*, 2003).

1.2.2.2 TRPV1/TRPV3

A report by Peier et al. (Peier *et al.*, 2002) revealed that a distinct expression of TRPV1 and TRPV3 in keratinocytes and sensory afferents. Moreover, heterologous co-expression of TRPV1 and TRPV3 was observed. However, only minor amounts of TRPV3 could be co-immunoprecipitated with TRPV1. Obviously, the respective homooligomeric configuration was clearly preferred. Also, FRET data for TRPV1/TRPV3 was unable to demonstrate an efficient heteromultimerization occurring between TRPV1 and TRPV3.

In addition, the confocal laser scanning microscopy revealed the poor colocalization of TRPV1 and TRPV3 and low correlation coefficients in intracellular compartments even through slightly higher colocalization in the plasma membrane region was observed. Therefore, an interaction between TRPV1 and TRPV3 subunits appears likely, but may occur with a lower efficiency compared to the formation of the respective homooligomers (Hellwig *et al.*, 2005).

1.2.2.3 TRPV5/TRPV6

Findings by Hoenderop *et al.* (2003) demonstrated that there was hetertetramer formation between TRPV5 and TRPV6 using the techniques of FRET, co-immunoprecipitation and confocal laser scanning microscopy (Hoenderop *et al.*, 2003). When TRPV5 was coexpressed with its phylogenetically closest relative, TRPV6, identical localization was observed in vesicular intracellular structures. Co-expression of TRPV5 and TRPV6 gave rise to a FRET efficiency which is even higher than the values of the respective homomultimers (Hellwig *et al.*, 2005). Data from chemical cross-linking, density gradient centrifugation, functional and

biophysical assays on TRPV5/TRPV6 constructs not only confirmed that TRPV5 and TRPV6 subunits assemble into the same pore complex but also re-affirmed the tetrameric stoichiometry of TRPV channel subunits for both isoforms. Furthermore, TRPV5 and TRPV6 are co-expressed in various epithelial tissues and their expression levels affect intestinal and renal Ca^{2+} absorption. Importantly, TRPV5 and TRPV6 have been implicated in many diseases and their heteromerization is likely to be of physiological relevance (van *et al.*, 2005).

1.2.3 TRPM subfamily

TRPM subfamily consists of eight members which can be divided into four groups: M1/M3, M6/M7, M2/M8, and M4/M5 (Clapham *et al.*, 2005). Assembly of the TRPM subunits has been less reported with an exception of heteromeric assembly of TRPM6/TRPM7 (Chubanov *et al.*, 2004).

It has been known for some time that TRPM6 specifically interacts with its closest homolog, the Mg^{2+}-permeable cation channel TRPM7, resulting in the assembly of functional TRPM6/TRPM7 complexes at the cell surface. Inward and outward currents at negative and positive voltages respectively could be observed in TRPM7-expressing oocytes. In addition, co-expression of TRPM6 markedly prolonged the TRPM7-like current, which was the most pronounced at positive membrane voltages. However, no obvious ion current in TRPM6a-, TRPM6b- and TRPM6c-injected oocytes was detected (Chubanov *et al.*, 2004). Consistent to the functional data, western blot analysis also showed that TRPM6a was present in the cell lysate but absent from the plasma membrane. Co-injection of TRPM6a and TRPM7 cRNA allowed for the detection of TRPM6 proteins in the cell membrane fraction (Chubanov *et al.*, 2004). This indicated that TRPM6 subunits were unable to form a functional channel complex in the *Xenopus* cell membrane when expressed alone, whereas TRPM7 was able to direct TRPM6 to the cell membrane. Furthermore, TRPM6 specifically requires TRPM7 for trafficking to the cell surface, most probably by means of heteromeric assembly. Also, based on the evidence from FRET, it suggests that TRPM6a directly interacts with TRPM7 to form a functional channel

complex on the cell surface. TRPM7 and TRPM6 contribute to magnesium absorption in epithelial cells (Chubanov *et al.*, 2004).

1.2.4 TRPP subfamily

The TRPP ("polycystin") family is divided into two groups based on the structure, (1) the polycystic kidney disease 1 (PKD1, also named TRPP1)-like proteins, which comprises PKD1/TRPP1, PKDREJ, PKD1L1, PKD1L2, and PKD1L3, and (2) the polycystic kidney disease 2 (PKD2, also named TRPP2)-like proteins, which comprises PKD2/TRPP2, PKD2L1/TRPP3, and PKD2L2/TRPP5 (Delmas, 2004;Moran *et al.*, 2004;Pedersen *et al.*, 2005).

TRPP1 and TRPP2 are two individual proteins related to the autosomal dominant polycystic kidney disease (ADPKD). They interact with each other to form a new complex. In this complex, TRPP1 with a large extracellular domain is not an ion channel. However, TRPP2, which has six trans-membrane domains, can form a non-selective cation channel. TRPP1-P2 complex plays an important role in the flow-induced Ca^{2+} influx. In this process, TRPP1 may sense the fluid flow, thus functions as a mechano-fluid stress sensor (Nauli *et al.*, 2003). TRPP2 receives the shear stress signaling from TRPP1, resulting in the opening of the channel pore to allow Ca^{2+} influx. In addition, TRPP1 is required for TRPP2 translocation to the plasma membrane. Recent studies by Nauli *et al.*, (Nauli *et al.*, 2008) and AbouAlaiwi *et al* (AbouAlaiwi *et al.*, 2009) showed that TRPP1-P2 complex is localized in the microsensory compartment (i.e., endothelial cilium), where it contributed to the shear stress-related responses (AbouAlaiwi *et al.*, 2009;Nauli *et al.*, 2008).

1.2.5 Mechanism of heteromeric coassembly within the same TRP subfamily

TRPC1 seems to have a special role in facilitating heteromerization among distantly related TRPCs, such as TRPC1/TRPC5, TRPC1/TRPC4, TRPC1/TRPC4/TRPC5 discussed above. Two interaction domains have been identified in the oligomerization of TRPC channels: the first interaction domain overlaps the N-terminal ankyrin repeats and the coiled-coil domains; the second

interaction domain encompasses the putative pore region, including the linker between the fourth and fifth trans-membrane segments and the cytosolic C-terminal tail. The first domain is responsible for the self-association of the N-terminus of adjacent TRPCs. For example, N-terminus is required for the heteromeric assembly of TRPC1/TRPC3 (Liu *et al.*, 2005). The second domain is responsible for the interaction between the N-terminus and the C-terminus of adjacent subunits *(Lepage et al., 2006).* In addition, tetramerization of TRPC4 or TRPC6 channels is mediated not only by the ankyrin repeat domain but also by a following coiled-coil motif and a second site comprising the pore region and part of the C-terminal tail *(Lussier et al., 2005).* Thus, according to the assembly mechanism of TRPC subfamily, both terminals and the putative pore region are involved in the heteromeric assembly.

For TRPV assembly, the trans-membrane domain and the cytosolic terminus of TRPV are involved in the specificity and the affinity of the subunit interaction. It was suggested that N-tail/N-tail, N-tail/C-tail, and C-tail/C-tail interaction are necessary for the homomeric assembly of TRPV5. It was speculated that interaction between both tails is not only necessary for the homomeric assembly but also for the heteromeric assembly of TRPV subfamily (Hellwig *et al.*, 2005).

The study by Chubanov *et al.* (2004) suggests that the mutation of S141L in TRPM6 disrupt the heteromeric assembly of TRPM6/TRPM7 leading to the lost of current amplification mediated by TRPM6/TRPM7 as well as TRPM7-assisted surface targeting of TRPM6 (Chubanov *et al.*, 2004). The protein kinase domain of TRPM7 has been crystallized and solved (Yamaguchi *et al.*, 2001). TRPM7 exhibits a dimer configuration other than tetrameric rotational symmetry. Thus, it is attempting to speculate that interacting cytosolic C- terminus of subunits located in different pore complexes is required for the TRPM6/TRPM7 functional channel complex.

TRPP1-like proteins are large (~460 kDa) integral membrane glycoproteins with an extended N-terminal extracellular region, 11 predicted transmembrane-spanning segments, and a short intracellular C-terminal domain (Hughes *et al.*, 1995). The extracellular region comprises up to ~3,000 amino acids (in the case of TRPP1) and contains a number of recognizable protein motifs including ligand binding sites and

adhesive domains (Bichet *et al.*, 2006). The presence of these domains suggests that TRPP1 is involved in interactions with proteins (homophilic and/or heterophilic interactions) and carbohydrates on the extracellular side of the membrane. Disease-causing mutations in both biochemical and electrophysiological assays demonstrated that channel activity of TRPP1/TRPP2 is dependent on an interaction through their respective C-terminal regions. A mutant TRPP1 protein, R4227X, which lacks the terminal 76 amino acids containing the coiled-coil domain of TRPP1 was found to have greatly reduced binding to full-length TRPP2, as measured by co-immunoprecipitation and whole-cell patch clamp assays. Likewise, a mutant TRPP2 protein, R742X which lacks the terminal 227 amino acids but contains all six trans-membrane domains and the possible pore region, failed to co-immunoprecipitate with full-length TRPP1. No currents were generated when R742X was co-expressed with full-length TRPP1 consistent with the biochemical analyses (Hughes *et al.*, 1995).

1.3. Heteromeric coassembly of TRP subunits across different TRP subfamilies and their functional roles in signal transduction

Heteromeric assembly across different TRP subfamilies is one of the hot focus recently in the TRP channel research field. Such association is reported between TRPC1 and TRPP2 (Bai *et al.*, 2008) and between TRPV4 and TRPP2 (Kottgen *et al.*, 2008). Both TRPC1/TRPP2 and TRPV4/TRPP2 heteromers have physiological function. In the result chapters of this thesis, we will show the details about the third example, TRPV4-TRPC1 heteromeric channel (Ma *et al.*, 2010).

1.3.1. TRPC1/TRPP2

TRPC1/TRPP2 heteromeric channel is the first identified inter-group heteromeric TRP channels (Bai *et al.*, 2008;Kobori *et al.*, 2009;Zhang *et al.*, 2009). TRPC1/TRPP2 is activated in response to G-protein-coupled receptor activation and shows a pattern of single-channel conductance, amiloride sensitivity and ion permeability distinct from that of TRPP2 or TRPC1 alone (Bai *et al.*, 2008). Most

recent study reported native TRPC1/TRPP2 activity in kidney cells by complementary gain-of-function and loss-of-function experiments. The existence of TRPC1/TRPP2 couple under physiological conditions is supported by colocalization at the primary cilium and by co-immunoprecipitation from kidney membranes. These findings suggest a role of heteromultimeric TRPC1/TRPP2 channel in mechanosensation and cilium-based Ca^{2+} signalling (Bai *et al.*, 2008;Zhang *et al.*, 2009)).

1.3.2. TRPP2/TRPV4

TRPP2 assembles with TRPV4 to form a mechano- and thermosensitive molecular sensor in the cilium as determined by FRET, co-immunoprecipitation and subcellular colocalization methods. Whole-cell patch clamp studies show that TRPP2/TRPV4 heteromers display electrophysiological properties different from those of homomeric TRPP2 or TRPV4 channels. "Knocking-down" TRPV4 in renal epithelial cells abolishes flow-induced Ca^{2+} transients, demonstrating that a requirement for TRPV4 in the ciliary mechanosensor. These findings demonstrate that TRPP2 and TRPV4 not only physically but also functionally interact with each other. Furthermore, the report provided important genetic evidence that TRPV4 and TRPP2 collectively mediate thermosensation at moderately warm temperatures in the mouse (Kottgen *et al.*, 2008).

1.3.3 Mechanism of heteromeric coassembly across different TRP subfamilies

The topological features of the homomeric TRPP2-, TRPC1- and heteromeric TRPP2-C1 channel complexes have been assessed by atomic force microscopy recently (Zhang *et al.*, 2009). The results were consistent with structural tetramers. TRPC1 homomeric channels have different average diameter and protruding height when compared to TRPP2 homomers. The contribution of individual monomers to the TRPP2-C1 heteromers was easily distinguishable in atomic force microscopy (Zhang *et al.*, 2009). The molecular mass of the protein isolated from cells expressing both TRPP2 and TRPC1 was intermediate between the masses of the two homomers, further supporting the formation of a heteromer. Another study using atomic force

microscopy found that TRPP2-C1 heterotetramers have the subunit stoichiometry of 2 TRPP2 vs. 2 TRPC1 with alternating subunit arrangement (Kobori *et al.*, 2009).

For TRPV4/TRPC1 heteromers, we found that deletion of either N-terminal or C-terminal cytoplasmic domain of both subunits (TRPC1 and TRPV4) could interrupt the interaction of TRPC1 with TRPV4 (Ma *et al.*, 2010). The requirement of both N- and C-terminal domain for TRP channel assembly are not very surprising, because other studies also had similar findings for TRPV channels (Hellwig *et al.*, 2005).

1.4. Physical interaction of TRP channels with Ca^{2+}-activated K^+ channels

Ca^{2+} influx through localized TRP channels may increase Ca^{2+} level within defined subcellular compartments of the cytoplasm. Evidence suggests that specific TRP channels may interact physically and/or functionally with Ca^{2+}-activated K^+ channels to form signaling complex. Activity of TRP channels may provide Ca^{2+} source for activation of Ca^{2+}-activated K^+ channels. Several studies suggest couples of TRPV4/BK_{Ca} (Earley *et al.*, 2005), TRPC1/BK_{Ca} (Kwan *et al.*, 2009), TRPC6/BK_{Ca} (Kim *et al.*, 2009) and TRPA1/IK_{Ca}/SK_{Ca} (Earley *et al.*, 2009). Thus, it is attempting to speculate that different subpopulations of Ca^{2+}-activated K^+ channels play different roles dependent on their coupling with specific TRP channels.

1.4.1 TRPV4/BKCa

The identification of the functional interaction between TRPV4 and BK_{Ca} brings forward a very interesting issue about the heteromeric assembly between TRP and BK_{Ca} channel. In freshly isolated cerebral myocytes, TRPV4 agonist 4α-PDD and the endothelium-derived arachidonic acid metabolite 11,12 epoxyeicosatrienoic acid (11,12 EET) evoked outwardly rectifying whole-cell currents with properties consistent with those of expressed TRPV4 channels. Using high-speed laser-scanning confocal microscopy, it is found that 11,12 EET increased the frequency of unitary Ca^{2+} release events (Ca^{2+} sparks) via ryanodine receptors located on the sarcoplasmic reticulum of cerebral artery smooth muscle cells. EET-induced Ca^{2+} sparks activated nearby sarcolemmal large-conductance Ca^{2+}-activated K^+ (BK_{Ca}) channels, measured

as an increase in the frequency of transient K^+ currents. Antisense-mediated suppression of TRPV4 expression in intact cerebral arteries prevented 11,12 EET-induced smooth muscle hyperpolarization and vasodilation. Thus, it suggests that TRPV4 forms a novel Ca^{2+} signaling complex with ryanodine receptors and BK_{Ca} channels to elicit smooth muscle hyperpolarization and arterial dilation (Earley *et al.*, 2005).

Recent data from our laboratory showed that TRPV4 can be pulled down together with BK_{Ca} in co-immunoprecipitation assay of vascular endothelial cells (Ma *et al.*, 2010), supporting the existence of TRPV4-BK_{Ca} complex.

1.4.2 TRPC1/BKCa

A physical interaction of TRPC1 with BK_{Ca} was reported by our research group (Kwan *et al.*, 2009). This TRPC1-BKCa complex plays an important role in membrane potential control in vascular smooth muscle cells (VSMCs). In coimmunoprecipitation experiments, an antibody against BK_{Ca} α-subunit (α-BK_{Ca}) could pull down TRPC1, and moreover an anti-TRPC1 antibody could reciprocally pull down α-BK_{Ca}. Double-labeling immunocytochemistry also showed that TRPC1 and BK_{Ca} were colocalized in the same subcellular regions, mainly on the plasma membrane indicating that TRPC1 physically associates with BK_{Ca} in VSMCs. With the use of potentiometric fluorescence dye DiBAC(4)(3), it was found that store-operated Ca^{2+} influx resulted in membrane hyperpolarization of VSMCs. The hyperpolarization was inhibited by an anti-TRPC1 blocking antibody T1E3 and two BK_{Ca} channel blockers, charybdotoxin and iberiotoxin. These data were confirmed by sharp microelectrode measurement of membrane potential in VSMCs of intact arteries. Furthermore, T1E3 treatment markedly enhanced the membrane depolarization and contraction of VSMCs in response to several contractile agonists including phenylephrine, endothelin-1, and U-46619. These data suggest that, TRPC1 physically associates with BK_{Ca} in VSMCs and that Ca^{2+} influx through TRPC1 activates BK_{Ca} to induce membrane hyperpolarization. The hyperpolarizing effect of TRPC1/BK_{Ca} coupling could serve to reduce agonist-induced membrane

depolarization, thereby preventing excessive contraction of VSMCs to contractile agonists (Kwan *et al.*, 2009). Because TRPC1 is a Ca^{2+}-permeable cation channel involved in diverse physiological function, it is attempting to speculate that TRPC1 may associate with other proteins, not only BK_{Ca}, to form a signaling complex, which is crucial for channel function.

1.4.3 TRPC6/BK_{Ca}

Based on the evidences from coimmunoprecipitation and GST pull-down assays, physical interaction between TRPC6 and BK_{Ca} channel was demonstrated. Co-expression of TRPC6 increased plasma membrane expression of a BK_{Ca} subunit splice variant (Slo1(VEDEC)) which is typically retained in intracellular compartments in HEK cells as measured by cell-surface biotinylation and confocal microscopy assays. Functional studies by patch clamp also showed that co-expression of TRPC6 increased currents through BK_{Ca} channels. Knockdown of endogenous TRPC6 by small interfering RNA reduced the steady-state surface expression of endogenous BK_{Ca} channels as well as voltage-evoked outward current through BK_{Ca} channels. In all, interactions of TRPC6 with certain splice variants of BK_{Ca} channels increase the expression of the resulting channel complex on the cell surface and the corresponding functional role (Kim *et al.*, 2009).

1.4.4 TRPA1/IKCa/SKCa

Recent report by Earley *et al.* (Earley *et al.*, 2009) suggest an association between TRPA1 and IKca/SKca (intermediate/small conductance Ca^{2+}-activated K^+ channels. Double immunostaining assays found the colocalization of TRPA1 and IKCa. Functional studies showed that in cerebral arteries, allyl isothiocyanate (AITC)-induced dilation was attenuated by disruption of the endothelium and presence of a TRPA1 channel blocker HC-030031. Consistently, the IK_{Ca} inhibitor TRAM34 significantly decreased AITC-induced vasodilation, whereas the combination of TRAM34 and SK_{Ca} blocker apamin abolished sustained AITC-induced vasodilation, indicating that SK_{Ca} and IK_{Ca} channel activity contribute

to TRPA1-mediated vasodilatory responses. SK_{Ca} and IK_{Ca} hyperpolarize the endothelial cell plasma membrane, and they are considered as the molecules of endothelium derived hyperpolarizing factor (EDHF). These findings provided the clue of the functional coupling between TRPA1 and $IK_{Ca}/SK_{Ca,}$ and potential role of such coupling in EDHF-type vasodilation (Earley *et al.*, 2009).

1.5. Protein-protein interaction of TRP channels with auxiliary proteins

TRP channels interact directly with auxiliary proteins that assemble the channels within Ca^{2+}-signaling complexes. Such auxiliary proteins may alter the permeation and regulation of TRP channels. These auxiliary proteins can be categorized into three groups: (1) proteins that directly interact with TRP channels at near-plasma membrane domain; (2) proteins that mediate insertion and retrieval of TRP channels from the plasma membrane; and (3) scaffolding proteins that mediate TRP channel-ER coupling (Kiselyov *et al.*, 2007).

1.5.1 Proteins that directly interact with TRP channels at near-PM domain

1.5.1.1 Calmodulin

Calmodulin is a ubiquitous protein, well known to be involved in Ca^{2+}-dependent feedback regulation of several ion channels (Levitan, 1999). Since TRPC channels are the key component in Ca^{2+} signaling, it is not surprising that they are subject to regulatory feedback loops mediated by Ca^{2+} itself. Two forms of regulation of TRPC channels by calmodulin exist. The first one is the, direct regulation of TRPC channels by calmodulin. It was reported that all the mammalian TRPC channels contain at least one calmodulin binding site which is located at their C-terminus (Tang *et al.*, 2001;Zhu, 2005). Interestingly, the calmodulin binding site at the C-terminus of TRPC channels overlaps with the inositol 1,4,5-trisphosphate receptors (IP_3R) binding site, and IP_3R and calmodulin appear to compete for binding to this site. It is important to note that TRPC channels will be activated if this site binds with IP_3R and will be inhibited if this site binds with calmodulin (Zhang *et al.*, 2001). Calmodulin also interacts with TRPC1 and mediates the Ca^{2+}-dependent inactivation of the

channel (Singh *et al.*, 2002). The second form is indirect regulation of TRPC channels by calmodulin via an intermediate protein. For instance, enkurin is a protein that binds to both calmodulin and TRPC channels (Sutton *et al.*, 2004), and may thus function as an adaptor for interaction of other calmodulin-regulated proteins with TRPC channels.

In TRPV subfamily, interaction between TRPV6 and calmodulin was demonstrated. Such interaction is Ca^{2+}-dependent and it involves the binding of calmodulin with speficic regions in the COOH and NH2 of TRPV5 and TRPV6 as well as the trans-membrane domain of TRPV6 (Lambers *et al.*, 2004;Niemeyer *et al.*, 2001). Deletion assay of TRPV6 or calmodulin also confirmed the functional interaction of TRPV6 and calmodulin. Deletion of the calmodulin-binding site in the COOH terminus of TRPV6 significantly reduced slow component of channel inactivation. Although it is clear that calmodulin can modulate TRPV6-mediated Ca^{2+} influx, it still remains to be established whether calmodulin functions as a general Ca^{2+} sensor for TRPV5/V6 channels.

1.5.1.2 INAD

INAD, the PDZ domain containing protein, is the near-membrane scaffold that assembles TRP channels and other Ca^{2+}-signaling proteins into signaling complexes (Chevesich *et al.*, 1997;Tsunoda *et al.*, 1997). Evidences showed the dependence of INAD for localization of TRP to the rhabdomeres and the requirement of the TRP-INAD interaction to prevent retinal degeneration. INAD binds calmodulin either directly or indirectly (Chevesich *et al.*, 1997). It is attempting to put forward the intriguing possibility of TRP-INAD-calmodulin association, in which INAD may serve as a Ca^{2+}-dependent regulatory protein in the TRP complex.

1.5.1.3 NHERF/EBP50

NHERF/EBP50 (Na^+/H^+ exchanger regulatory factor-ezrin/moesin/radixin -binding phosphoprotein 50) are the bivalent scaffolding protein that can interact with TRPC4 and TRPC5 at their C-terminus (Mery *et al.*, 2002;Obukhov and Nowycky, 2004;Tang *et al.*, 2000). The activation of TRPC4 and TRPC5 can be inhibited or

delayed by disrupting the interaction of TRPs with NHERF/EBP50 (Obukhov *et al.*, 2004).

Co-expression of TRPV5 with two PDZ domain-containing proteins NHERF2 and serum- and glucocorticoid-inducible kinase 1/3 (SGK1/3) resulted in increased TRPV5 activity (Embark *et al.*, 2004). However, co-expression of TRPV5 with NHERF2 or SGK alone could not activate TRPV5 (Embark *et al.*, 2004), indicating the requirement of both NHERF2 and SGK for TRPV5 activity. Such view was confirmed by the observation that deletion of the first PDZ domain in NHERF2 abolished the activating effect of SGK/NHERF2 on TRPV5 activity (Palmada *et al.*, 2005). Furthermore, it is demonstrated that NHERF2 specifically interacts with the three amino acids (YHF) at of the COOH terminus of TRPV5 (Palmada *et al.*, 2005). However, TRPV6 does not bind NHERF2 (Palmada *et al.*, 2005). Perhaps such a modulation just acts on the TRPV5 homotetramer rather than TRPV5/TRPV6 heteromeric complex, or also can act on TRPV5/TRPV6 complex through the modulation on TRPV5 subunit.

1.5.1.4 Neurabin

Neurabin is homologous scaffolds. Neurabin-II is also known as spinophilin. It consists of actin and protein phosphatase 1 binding domains, a PDZ domain, and three (spinophilin) or four (neurabin) coiled-coil domains (Allen *et al.*, 1997;McAvoy *et al.*, 1999;Nakanishi *et al.*, 1997;Satoh *et al.*, 1998). Spinophilin binds the third intracellular loop of G-protein-coupled receptors (GPCRs) and several regulators of G proteins signaling proteins (Wang *et al.*, 2005). Generally, the increase in Ca^{2+} is achieved by the generation of IP_3, activation of IP_3-receptors, release of stored intracellular Ca^{2+}, and Ca^{2+} entry through plasma membrane cation channels including TRP channels. Hence, spinophilin and neurabin may bind TRP channels to coordinate the activity of the Ca^{2+}-signaling complex. Such speculation was supported by the recent evidences that neurabin binds TRPC5 and TRPC6 in rat brain lysates by immunoprecipitation (Goel *et al.*, 2005).

1.5.1.5 Caveolin

Another potential TRP scaffold is caveolin which is essential membrane protein found in caveolae. A report by Brazer *et al.* (2003) showed that TRPC1 binds to caveolin and the interaction play a key role in assembly of TRPC1 as store-operated Ca^{2+} influx channel in which the important step is insertion of TRPC1 into caveolae (Brazer *et al.*, 2003). Both dominant-negative caveolin and truncation of the ankyrin repeats at the N-terminus of TRPC1 can inhibit insertion of TRPC1 to the plasma membrane (Brazer *et al.*, 2003). The role of caveolin in the endocytosis of TRPV5 was also reported. Cha *et al.* (2008) showed that protein kinase C (PKC) activator 1-oleoyl-acetyl-sn-glycerol (OAG) can increase TRPV5 current density and surface expression. Importantly, knocking-down of caveolin-1 using either knockout mice or small interference RNA abrogated the OAG activation of TRPV5 (Cha *et al.*, 2008). It has been suggested that protein association between TRPV5 and caveolin-1 may directly or indirectly may responsible for protein targeting to caveolae (Cohen *et al.*, 2004).

1.5.2. Proteins that mediate insertion and retrieval of TRP channels from the plasma membrane

1.5.2.1 VAMP2

Vesicle-associated membrane protein 2 (VAMP2) is present on the membrane of intracellular trafficking vesicles and is involved in fusion of the vesicles to the plasma membrane. VAMP2 was shown to interact with TRPC3 at its N-terminus by yeast two-hybrid screen, immunoprecipitation and immunolocalization studies (Singh *et al.*, 2004). Cleavage of VAMP2 with tetanus toxin did not prevent trafficking of TRPC3-containing vesicles to the plasma membrane region but does suppress insertion of the channel into the surface membrane, indicating that interaction with VAMP2 is required for fusion of TRPC3-containing vesicles with the plasma membrane (Singh *et al.*, 2004).

1.5.2.2 PLCγ

It was previously demonstrated that phospholipase C (PLC)γ interacts and regulates activity of TRPC3 channel and PLCγ is a candidate for lipid-mediated fusion of TRPC3 with the plasma membrane (Patterson *et al.*, 2002;van Rossum *et al.*, 2005). PLCγ has the well-established protein interacting sites, SH3 domains. In interaction of TRPC3 with PLCγ-1, an amino-terminal portion of TRPC3 binds to PLCγ-1 via a region that includes the SH3 domain and the carboxy-terminal half of a split PH domain (Patterson *et al.*, 2002;van Rossum *et al.*, 2005). These data imply a role of TRPC3-PLCγ-1 interaction in regulating surface expression and the subsequent function of TRPC3 (van Rossum *et al.*, 2005).

1.5.2.3 MxA

MxA, an interferon-induced 76-kDa GTPase that inhibits the multiplication of several RNA viruses, is one of the proteins that interact with the ankyrin-like repeat domains. Ankyrin-like repeat domains is one of the most common protein-protein interaction motifs (Lussier *et al.*, 2005). Lussier *et al.* (Lussier *et al.*, 2005) showed that MxA specifically interacted with TRPC1, -3, -4, -5, -6, and -7 at the second ankyrin-like repeat domain of TRPCs by GST pull-down and co-immunoprecipitation assays. Such interaction may also affect the channel function, because co-expression of MxA with TRPC6 enhanced agonist-induced or OAG-induced Ca^{2+} entry (Lussier *et al.*, 2005).

1.5.2.4 SNARE

Interaction of TRPC3 with VAMP2, and TRPC3 with αSNAP was identified by yeast two-hybrid screen, immunoprecipitation and immunolocalization studies (Singh *et al.*, 2004). αSNAP is a soluble N-ethylmaleimide-sensitive factor attachment protein. In rat hippocampal neurons, endogenous TRPC3 interacts with the αSNAP, VAMP2 and several other soluble N-ethylmaleimide-sensitive factor attachment protein receptor (SNARE) proteins (Singh *et al.*, 2004). Such interaction may play a role in membrane protein trafficking and/or regulation of TRP channel activity.

In TRPV subfamily, it is reported that TRPV1 interacts with SNARE proteins including snapin and synaptotagmin IX. Two SNARE proteins participate in channel exocytosis and distribution in intracellular vesicular compartments. Moreover, it was shown that insulin and IGF-1 can induce translocation of TRPV1 which is mediated by activation of PI3K and PKC (Morenilla-Palao *et al.*, 2004;Van Buren *et al.*, 2005). Also, PKC promotes insertion of the TRPV1 channel into the plasma membrane via a mechanism regulated by SNARE proteins. Thus, it is attempting to speculate that TRPV1/SNARE interaction favors the plasma membrane expression and function of TRPV1.

1.5.3 Scaffolding proteins that mediate TRP channel-ER coupling

1.5.3.1 Junctate

Junctate, an integral Ca^{2+} binding protein located on ER membrane, induces and/or stabilizes peripheral couplings between the ER and the plasma membrane, and forms a complex with the IP_3 receptors at its NH2-domain (Treves *et al.*, 2004). Over-expression of junctate increases agonist-induced and store depletion-induced Ca^{2+} influx, whereas its down regulation dissociates the IP_3R-junctate-TRPC3 complex, and reduces both agonist-activated Ca^{2+} release from intracellular stores and Ca^{2+} entry via TRPC3 (Treves *et al.*, 2004). Functional studies support a view that junctate binding IP_3Rs and TRPC3 forming the tertiary complex IP_3R-junctate-TRPC3 that is the molecular basis of the peripheral coupling in TRPC3-overpressing HEK293 cells. Such view was further confirmed by coimmunoprecipitation and pull-down assay (Stamboulian *et al.*, 2005;Treves *et al.*, 2000;Treves *et al.*, 2004).

A report by Stamboulian *et al.* (2005) showed that junctate also binds TRPC5 and TRPC2. However, it is interesting to note that junctate does not bind to TRPC1 which has the ubiquitous distribution in rodent sperms (Stamboulian *et al.*, 2005).

1.5.3.2 Homer

Homer proteins are coded by three genes, homer-1, -2, and -3, and bind many Ca^{2+} signaling proteins to regulate Ca^{2+} signaling (Brakeman *et al.*, 1997;Fagni *et al.*, 2002;Olson *et al.*, 2005;Stiber *et al.*, 2005;Tu *et al.*, 1998;Xiao *et al.*, 1998;Yamamoto *et al.*, 2005). Homer proteins contain an Ena/VASP homology (EVH) domain that binds proline-rich sequences and they can assemble and regulate Ca^{2+}-signaling complexes (Fagni *et al.*, 2002;Xiao *et al.*, 2000) which may include metabotropic glutamate receptor, IP_3 receptors, plasma membrane Ca^{2+}-ATPase (PMCA) pump, sarcoplasmic/ endoplasmic Ca^{2+}-ATPase (SERCA) pump, and ER luminal Ca^{2+} binding proteins (Sala *et al.*, 2005). It is interesting to note that all TRPC and several other TRP channels contain a highly conserved proline-rich sequence at their C-terminus (Yuan *et al.*, 2003). Thus, it is possible that homer proteins interact with TRP channels via proline-rich sequences. Such view was supported by the observation that homer mediates the interaction and gating of TRPC channels by IP3 receptor (Yuan *et al.*, 2003). Observation of dissociation the TRPC1/Homer/IP_3R complex making TRPC1 channel constitutively active, and deletion of homer-1 in mice induced an increased spontaneous Ca^{2+} influx in native cells (Yuan *et al.*, 2003). This indicates an inhibiting regulation of TRPC1/Homer/IP_3R interaction on TRPC1 activity.

1.5.3.3 STIM1

Stromal interacting molecule 1 (STIM1) can bind TRPC1 (Lu *et al.*, 2010;Pani *et al.*, 2009;Yuan *et al.*, 2007). Such interaction would allow TRPC1 to function as a store-operated Ca^{2+} channel because STIM1 has been indicated to regulate store-operated Ca^{2+} channels by function as an ER Ca^{2+} sensor (Spassova *et al.*, 2006;Zhang *et al.*, 2005). The evidences support a model in which STIM1 would activate store-operated Ca^{2+} channel, TRPC1, by binding to channels and subsequently activating the channel. During store depletion of the cell, there is Ca^{2+} outflux in the ER and STIMI1 can sense such Ca^{2+} outflux process. The physical interaction between STIM1 and TRPC1 allows TRPC1 easily receive the signal sensed by STIM1. Three mechanisms have been proposed to explain how STIM1 can

activate the store-operated Ca^{2+} channel: first, STIM1 may interact with a putative pore-forming subunit fo TRPC1; Second, STIM1 may activate Ca^{2+} influx by means of conformational coupling through its coiled-coil domain; Third, STIM1 may assemble with additional STIM1 monomers to form a unique functional Ca^{2+} channel (Zhang *et al.*, 2005).

1.5.3.4 AKAP79/150

The AKAP (a kinase anchoring protein) family of scaffolding proteins was originally named for their ability to target PKA to appropriate substrates but were now known to assemble a wide range of kinases and phosphatases into signaling complexes with appropriate targets (Bregman *et al.*, 1989;Leiser *et al.*, 1986). A recent report by Zhang *et al.* showed that the scaffolding protein AKAP79/150 can modulate the sensitivity of the heat-activated TRPV1 channel. Also, it has been identified that TRPV1 interacts with AKAP79/150 at its C-terminal. Formation of such signal complex allows the regulation of TRPV1 channel activity by the protein kinases PKA and PKC and by the phosphatase calcineurin. This complex plays an important role in heat hyperalgesia (Zhang *et al.*, 2008).

1.6. Concluding remarks and perspectives

Much effort have been made to explore the protein-protein interaction involving TRP channels and the functional roles of such interaction in signal transduction. Several preliminary conclusions can be drawn: (1) The potential importance of heteromultimerization of TRP subunits within the same TRP subfamily or across different TRP subfamilies is an emerging area of research. The heteromultimerization may drastically alter ion selectivity, voltage-dependence and other electrophysiological/pharmacological properties, resulting in the formation of new hetermeric channels that behave differently from the homomultimers; (2) Physical interaction of TRP channels with Ca^{2+}-activated K^+ channels may allow TRP channels to serve as a source of Ca^{2+} for the activation of Ca^{2+}-activated K^+ channels which allow Ca^{2+}-activated K^+ channels to play different roles; (3) TRP channels interact

directly with auxiliary proteins that assemble them within Ca^{2+}-signaling complexes. Such auxiliary proteins may alter the permeation and regulation of TRP channels.

Clearly, further studies are needed to determine how TRP channels heteromultimerize. Classical TRPC and TRPV channels are structurally related to voltage-dependent K^+ channels (K_V). Studies on tetramerization of the K_V1 and K_V2 families showed that an N-terminal T1 domain (first tetramerization domain) is responsible for regulating channel assembly. The T1 domain of K_V1 allows the recognition of members of the same family and prevents co-assembly with members of other K_V families (Long *et al.*, 2005). The C-terminus of K_V 1.1 and K_V 2.1 surrounds the T1 domain and can interact with the N-terminus of the adjacent subunit (Ju *et al.*, 2003;Schulteis *et al.*, 1996). Both TRP and K_V superfamilies have two subunit interaction sites that appear to control the selectivity of subunit assembly. The first interaction site is located at the N-terminus, and the second interaction lies between the N- and C-terminus of adjacent subunits (Lepage and Boulay, 2007). Thus, knoweledge on the assembly mechanism and structure of K_V family may provide clue for similar studies about TRP superfamily.

It appears that more detailed studies are needed in the area of protein-protein interaction involving TRP channels. Some of these areas include stoichiometry analysis, protein surface analysis, map of interacting domains and biological important functions of these heteromers. Future studies in these areas should help understand the mechanism of protein-protein interaction, and may shed some light on biologically important functions of these interactions.

Chapter 2

Objective of the present study

Hemodynamic blood flow is one of most important physiological factors that control vascular tone. Flow shear stress acts on the endothelium to stimulate the release of vasodilators such as nitric oxide (NO), prostacyclin and endothelium-derived hyperpolarizing factors, causing endothelium-dependent vascular relaxation. In many cases, a key early signal in this flow-induced vascular dilation is Ca^{2+} influx in endothelial cells in response to flow. There is intense interest in searching for the molecular identity of the channels that mediate flow-induced Ca^{2+} influx. Functional TRP complexes are presumed to be homo- as well as heterotetramers, and there are growing efforts to identify the subunit composition of these homo- and heterotetramers and to clarify the roles of these functional TRP complexes in the regulation of physiological processes. The objective of this project is to determine the basic molecular identity of flow-induced Ca^{2+} influx and subsequent vasodilation.

In order to attain this objective, I aim to achieve the following:

1. To identify heteromeric assembly of TRPV4 and TRPC1.
2. To identify typical pore properties of TRPV4-TRPC1 heteromeric channel.
3. To examine if the depletion of intracellular Ca^{2+} stores can stimulate the subcellular trafficking of TRPV4-TRPC1 heteromeric channel;
4. To examine functional role of TRPV4-TRPC1 heteromeric channel in flow-induced $[Ca^{2+}]_i$ rise and vasodilation

Chapter 3

Heteromeric assembly of TRPV4 and TRPC1

3.1 Introduction

All transient receptor potential (TRP) channels are cation channels, though the permeability for different mono- and divalent cations varies greatly among isoforms. A typical TRP subunit is composed of six membrane-spanning domains and a hydrophobic segment between the fifth and sixth trans-membrane domains that forms the putative pore region loop. Cytosolic N-terminus and C-terminus tails flank the six trans-membrane domains (Pedersen *et al.*, 2005). Functional TRP complexes are presumed to be homo- as well as heterotetramers (Hellwig *et al.*, 2005;Lepage *et al.*, 2007). Also, each TRP subunit contains typical domains that interact with other proteins (Hellwig *et al.*, 2005;Lepage *et al.*, 2007). There are growing efforts to identify the specific TRP channels that are responsible for defined cellular functions and/or physiological processes.

There are two possibilities. First, a specific TRP subunit may co-assemble with different types of TRP subunits to form heterotetrameric channels. The heretomeric coassembly usually occurs between the members within the same subfamily such as between TRPC1 and TRPC5, and between TRPV5 and TRPV6. However, there are also reports that heteromeric coassembly could occur between the members across different TRP subfamilies, such as association between TRPC1 and TRPP2 (Bai *et al.*, 2008) and between TRPV4 and TRPP2 (Kottgen *et al.*, 2008). Those heteromeric channels display the electrophysiological and/or pharmacological properties different from those of the homomeric TRP channels. Second, two TRP channels, each of which are composed of four subunits, may interact with each other through their N- or

C-terminus.

In this chapter, I used multiple techniques, including fluorescence resonance energy transfer (FRET), co-immunoprecipitation and subcellular colocalization, to explore the possible heteromeric assembly of TRPV4 and TRPC1 (data are published recently, (Ma *et al.*, 2010). My results strongly suggest that TRPV4 physically interact with TRPC1 to form a complex.

3.2 Materials and Methods

3.2.1 Cell culture

All animal experiments were conducted in accordance with the regulation of the U.S. National Institute of Health (NIH publication No.8523). HEK293 cells were cultured in DMEM supplemented with 10% FBS, 100 μg/ml penicillin and 100 U/ml streptomycin.

3.2.2 Cloning and transfection

Mouse TRPV4 gene (NM_022017) was a gift from Dr. Bernd Nilius, Belgium. Human TRPC1 cDNA (NM_003304) was obtained by RT-PCR from human coronary endothelial cells CC2585 (BioWhittaker). For subcellular co-localization and FRET, TRPV4 was tagged with CFP or YFP at its C-terminus, and TRPC1 was tagged with CFP or YFP at its N-terminus. For N- or C- terminal deletion of TRPV4, aa6-aa465 or aa723-aa866 was deleted in YFP-tagged TRPV4 construct, respectively. For N- or C-terminal deletion of TRPC1, aa10-342 or aa653-751 was deleted in YFP-tagged TRPC1 construct, respectively. All genes were cloned into pcDNA6 vector for expression. The nucleotide sequences of all constructs were verified with DNA sequencing.

Transfection condition was as described elsewhere (Kwan *et al.*, 2009). Briefly, HEK293 cells were transfected with various constructs using Lipofectamine 2000. Abound 6×10^4 HEK293 cells were grown in each well of the 6-well plates. Transfection was done with 4 μg plasmid and 6 μl Lipofectamine 2000 in 200 μl

Opti-MEM reduced serum medium in 6-well plates.

3.2.3 Subcellular localization

HEK cells were co-transfected with CFP-tagged TRPV4 and YFP-tagged TRPC1. Fluorescence imaging at subcellular level was analyzed 2 days posttransfection using a FV1000 confocal laser scanning system. For colocalization with a plasma membrane fluorescent di-8-ANEPPS, HEK cells were co-transfected with CFP-tagged TRPV4 and un-tagged TRPC1. 2 days posttransfection, plasma membrane was labeled with 2 μM di-8-ANEPPS in normal physiological saline solution (NPSS) for 10 min in dark immediately before imaging experiments. Free dye was washed away before imaging. CFP and Di-8-ANEPPS fluorescence was recorded by FV1000 confocal system.

3.2.4 Immunoprecipitation and immunoblots

Immunoprecipitation and immunoblots were as described elsewhere (Kwan *et al.*, 2009). The whole cell lysates from HEK cells were extracted with detergent extracted buffer, which contained 1% (vol/vol) Nonidet P-40, 150 mmol/L NaCl, 20 mmol/L Tris-HCl, pH 8.0, with addition of protease inhibitor cocktail tablets. TRPV4 or TRPC1 proteins were immunoprecipitated by incubating 800 μg of the extracted proteins with 5 μg of anti-TRPV4 (Alomone Lab) or anti-TRPC1 (Alomone Lab) antibody on a rocking platform overnight at 4°C. Protein A agarose was then added, followed by a further incubation at 4°C for 3 hr. The immunoprecipitates were washed and resolved on an 8% SDS/PAGE gel.

For immunoblots, the PVDF membrane carrying the transferred proteins was incubated at 4°C overnight with the primary anti-TRPV4 (1:200), anti-TRPC1 (1:200), or T1E3 (1:200) antibodies. Immunodetection was accomplished using horseradish peroxidase-conjugated secondary antibody, followed by ECL detection system.

3.2.5 FRET detection and subcellular localization of TRPV4-CFP/TRPC1-YFP

CFP (or YFP)-tagged TRPV4 and YFP (or CFP)-tagged TRPC1 were co-transfected into these cells. FRET signals were detected as described elsewhere (Qiu et al., 2005). Briefly, an inverted microscope equipped with three-cube FRET filters and CCD camera was used to measure FRET. Three-cube FRET filter cubes were listed as follows (excitation; dichroic; emission): YFP (S500/20 nm; Q515lp; S535/30 nm); FRET (S430/25 nm; 455dclp; S535/30 nm); and CFP (S430/25 nm; 455dclp; S470/30 nm). Average background signal was subtracted. FRET ratio (FR) was calculated by the following equation:

$$FR = \frac{F_{AD}}{F_A} = \frac{[S_{FRET}(DA) - R_{D1} * S_{CFP}(DA)]}{R_{A1} * [S_{YFP}(DA) - R_{D2} * S_{CFP}(DA)]}$$

in which F_{AD} represents the total YFP emission with 430/25-nm excitation, and F_A represents the direct YFP emission with 500/20-nm excitation. In S_{CUBE}(SPECIMEN), CUBE indicates the filter cube (CFP, YFP, or FRET), and SPECIMEN indicates whether the cell is expressing donor (D, CFP), acceptor (A, YFP), or both (DA). $R_{D1} = (S_{FRET}(D))/(S_{CFP}(D))$, $R_{D2} = (S_{YFP}(D))/(S_{CFP}(D))$, and $R_{A1} = (S_{FRET}(A))/(S_{YFP}(A))$ are predetermined constants that require measurement of the bleed-through of the emission of only CFP- or YFP-tagged molecules into the FRET channel and the emission of only CFP-tagged molecules into the YFP channel.

3.2.6 Statistics

Student's t-test was used for statistical comparison, with probability $p<0.05$ as a significant difference. For comparison of multiple groups, One-way ANOVA with Newman-keuls was used.

3.3 Results

3.3.1 Colocalization of TRPV4 and TRPC1 in co-transfected HEK293 cells

Subcellular localization of TRPC1 and TRPV4 were examined in living HEK293 cells co-transfected with TRPC1 and TRPV4. TRPV4 was tagged with CFP, and TRPC1 was tagged with YFP. As shown in Figure 1, TRPV4 (Chapter 3 Figure 1A,

green) and TRPC1 (Chapter 3 Figure 1B, red) were localized both in cytosol and plasma membrane. There was very strong overlapping of TRPV4 and TRPC1 fluorescence as is apparent in merged images (Chapter 3 Figure 1C, yellow) and intensity profile of TRPV4-CFP and TRPC1-YFP (Chapter 3 Figure 1D). These data suggest that TRPV4 is co-localized with TRPC1 in co-transfected HEK293 cells. A fluorescence plasma membrane marker Di-8-ANEPPS was also used (Cheng *et al.*, 2007). In TRPV4-TRPC1 co-expressing cells, Di-8-ANEPPS fluorescence was found to significantly overlap with that of TRPV4-CFP in the plasma membrane (Chapter 3 Figure 2), confirming that some TRPV4 proteins were indeed localized in the plasma membrane.

3.3.2 Co-immunoprecipitation of TRPV4 and TRPC1 in co-transfected HEK293 cells

Co-immunoprecipitation was used to determine whether TRPV4 and TRPC1 are physically associated. Two antibodies for co-immunoprecipitation, one targeting against TRPC1 (Alomone Lab) and the other targeting against TRPV4 (Alomone Lab), were both reported to be highly specific (Maroto *et al.*, 2005;Yang *et al.*, 2006). This was verified in the present study by immunoblots, in which both antibodies recognized the expected band in HEK293 cells expressing respective genes (Chapter 3, Figure 3A and 3B). No band was observed if these antibodies were preabsorbed by excessive amount of respective peptide antigen (Chapter 3 Figure 3A and B). Co-immunoprecipitation experiments demonstrated that the anti-TRPC1 antibody was able to pull-down TRPV4 in the proteins lysates freshly prepared from TRPV4-TRPC1 co-expressing HEK293 cells (Chapter 3 Figure 4A). Furthermore, reciprocal co-immunoprecipitation demonstrated that the anti-TRPV4 antibody was also able to pull down TRPC1 (Chapter 3 Figure 4B). In control experiments, in which immunoprecipitation was performed with IgG purified from pre-immune serum, no band could be observed (Chapter 3 Figure 4A and B). These data indicate that TRPV4 indeed physically associates with TRPC1.

3.3.3 Fluorescence resonance energy transfer (FRET) in co-transfected HEK293 cells

FRET is a sensitive reporter of the proximity of two fluorophores, because distances closer than 10 nm between appropriate fluorophores are required to elicit FRET (Hofmann *et al.*, 2002). It provides a non-invasive means of monitoring the subunit assembly of ion channels and other proteins (Hofmann *et al.*, 2002;Qiu *et al.*, 2005). To measure steady-state FRET, cells transfected with different fusion proteins were imaged using epifluorescence microscope though CFP, YFP, and FRET filter channels. Strong FRET signal was detected in HEK293 cells that were co-expressed with CFP-tagged TRPV4 and YFP-tagged TRPC1 (Chapter 3 Figure 5), and in cells that were co-expressed with YFP-tagged TRPV4 and CFP-tagged TRPC1 (Chapter 3 Figure 5). In addition, strong FRET signal was detected in cells that were co-expressed with CFP-tagged TRPV4 and YFP-tagged TRPV4, and also in cells that were co-expressed with CFP-tagged TRPV4 and YFP-tagged TRPV4 (Chapter 3 Figure 5). These data strongly suggest that, when TRPV4 and TRPC1 were co-expressed, TRPV4 form heteromeric channels with TRPC1, and that when either TRPV4 or TRPC1 was expressed alone, homomeric channels were formed. Two negative control experiments were performed: 1) cells were co-transfected with CFP and YFP (without attaching to TRP channels); 2) cells were co-transfected with CFP-tagged TRPV4 and YFP-tagged GirK4. GirK is an inward rectifying K^+ channel bearing no similarity to TRP channels. No FRET signal was detected in both negative controls (Chapter 3 Figure 5). On the other hand, in cells that were co-expressed with the CFP-YFP concatemer, a positive control for FRET, significant FRET signals could be observed (Chapter 3 Figure 5).

3.3.4 The requirement of both N- and C-terminal domains for TRPV4 and TRPC1 channel assembly

Ample amount of evidence suggests that TRP channels interact with other TRP isoforms through N-terminal or C-terminal cytoplasmic domain (Hellwig *et al.*, 2005). Therefore, we made cDNA constructs with either N-terminal or C-terminal deletion

for both TRPC1 and TRPV4. Then we determined whether a particular deletion could abolish the interaction between TRPV4 and TRPC1 using FRET assay. Information on the topology of TRPV4 and TRPC1 was provided by previous publications (Dohke *et al.*, 2004;Nilius *et al.*, 2004). Our experimental results indicate that deletion of either N-terminal or C-terminal cytoplasmic domain of TRPC1 abolished the interaction of TRPC1 with TRPV4 (Chapter 3 Figure 6). In addition, deletion of either N-terminal or C-terminal cytoplasmic domain of TRPV4 also abolished the interaction (Chapter 3 Figure 6). In other words, C-terminal and N-terminal domains of both channels are required for their interaction. The requirement of both N- and C-terminal domain for TRP channel assembly are not very surprising, because other studies also had similar findings before (for TRPV1, (Hellwig *et al.*, 2005)). We also found that only N-terminus (but not C-terminus) is required for TRPV4 self-assembly (data not shown).

3.4 Discussion and conclusion

With the use of fluorescence resonance energy transfer (FRET), co-immunoprecipitation and subcellular colocalization methods, it was found that TRPC1 interacts physically with TRPV4 to form a heteromeric channel complex. In addition, our experimental results indicate that C-terminal and N-terminal domains of both channels are required for their interaction.

The results from the present study provided some clue as to how TRPV4 and TRPC1 interact with each other. FRET data suggest that TRPV4 interacts directly with TRPC1 without the presence of a third protein between them. Two possibilities exist: 1) TRPV4 may coassemble with TRPC1 to form heterotetrameric channels. Heteromeric assembly across different TRP subfamilies has been reported between TRPC1 and TRPP2 (Bai *et al.*, 2008) and between TRPV4 and TRPP2 (Kottgen *et al.*, 2008). 2) TRPV4 and TRPC1 may each form homotetrameric channels, and two homotetrameric channels then interact with each other through their N- or C-terminus.

The fluorescent proteins CFP and YFP have previously been shown to function as a FRET pair with a characteristic distance for 50% transfer efficiency of approximately 50 Å (Miyawaki *et al.*, 1997), which makes them optimal for reporting the presence of two fluorescently tagged subunits in the same channel (Zheng *et al.*, 2002). These evidences suggest that the pore regions of TRPC1 and TRPV4 are closely appositioned to each other, likely forming heterotetrameric channels sharing a common pore, similar to the reported heterotetrameric channels of TRPP2-TRPC1 (Bai *et al.*, 2008). Our experimental results also demonstrated that deletion of either N-terminal or C-terminal cytoplasmic domain of TRPC1 abolished the interaction of TRPC1 with TRPV4. In addition, deletion of either N-terminal or C-terminal cytoplasmic domain of TRPV4 also abolished the interaction.

In conclusion, in the present study, we demonstrated that TRPC1 interacts physically with TRPV4 to form a heteromeric channel complex in which C-terminal and N-terminal domains of both channels are required for their interaction.

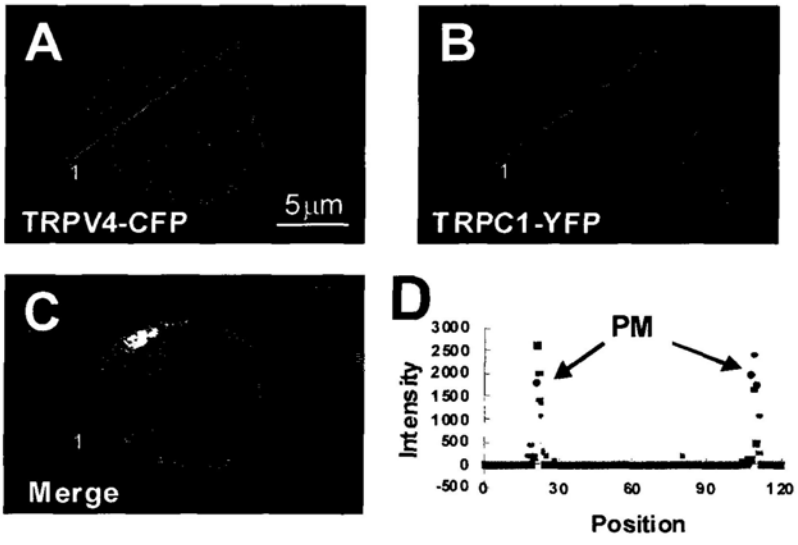

Chapter 3 Figure 1. Subcellular colocalization of TRPV4 and TRPC1 in heterologously expressed HEK cells. A-D, colocalization of TRPV4-CFP (A, green peusdocolor) and TRPC1-YFP (B, red peusdocolor) in a co-expressing cell. C, overlay image of CFP/YFP; D, fluorescence intensity of TRPV4-CFP and TRPC1-YFP along the red marked line in A and B. PM stands for plasma membrane. Representatives of 10-36 individual cells from 4 experiments.

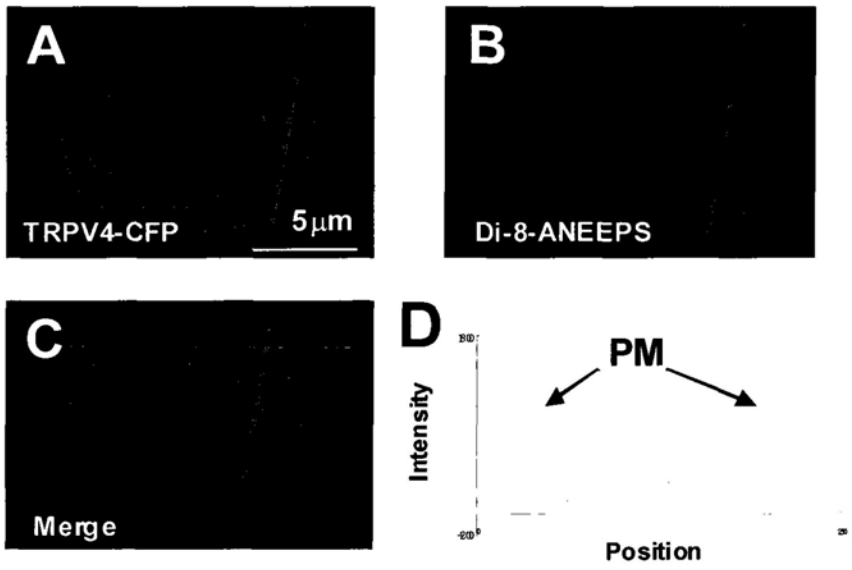

Chapter 3 Figure 2. Co-localization of TRPV4 and di-8-ANEPPS in TRPV4-TRPC1 co-expressing HEK cells. Representative images from TRPV4-TRPC1 co-expressing cells. A-D, Co-localization of di-8-ANEPPS, a plasma membrane marker fluorophore (B, red), and TRPV4-CFP (A, green). C, overlay image of A and B; D, fluorescence intensity of di-8-ANEPPS and TRPV4-CFP along the red marked line in A and B. PM stands for plasma membrane. Representatives of 10-36 individual cells from 4 experiments.

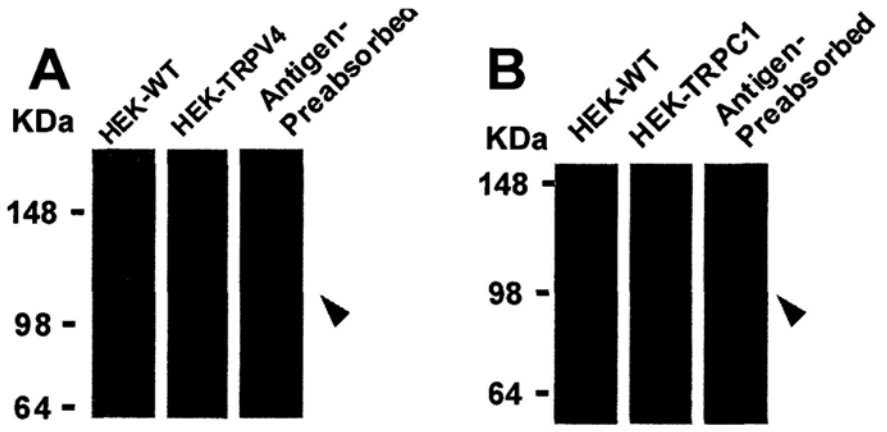

Chapter 3 Figure 3. Immunoblots showing the specificity of antibodies to their respective targets. HEK cells were transfected with TRPV4 (A) or TRPC1 (B). The extracted proteins were immunoblotted with anti-TRPV4 (Alomone Lab) (A), anti-TRPC1 (Alomone Lab) (B). Wild-type HEK cells were used a control. n = 3-4 for all experiments.

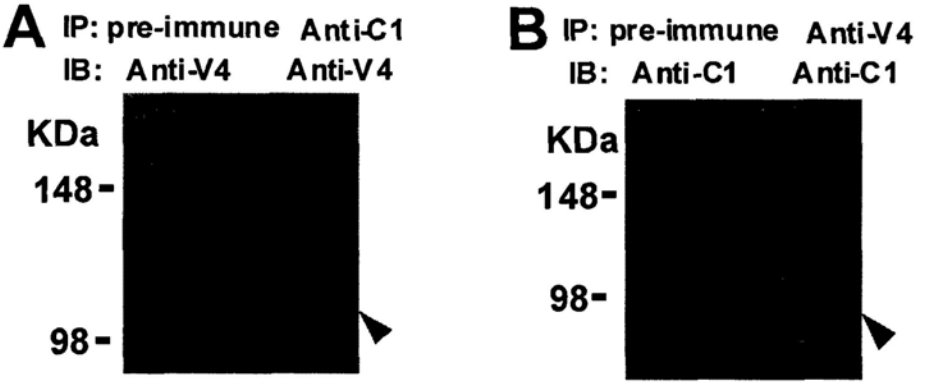

Chapter 3 Figure 4. Co-immunoprecipitation of TRPV4 and TRPC1 in heterologously expressed HEK cells. The pulling antibody and the blotting antibody were indicated in the figure. Control immunoprecipitation was done using the preimmune IgG (labeled as pre-immune). IP, immunoprecipitation; IB, immunoblot; anti-V4, anti-TRPV4; anti-C1, anti-TRPC1. n = 3-4 experiments.

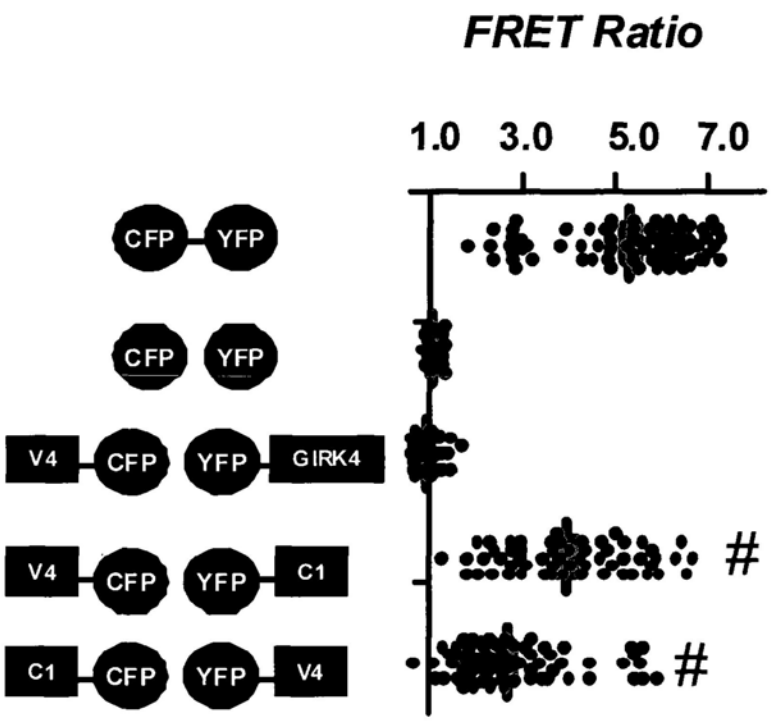

Chapter 3 Figure 5. FRET detection by three-cube FRET in transfected HEK cells. Horizontal axes indicate FRET ratio (FR) of living cells expressing indicated constructs. Each point represents the FRET ratio of a single cell. The red lines and error bars indicate the average FR values and standard error. FR= 1, no FRET. FR> 1, having FRET. Mean ± SE (n = 50-81). #, P< 0.001 compared to negative control.

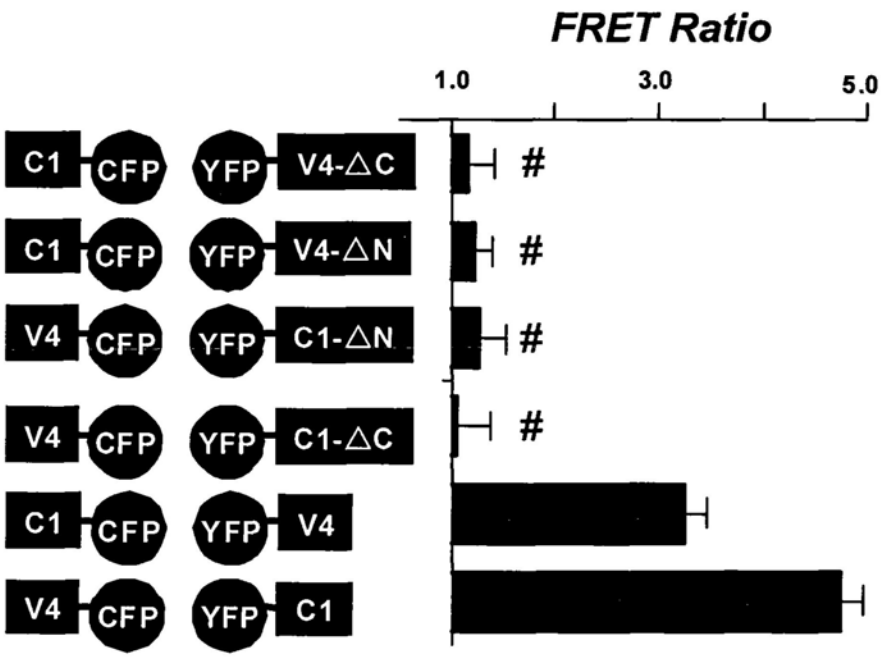

Chapter 3 Figure 6. FRET detection by three-cube FRET system in transfected HEK cells. Horizontal axes indicate FRET ratio (FR) on living cells expressing indicated constructs. FR = 1, no FRET. FR > 1, having FRET. Mean ± SE (n = 17-89). △N or △C represents YFP-tagged construct with deletion at N- or C- terminus of either TRPC1 or TRPV4. #, $P<0.001$ compared to C1-CFP plus V4-YFP.

Chapter 4

Basic electrophysiological properties of TRPV4-TRPC1 heteromeric channel

4.1 Introduction

TRPV4 is a Ca^{2+}-permeable nonselective cation channel of the vanilloid-type transient receptor potential channel subfamily (Nilius et al., 2004). TRPV4 can be polymodally activated by hypotonic cell swelling, moderate heat, arachidonic acid and its metabolite epixyeicosatrienoic acids (EETs), synthetic phorbol ester 4α-phorbol 12,13-didecanoate (4α-PDD) (Nilius et al., 2004); (Plant and Strotmann, 2007a). TRPV4 is also involved in the flow sensation. TRPV4 is activated by flow shear stress in TRPV4-overexpressing HEK293 cells and native renal epithelial cells (Gao *et al.*, 2003;Wu *et al.*, 2007). Importantly, there is convincing evidence that TRPV4 is involved in the endothelium-dependent vascular dilation to flow (Hartmannsgruber et al., 2007;Kohler et al., 2006).

In the chapter 3, based on the results from fluorescence resonance energy transfer (FRET), co-immunoprecipitation and subcellular colocalization methods, I have suggested that TRPC1 can interact physically with TRPV4 to form a complex. Similar heterotetrameric channels have been reported previously by others. One example is the heteromeric channels of TRPP2-TRPC1 (Bai et al., 2008;Tsiokas et al., 1999).

In this chapter, I will examine some basic electrophysiological properties of this TRPV4-TRPC1 heteremeric channels, with special emphasis on the channel pore properties including permeability ratio to different cations, I-V curve rectification, and voltage-dependent block of extracellular Ca^{2+} (Voets *et al.*, 2002a). Our data show that TRPV4-TRPC1 heteromeric channel has distinct properties that are different

(although not drastically different) from homomeric TRPV4 channels with regard to I-V relationships, kinetics of cation current, permeability ratio to different cations and and voltage-dependent block by extracellular Ca^{2+}.

4.2 Materials and methods

4.2.1 Cell culture

All animal experiments were conducted in accordance with the regulation of the U.S. National Institute of Health (NIH publication No.8523). HEK293 cells were cultured in DMEM supplemented with 10% FBS, 100 μg/ml penicillin and 100 U/ml streptomycin.

4.2.2 Cloning and transfection

Mouse TRPV4 gene (NM_022017), $TRPV4^{M680D}$ was a gift from Dr. Bernd Nilius, Belgium. Human TRPC1 cDNA (NM_003304) was obtained by RT-PCR from human coronary endothelial cells CC2585 (BioWhittaker). TRPC1Δ567-793 and $TRPC1^{Mut\text{-}pore}$ were gifts from Dr. Indu Ambudkar, NIH, USA.

Transfection condition was as described elsewhere. Briefly, HEK293 cells were transfected with various constructs using Lipofectamine 2000. Abound 6×10^4 HEK293 cells were grown in each well of the 6-well plates. Transfection was done with 4 μg plasmid and 6 μl Lipofectamine 2000 in 200 μl Opti-MEM reduced serum medium in 6-well plates. Functional studies were performed 2-3 days post-transfection.

4.2.3 FRET detection and subcellular localization of TRPV4-CFP/TRPC1-YFP

CFP (or YFP)-tagged TRPV4 and YFP (or CFP)-tagged TRPC1 were co-transfected into these cells. FRET signals were detected as described elsewhere (Qiu et al., 2005). Briefly, an inverted microscope equipped with three-cube FRET filters and CCD camera was used to measure FRET. Three-cube FRET filter cubes were listed as follows (excitation; dichroic; emission): YFP (S500/20 nm; Q515lp;

S535/30 nm); FRET (S430/25 nm; 455dclp; S535/30 nm); and CFP (S430/25 nm; 455dclp; S470/30 nm). Average background signal was subtracted. FRET ratio (FR) was calculated by the following equation:

$$FR = \frac{F_{AD}}{F_A} = \frac{[S_{FRET}(DA) - R_{D1} * S_{CFP}(DA)]}{R_{A1} * [S_{YFP}(DA) - R_{D2} * S_{CFP}(DA)]}$$

in which F_{AD} represents the total YFP emission with 430/25-nm excitation, and F_A represents the direct YFP emission with 500/20-nm excitation. In S_{CUBE}(SPECIMEN), CUBE indicates the filter cube (CFP, YFP, or FRET), and SPECIMEN indicates whether the cell is expressing donor (D, CFP), acceptor (A, YFP), or both (DA). R_{D1} = (S_{FRET}(D))/(S_{CFP}(D)), R_{D2} = (S_{YFP}(D))/(S_{CFP}(D)), and R_{A1} = (S_{FRET}(A))/(S_{YFP}(A)) are predetermined constants that require measurement of the bleed-through of the emission of only CFP- or YFP-tagged molecules into the FRET channel and the emission of only CFP-tagged molecules into the YFP channel.

4.2.4 Preparation of T1E3 and preimmune IgG

T1E3 antibody was raised in rabbits using the strategy developed by Xu *et al* (Xu and Beech, 2001). Briefly, a peptide corresponding to TRPC1 putative pore-region (CVGIFCEQQSNDTFHSFIGT) was synthesized and conjugated to keyhole limpet hemocyanin (KLH) at Alpha Diagnostic International (USA). The coupled T1E3 peptide (0.5 mg) was injected into the ear vein of a rabbit (day 0), followed by two boost doses at day 21 and day 42 respectively. Antiserum was collected four weeks after the second boost. Immunoglobin G was purified from the T1E3 antiserum using a HiTrap Protein G column (GE Healthcare). For control, pre-immune serum was purified with a HiTrap Protein G column to obtain the immunoglobin G, and then was used in experiments. The applied T1E3 and preimmune IgG were of similar protein quantities in order to balance possible osmotic effect.

In antigen preabsorption control, T1E3 was preabsorbed with excessive amount of peptides (16 μg peptide per μg T1E3) for 2.5 hr at room temperature in PBS with 1% BSA.

4.2.5 Whole-cell patch clamp

As previous report (Voets *et al.*, 2002b), whole cell membrane currents were monitored with an EPC-9 (HEKA Elektronik, Lambrecht, Germany; 8-Pole Bessel filter, 2.9 kHz) using ruptured patches. Patch electrodes had a DC resistance between 2 and 4 mΩ when filled with intracellular solution. An Ag-AgCl wire was used as a reference electrode. Capacitance and access resistance were monitored continuously. Between 50 and 70% of the series resistance was electronically compensated to minimize voltage errors. Unless mentioned otherwise, we have applied a ramp protocol consisting of a 20-ms voltage step to −100 mV followed by a 380-ms linear ramp to +100 mV. This protocol was repeated every 5 s. The currents were sampled at 1.25 kHz. The time course of the whole cell current and current densities were obtained by averaging the current in a narrow window around −80 mV during the voltage ramp protocol. All of the experiments were performed at room temperature (20–23 °C).

As previous report (Voets *et al.*, 2002b), the standard extracellular solution contained 150 mm NaCl, 1 mm $MgCl_2$, 5 mm $CaCl_2$, 10 mm glucose, 10 mm HEPES, buffered at pH 7.4 with NaOH. When indicated in the figure legends, the Ca^{2+} concentration of this solution was varied between 0 and 30 mm. To study the relative permeability of mono- and divalent cations, we used extracellular solutions containing 1 mm $MgCl_2$, 10 mm glucose, 10 mm HEPES, and either 150 mm XCl (where X = sodium, cesium, or potassium) or 30 mm $CaCl_2$ and 120 N-methyl-d-glucamine chloride. These solutions were titrated to pH 7.4 with the appropriate base. Two different intracellular solutions were used yielding virtually identical results after correcting for the liquid junction potential. The cesium-based solution contained 20 mmCsCl, 100 mm cesium aspartate, 1 mm$MgCl_2$, 4 mm Na_2ATP, 0.022 mm $CaCl_2$, 10 mm BAPTA, 10 mm HEPES, pH adjusted to 7.2 with CsOH. The sodium-based solution contained 150 mm NaCl, 1 mm$MgCl_2$, 4 mm Na_2ATP, 0.037 mm $CaCl_2$, 5 mm EGTA, 10 mm HEPES, pH adjusted to 7.2 with NaOH. Free intracellular Ca^{2+}

was calculated to be ~1 nm for both solutions. The specific TRPV4 activator 4α-PDD was applied to the extracellular solution at a concentration of 5 μmol/L.

4.2.6 Cell-attached single channel patch clamp

Cell-attached single channel currents were monitored with an EPC-9 (HEKA Elektronik, Lambrecht, Germany) as described elsewhere (Watanabe *et al.*, 2003). Single-channel currents were sampled at 200- and 500-s intervals and filtered at 2 and 1 kHz for HEK-293 cells. The pipette solution contained (in mM): 150 NaCl, 1 MgCl2, 10 Na-HEPES pH 7.4 and the bath solution was 150 KCl, 5 MgCl2, 10 HEPES, 10 glucose (pH adjusted to 7.4 with KOH). The recordings were made before and after 4α-PDD (5 μmol/L) application.

4.2.7 Statistics

Student's t-test was used for statistical comparison, with probability $p<0.05$ as a significant difference. For comparison of multiple groups, One-way ANOVA with Newman-keuls was used.

4.3 Results

4.3.1 Determination of subunit coassembly using FRET.

The fluorescent proteins CFP and YFP have previously been shown to function as a FRET pair with a characteristic distance for 50% transfer efficiency of approximately 50 Å ((Miyawaki et al., 1997); (Patterson et al., 2000)) which makes them optimal for reporting the presence of two fluorescently tagged subunits in the same channel (Zheng *et al.*, 2002). In chapter 3, I have shown the heteromeric assembly of TRPV4 and TRPC1 in cells coexpressed with TRPV4 and TRPC1 (Ma *et al.*, 2010). Here, HEK cells were transfected either TRPV4 or TRPC1 clone. Positive FRET signals were detected in both types of cells, suggesting that TRPV4 and TRPC1 can each form homomeric channels. Therefore, in HEK cells co-transfeted with TRPV4 and TRPC1, three types of channels may be formed: TRPV4-TRPC1

heteromeric channels, TRPC1 homomeric channels and TRPV4 homomeric channels.

4.3.2 Cation current kinetics, I-V relationship, and ratio of heteromeric TRPV4-TRPC1 vs. homomeric TRPV4 channels

4.3.2.1 Kinetics of cation current

In order to provide evidence for the formation of functional heteromeric channels, whole-cell patch clamp was used. A TRPV4-specific agonist 4α-PDD (5 μmol/L) activated a transient cation current in TRPV4-expressing HEK cells (Chapter 4 Figure 2) with a decay t/1/2 of 41 ± 4 sec (n = 14). Interestingly, TRPC1 co-expression markedly slowed down the decay phase of 4α-PDD-stimulated current transient (Chapter 4 Figure 2). 4α-PDD-stimulated cation current was inhibited by ruthenium red (5 μmol/L) (Chapter 4 Figure 2), confirming a requirement for TRPV. As controls, this current was absent in wild-type HEK cells (Chapter 4 Figure 2) and in HEK cells only overexpressed with TRPC1 (Chapter 4 Figure 2).

4.3.2.2 Whole-cell and single-channel I/V relationship

To provide further evidence for the formation of functional heteromeric channels, whole-cell and cell-attached single channel patch clamp were performed. In whole-cell patch clamp, current-voltage (I-V) relation measured from TRPV4 and -C1 coexpressing cells was distinct from that of TRPV4 expressing cells (Chapter 4 Figure 2). Single channel slope conductance was estimated based on I-V curve of single channel currents. The conductance was ~78 pS for inward currents and ~95 pS for outward currents for TRPV4-TRPC1 heteromeric channels, and ~63 pS and ~85 pS for TRPV4 homomeric channels (Chapter 4 Figure 3). These data support the notion that TRPV4 and TRPC1 coexpression produces a dictinct TRPV4-TRPC1 heteromeric channels.

4.3.2.3 Ratio of heteromeric TRPV4-TRPC1 vs. homomeric TRPV4 channel

As the strategy described in Chapter 4 Figure 4, because 4α-PDD is TRPV4-specific agonist which lack effect on TRPC1 homotretramer, we can rule out the participation of TRPC1 homotretramer, thus we can explore the ratio of TRPV4-TRPC1 heterotretramers vs. TRPV4 homotretramers in TRPV4-TRPC1 co-expressing HEK cells.

First, we used a polyclonal anti-TRPC1 antibody T1E3, which can plug the pore of TRPC1 channel (Xu *et al.*, 2001). Pre-incubation with T1E3 (1:100) for 1 hr at 37°C diminished the 4α-PDD-stimulated whole cell cation current (Chapter 4 Figure 4) in TRPV4-TRPC1 co-expressing HEK293 cells. The blocking effect on cation current was absent if T1E3 was preabsorbed by excessive amount of peptide antigen (Chapter 4 Figure 4). The specificity of T1E3 was verified by immunoblot and patch clamp studies. In immunoblots, T1E3 recognized the expected band in TRPC1-expressing HEK293 cells (Chapter 4 Figure 8). In patch clamp study, T1E3 had no direct action on TRPV4 homomeric channels, indicated by lack of action of T1E3 on 4α-PDD-elicited cation current in TRPV4-expressing HEK293 cells (Chapter 4 Figure 8).

Then we used two dominant-negative constructs of TRPC1, TRPC1Δ567-793 and $TRPC1^{Mut\text{-}pore}$. TRPC1Δ567-793 has deletion at TRPC1 pore region, whereas $TRPC1^{Mut\text{-}pore}$ carries several point mutations in TRPC1 pore region. Both mutants are able to coassemble with wild-type TRPC1 subunits to form multimeric complex, thereafter disrupting the function of TRPC1, thus exerting dominant-negative function (Liu et al., 2005). In the present study, co-transfection of TRPV4 with either TRPC1Δ567-793 or $TRPC1^{Mut\text{-}pore}$ each abolished 4α-PDD-stimulated whole cell cation current (Chapter 4 Figure 4). Taken together, these data support that TRPV4 and TRPC1 coassemble to form a functional heteromeric channels.

Interestingly, all three treatments, including T1E3 and two dominant negative constructs of TRPC1, each reduced the 4α-PDD-stimulated whole cell cation by a simlar degree, which was ~80% (Chapter 4 Figure 4).

4.3.3 Mono- and divalent cations permeability

Relative permeability of different channel complexes to Na^+, K^+ and Ca^{2+} was estimated based on reverse potential measurement of 4α-PDD-stimulated cation current using equation established by others (Voets *et al.*, 2002b). Similar to the previous report (Voets *et al.*, 2002b), TRPV4 is moderately selective for Ca^{2+} over Na^+ ions with permeability ratio of $P_{Ca}:P_K:P_{Cs}:P_{Na}$ = *7.1:1.4:1.2:1.* Compared to TRPV4 homomeric channels, TRPV4-TRPC1 heteromeric channel was slightly more permeable to Ca^{2+} but had similar permeability to monovalent cations with permeability ratio of $P_{Ca}:P_K:P_{Cs}:P_{Na}$ = *9.2:1.4:1.2:1* (Chapter 4 Figure 5 and 6).

We used a TRPV4 mutant $TRPV4^{M680D}$, which has point mutation at a crucial position within the putative pore region of TRPV4. Reversal potential measurement shows that changing of extracellular medium from NaCl to CaCl2 caused a drastic leftward shift of the reversal potential in $TRPV4^{M680D}$-expressing cells. These results are consistent with those in a previous report (Voets *et al.*, 2002b), supporting that $TRPV4^{M680D}$ had very low Ca^{2+} permeability (PCa/PNa values <<1) (Chapter 4 Figure 5 and 6) and that Met680 is a crucial amino acid controlling Ca selectivity in TRPV4 homomeric channels. Furthermore, in cells co-expressed with TRPC1 and $TRPV4^{M680D}$, changing of extracellular medium from NaCl to CaCl2 caused even more drastic leftward shift of the reversal potential. These data suggest that Met680 is also a very crucial amino acid controlling Ca selectivity in TRPV4-TRPC1 heteromeric channels. On the other hand, mutation at M680 had no significant effect on the relative permeability to monovalent cations (K^+ and Cs^+) both in TRPV4 homomeric channels and TRPV4-TRPC1 heteromeric channels (Chapter 4 Figure 5 and 6).

4.3.4 Ca^{2+}-dependent rectification of whole-cell I-V curve

The whole-cell I-V relationship for TRPV4-expressing cells bathed in "physiological" concentrations of mono- and divalent cations showed slight rectification (Chapter 4 Figure 7A). However, the shape of I-V curve strongly

depends on the extracellular Ca^{2+} concentration. In the absence of divalent cations, the current-voltage relation is linear with identical current amplitudes at +100 and -100 mV. Increasing concentrations of Ca^{2+} caused an inhibition of the current, which was more pronounced at negative potentials (Chapter 4 Figure 7), characteristic of a voltage-dependent block. However, similar to the previous report (Voets *et al.*, 2002b), the inward current could not be completely blocked by extracellular Ca^{2+} even when its concentrations reached up to 30 mM (Chapter 4 Figure 7), presumably because Ca^{2+} itself permeates the channel. The whole-cell I-V relationship was also studied in cells that were co-expressed with TRPV4 and TRPC1. Similar to TRPV-overexpressing cells, the TRPV4-TRPC1 coexpressing cells also displayed a straight I-V curve without apparent rectification when the cells were bathed in "physiological" concentrations of mono- and divalent cations. However, voltage-dependent inhibition by extracellular Ca^{2+} was markedly reduced in TRPV4-TRPC1 co-expressing cells when compared to TRPV4-expressing cells (Chapter 4 Figure 7B-D).

4.4 Discussion and conclusion

It is well-recognized that a specific TRP subunit may co-assemble with a different TRP subunit to form a heteromeric channel (Hofmann et al., 2002;Strubing et al., 2001). The heretomeric coassembly usually occurs between the members within the same subfamily (Hofmann et al., 2002;Strubing et al., 2001), but occationally also occurs between the members across different TRP subfamilies (Bai *et al.*, 2008). In chapter 3, I presented biochemical evidence, including co-immunoprecipitation and FRET, that TRPV4 could coassemble with TRPC1 to form a complex when they were co-expressed in HEK cells. In this chapter, I used patch clamp to study the whole-cell current of TRPV4-TRPC1-coexpressing HEK cells. Compared to TRPV4-expressing cells, TRPV4-TRPC1-coexpressing cells displayed a slower decay in whole-cell current, slightly increased Ca^{2+} permeability, a markedly reduced inhibition of inward current by extracellular Ca^{2+}. Majority of cell-attached patches from

TRPV4-TRPC1-coexpressing cells showed a slightly increased single channel slope conductance compared to those of TRPV4-expressing cells. These data indicate that heterologous expression of TRPV4 and TRPC1 can produce functionally distinct TRPV4-TRPC1 heteromeric channel.

When TRPV4 and TRPC1 are over-expressed in HEK cells, multiple channels may form, which include homomeric TRPV4, homomeric TRPC1 and heretemeric TRPV4-TRPC1 complex. Indeed, FRET studies (Figure 5.1) unequivocally demonstrated the existence of homomeric TRPV4, homomeric TRPC1, and heretemeric TRPV4-TRPC1 complex in overexpressed HEK cells. In this chaper, we used 4α-PDD to study the whole-cell current mediated by TRPV4-TRPC1 heteromeric channels. From figures 5.2 and 5.4, it is apparent that 4α-PDD can activate both TRPV4 homomeric channels and TRPV4-TRPC1 heteromeric channels. An important concern is the relative contribution of TRPV4 homomeric channels *vs.* TRPV4-TRPC1 heteromeric channels toward the whole-cell current in TRPV4-TRPC1 co-expressing cells. If there is a large contribution of TRPV4 homomers toward the overall 4α-PDD-stimulated whole-cell current, then it will not be justified to use 4α-PDD-stimulated whole-cell current as a functional index for TRPV4-TRPC1 heteromeric channels. In this regard, I utilized three different tools, an anti-TRPC1 blocking antibody and two dominant negative constructs of TRPC1, each of which is expected to interfere with the function of TRPV4-TRPC1 heteromers but not TRPV4 homomers. Interestingly, all three treatments reduced the 4α-PDD-stimulated whole-cell current by similar larger margin, which is ~80% (Chapter 4 Figure 4). Thus, I could estimate that the number of TRPV4-TRPC1 complex should surpass that of TRPV4 homomers by a larger margin with estimated ratio of at least 4:1. This ratio might be underestimated because none of these treatments is expected to fully abolish TRPV4-TRPC1-mediated current. Based on these evidences, I can reasonably use 4α-PDD-stimulated whole-cell current as functional index to study TRPV4-TRPC1 heteromeric channels in TRPV4-TRPC1 co-expressing cells.

TRPV1, TRPV2, and TRPV4 are only weakly Ca^{2+}-selective with PCa/PNa values below 10 (Caterina *et al.*, 1999;Caterina *et al.*, 1997;Liedtke *et al.*, 2000;Nilius *et al.*, 2001;Strotmann *et al.*, 2000;Watanabe *et al.*, 2002) and their monovalent cation permeability sequences are more indicative of a weak field strength binding site (Caterina *et al.*, 1999;Caterina *et al.*, 1997;Liedtke *et al.*, 2000;Nilius *et al.*, 2001;Strotmann *et al.*, 2000;Watanabe *et al.*, 2002). Previous evidences (Voets et al., 2002b) indicate that Met^{680} is crucial for the proper functioning of the TRPV4 pore. Introducing a negative charge at this position (mutant M680D) causes a further reduction of the current density and a complete loss of Ca^{2+} permeation. One possible explanation is that this additional negative charge on top of its usual negative charged amino acid at position 682 enhances the affinity of the Ca^{2+}-binding site to such an extent that it can no longer permeate the channel. In the present study, we found that convertion of Met680 to aspartic acid (D) also caused a drastic changes in the Ca^{2+} permeability in TRPV4-TRPC1 co-expressing HEK cells. These data suggest that Met^{680} is not only crucial for the proper functioning of the TRPV4 pore, but also for the proper functioning of the TRPV4-TRPC1 pore.

In conclusion, with the use of FRET and patch clamp studies we have demonstrated that heterologous expression of TRPV4 and TRPC1 can produce functional TRPV4-TRPC1 heteromeric channel. TRPV4-TRPC1 heteromeric channels display distinct channel properties with regard to its kinetics of cation current, permeability ratio to different cations, and voltage-dependent block by extracellular Ca^{2+}.

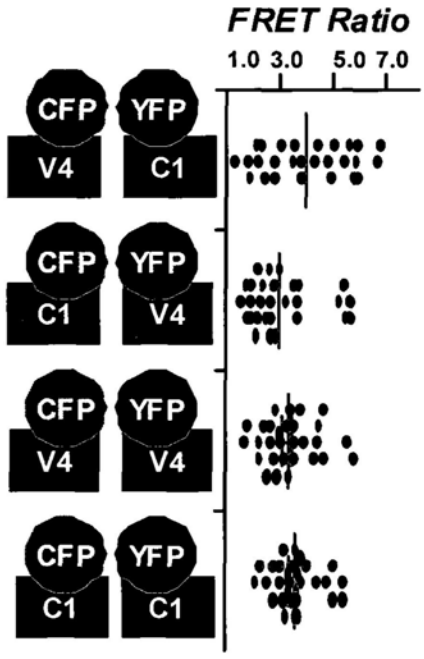

Chapter 4 Figure 1. FRET detection by three-cube FRET in transfected HEK cells. Horizontal axes indicate FRET ratio (FR) of living HEK cells expressing indicated constructs. Each point represents the FRET ratio of a single cell. Error bars indicate the average FR values and standard error. FR= 1, no FRET. FR> 1, having FRET. Mean ± SE (n = 30-35).

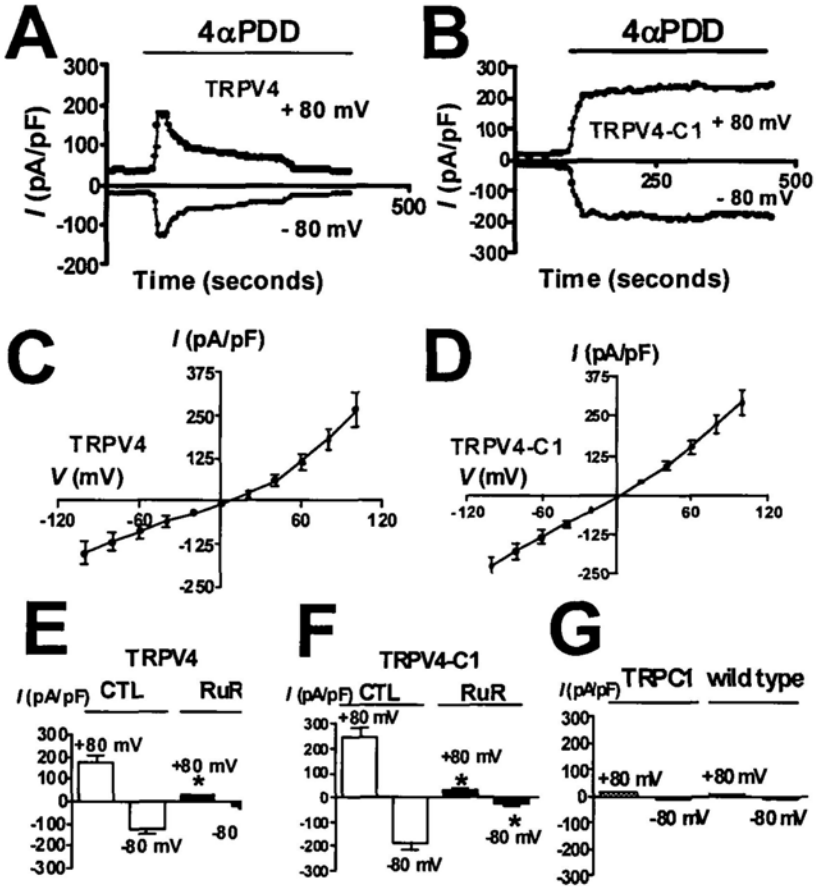

Chapter 4 Figure 2. Whole-cell current voltage relationship of 4α-PDD-stimulated cation current in TRPV4-expressing and TRPV4-TRPC1 co-expressing HEK cells. A and B, representative time course of 4α-PDD-stimulated whole cell current at ± 80 mV in TRPV4-expressing (A) and TRPV4-TRPC1 co-expressing (B) HEK cells. Cells were clamped at 0 mV. Whole cell currents were recorded in response to successive voltage pulses of +80 mV and -80 mV for 100 ms duration. These current values were then plotted *vs.* time. Solid bar on top of the traces indicates the time period when 4α-PDD (5 μmol/L) was applied. C and D, current voltage relationship taken at the time points shown in A (as in C) and B (as in D). Mean ± SE (n = 4-5 patches). E, F and G, summary for the peak whole cell current in response to 4α-PDD. WT, wild-type HEK cells; TRPC1, TRPC1-expressing HEK cells; Ctl, control; RuR, 5 μmol/L ruthenium red. Values are Mean ± SE (n = 5 to 11). #, P<0.05 compared to control. *, P<0.05 compared to the cells transfected with TRPV4 alone.

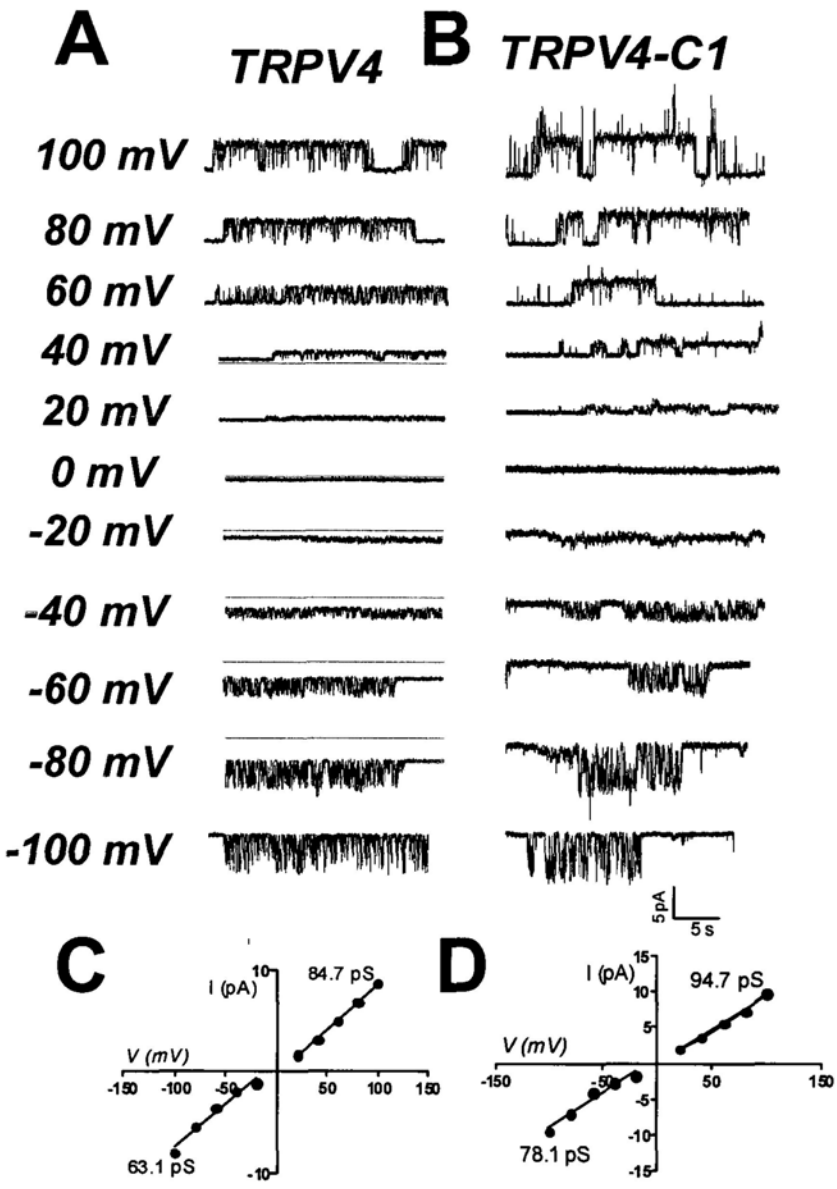

Chapter 4 Figure 3. Cell-attached current voltage relationship of 4α-PDD-stimulated cation current in TRPV4-expressing and TRPV4-TRPC1 co-expressing HEK cells. A and B, representative time course of 4α-PDD-stimulated cell-attached current in TRPV4-expressing (A) and TRPV4-TRPC1 co-expressing (B) HEK cells. C and D, the averaged data indicate a single-channel conductance of TRPV4-expressing (C) and TRPV4-TRPC1 co-expressing HEK cells (D). Mean ± SE (n = 4-5 patches).

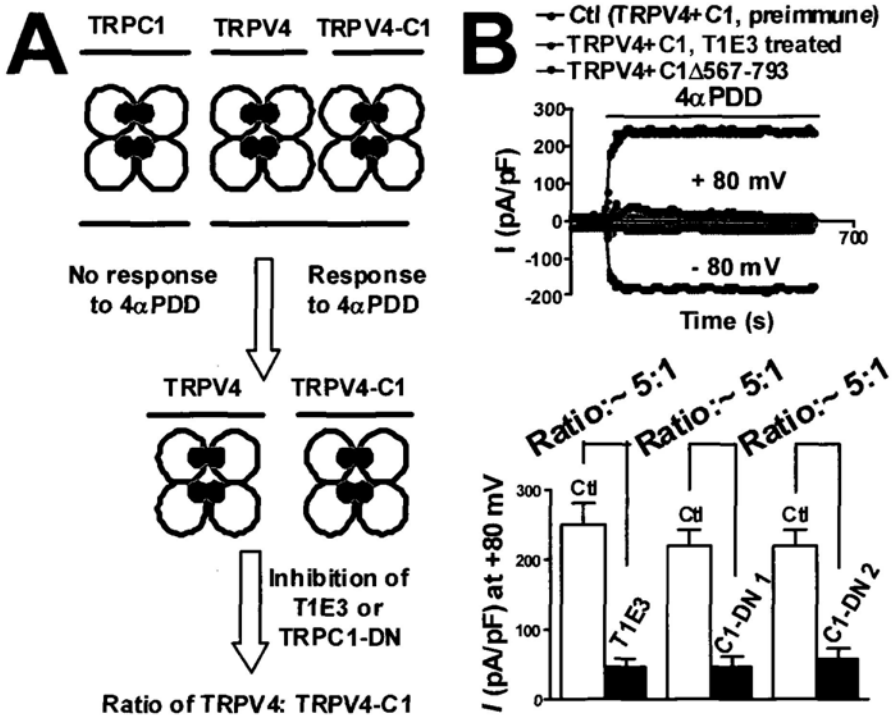

Chapter 4 Figure 4. Determination the ratio of TRPV4-TRPC1 heteromeric channel:TRPV4 homomeric channel in TRPV4-TRPC1 coexpressed HEK cells with T1E3, TRPC1Δ567-793 and TRPC1$^{Mut\text{-}pore}$. **A,** Diagram shown the strategy of determination the ratio of TRPV4-TRPC1 heteromeric channel:TRPV4 homomeric channel in TRPV4-TRPC1 coexpressed HEK cells with T1E3, TRPC1Δ567-793, TRPC1$^{Mut\text{-}pore}$. B and C, Representative traces (B) and summary (C) shown effect of T1E3, TRPC1Δ567-793 and TRPC1$^{Mut\text{-}pore}$ on 4α-PDD-stimulated cation current in HEK cells. Cells were co-transfected with TRPV4 and TRPC1. For those labeled as TRPV4+C1Δ567-793 and TRPV4+C1$^{Mut\text{-}pore}$ cells were co-transfected with TRPV4 plus TRPC1Δ567-793 or TRPV4 plus TRPC1$^{Mut\text{-}pore}$. For T1E3 experiments, cells were pre-incubated with T1E3 (1:100) or preimmune IgG (1:100, as control) for 1 hr at 37°C. C1-DN-1 stands for TRPC1Δ567-793; C1-DN-2 stands for TRPC1$^{Mut\text{-}pore}$. Values are Mean ± SE (n = 5-18). #, P<0.05 compared to control.

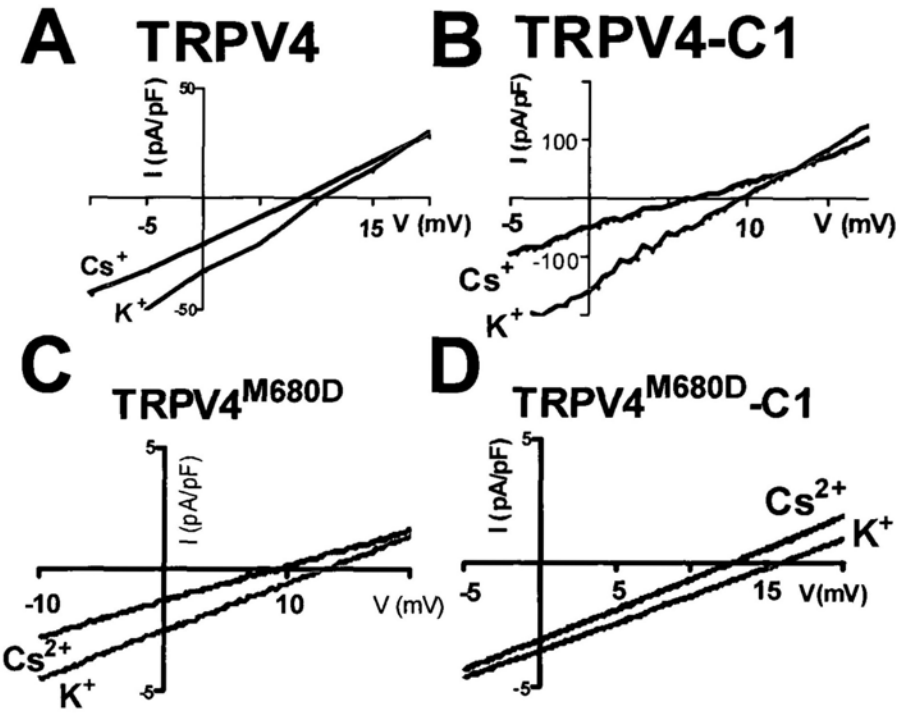

Chapter 4 Figure 5. Monovalent permeability sequence in TRPV4-expressing and TRPV4-TRPC1 co-expressing HEK cells. A-D, the monovalent currents through TRPV4 (A), TRPV4-TRPC1 (B), $TRPV4^{M680D}$(C) and $TRPV4^{M680D}$-TRPC1 (D) in extracellular solutions containing 150 mM of the indicated monovalent cation as sole charge carrier are shown. Representatives of 6-7 individual cells.

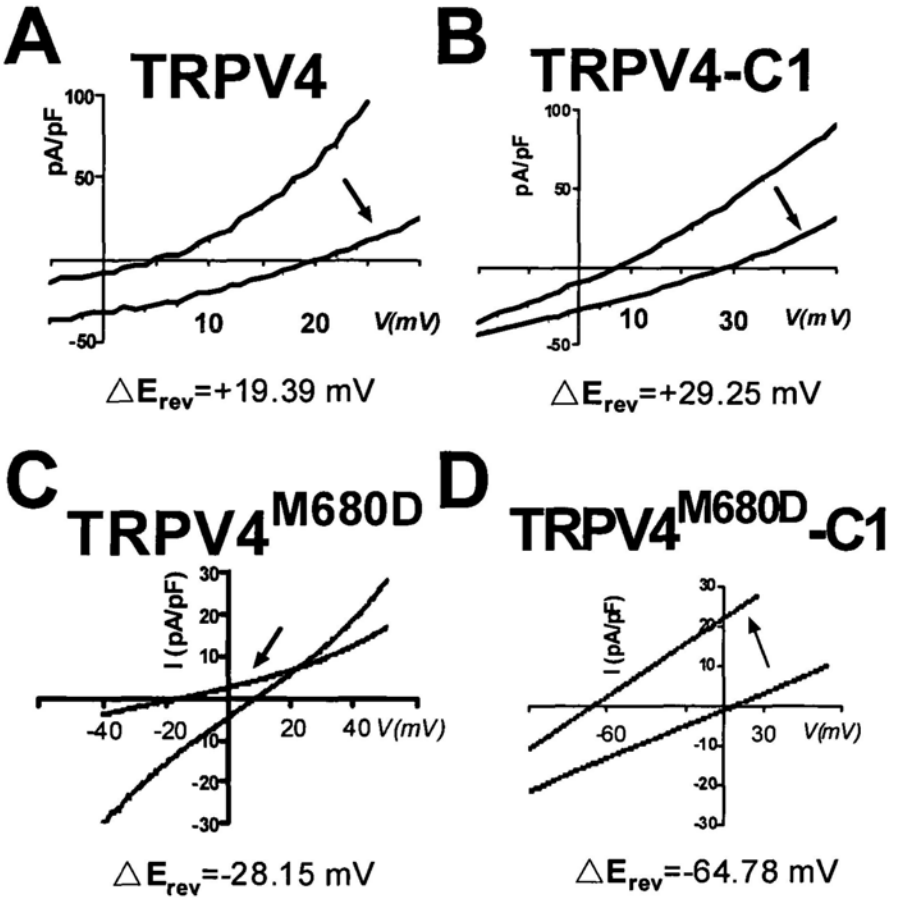

Chapter 4 Figure 6. Ca^{2+} permeability in TRPV4-expressing and TRPV4-TRPC1 co-expressing HEK cells. A-D, typical examples of currents through fully activated TRPV4 (A), TRPV4-TRPC1 (B), $TRPV4^{M680D}$(C) and $TRPV4^{M680D}$-TRPC1 (D) in standard extracellular solution and in an extracellular solution containing 30 mM Ca^{2+} as the sole charge carrier (arrow). In each panel, the resultant shift in reversal potential is indicated. Representatives of 6-7 individual cells.

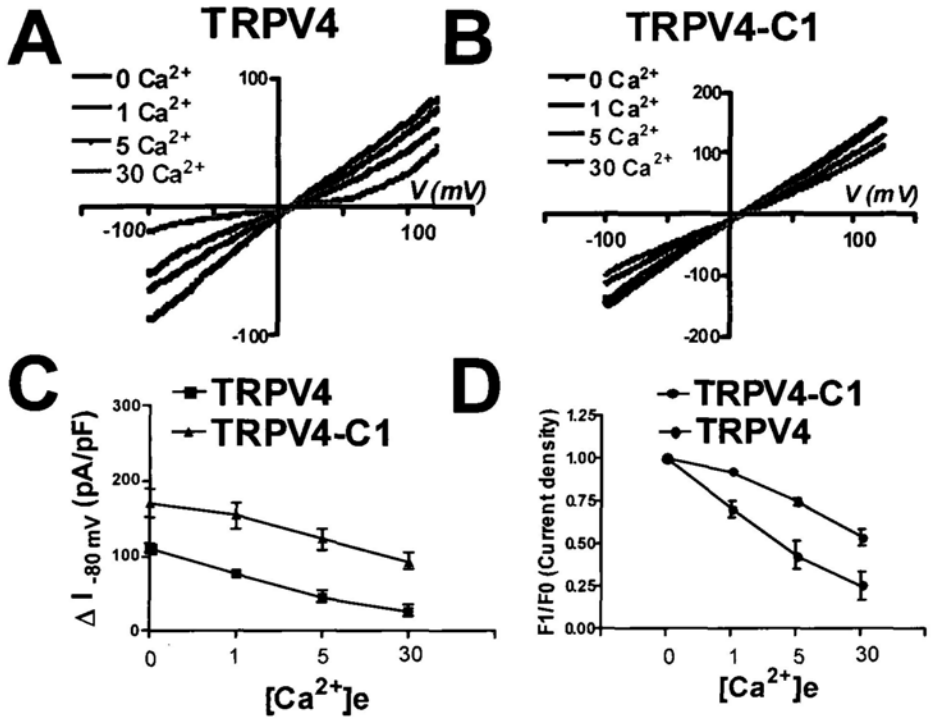

Chapter 4 Figure 7. Ca^{2+}-dependent rectification in TRPV4-expressing and TRPV4-TRPC1 co-expressing HEK cells. A and B, current-voltage relations for TRPV4 (A), TRPV4-TRPC1 (B) in standard extracellular solution containing the indicated Ca^{2+} concentrations. Note the appearance of inward and outward rectification in the presence of Ca^{2+}. C and D, Ca^{2+} dependence of rectification properties for TRPV4 and TRPV4-TRPC1. Shown are the average values (C) and ratio (D) of the currents measured at -80 mV.

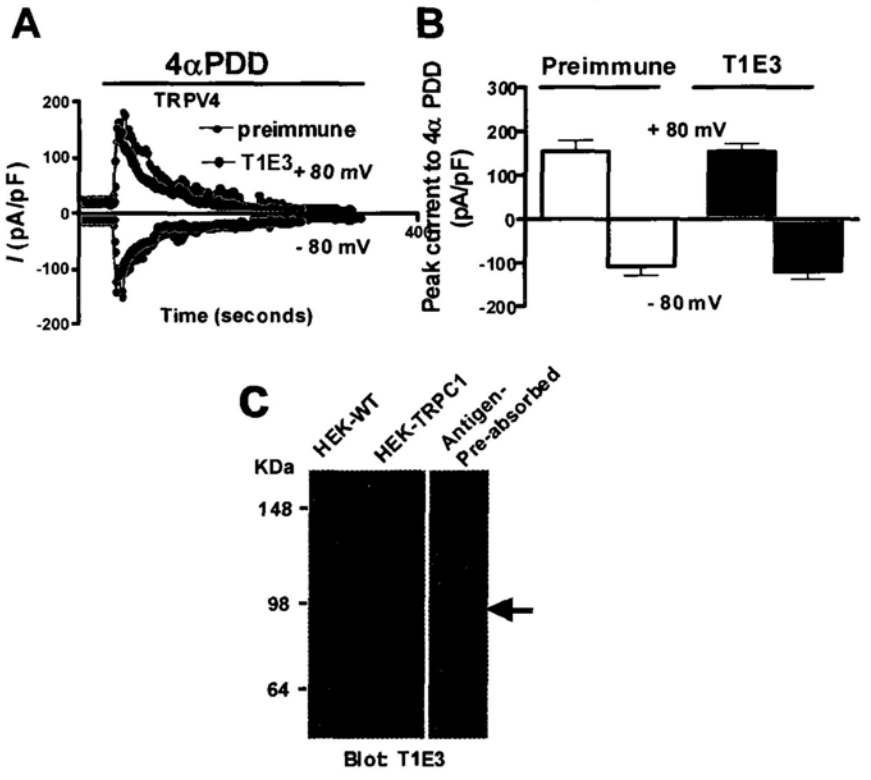

Chapter 4 Figure 8. A and B, Lack of effect of T1E3 on 4α-PDD-stimulated current in TRPV4-expressing HEK cells. Representative traces (A) and summary of data (B) of 4α-PDD-stimulated whole-cell current. Cells were clamped at 0 mV. Whole cell currents were recorded in response to successive voltage pulses of +80 mV and -80 mV for 100 ms duration. These current values were then plotted *vs.* time. Solid bar on top of the traces indicates the time period when 4α-PDD (5 μmol/L) was applied. The cells were pre-incubated with preimmune IgG (1:100) or T1E3 (1:100) for 1 hr at 37°C. Values are Mean ± SE (n = 5-12). C, Immunoblots showing the specificity of antibodies to their respective targets. HEK cells were transfected with TRPV4 (A) or TRPC1 (B and C). The extracted proteins were immunoblotted with anti-TRPV4 (Alomone Lab) (A and B), anti-TRPC1 (Alomone Lab) (A and B) or T1E3 antibody (C). Wild-type HEK cells were used a control. n = 3-4 for all experiments.

Chapter 5

Functional role of TRPV4-TRPC1 heteromeric channel in flow-induced $[Ca^{2+}]_i$ rise and vasodilation

5.1 Introduction

Hemodynamic blood flow is one of most important physiological factors that control vascular tone (Bevan, 1997;Busse and Fleming, 2003). Flow shear stress acts on the endothelium to stimulate the release of vasodilators such as nitric oxide, prostacyclin and endothelium-derived hyperpolarizing factors, causing endothelium-dependent vascular relaxation (Busse *et al.*, 2003;Davies, 1995). In many cases, a key early signal in this flow-induced vascular dilation is Ca^{2+} influx in endothelial cells in response to flow (Cooke *et al.*, 1991;Falcone *et al.*, 1993;Hartmannsgruber *et al.*, 2007;Kohler *et al.*, 2006;Liu *et al.*, 2006). There is intense interest in searching for molecular identity of the channels that mediate flow-induced Ca^{2+} influx. Several candidate channels have been proposed. In renal epithelial cells, it was found that polycystin 1 and polycystin 2 form a flow-sensitive channel complex to allow Ca^{2+} influx in response to fluid flow (Nauli *et al.*, 2003). In vascular endothelial cells, flow may activate $P2X_4$ purinoceptors, which is a Ca^{2+}-permeable channel (Yamamoto *et al.*, 2000). Flow-induced vascular dilation was found to be impaired in $P2X_4$ knockout mice ($P2X_4$ -/-) (Yamamoto *et al.*, 2006). Interestingly, several recent studies demonstrated that TRPV4 is a key channel in flow-induced endothelial Ca^{2+} influx and subsequent vascular dilation (Hartmannsgruber *et al.*, 2007;Kohler *et al.*, 2006).

TRP channels are a superfamily of cation channels that can be divided into seven

subfamilies, which include TRPC, TRPV, and five others (Montell, 2005). TRPV4 is a member of TRPV subfamily (Nilius *et al.*, 2004). The channel is Ca^{2+}-permeable and can be polymodally activated by hypotonic cell swelling, moderate heat, synthetic phorbol ester 4α-PDD, arachidonic acid and its metabolite epixyeicosatrienoic acids (Nilius *et al.*, 2004;Plant and Strotmann, 2007b). TRPV4 is also involved in flow sensation. TRPV4 is activated by flow shear stress in TRPV4-expressing HEK293 cells and in native renal epithelial cells (Gao *et al.*, 2003;Wu *et al.*, 2007). Importantly, there is convincing evidence that TRPV4 is involved in endothelium-dependent vascular dilation to flow (Hartmannsgruber *et al.*, 2007;Kohler *et al.*, 2006). In rat carotid arteries and gracilis artery, shear stress-induced dilation is blocked by a TRPV blocker ruthenium red (Kohler *et al.*, 2006). Furthermore, endothelium-dependent vascular dilation to flow shear stress is significantly reduced in TRPV4 knockout (-/-) mice (Hartmannsgruber *et al.*, 2007).

Previous studies from our group have demonstrated an interaction between flow-induced Ca^{2+} influx and store-operated Ca^{2+} influx in vascular endothelial cells (Kwan *et al.*, 2003). Depletion of intracellular Ca^{2+} stores was found to enhance flow-induced Ca^{2+} influx (Kwan *et al.*, 2003) and its associated vascular dilation (Liu *et al.*, 2006). Although still under debating, TRPC1 is one of possible candidates that have been suggested to mediate store-operated Ca^{2+} influx (Beech, 2005). In the present studies, we hypothesized that there may exist interaction between flow-sensing TRPV4 and another TRP isoform TRPC1, which is a ubiquitous expressed TRPC isoforms (Beech, 2005). Our results suggested that TRPC1 associates with TRPV4 to form a heteromeric channel. Such an association altered the kinetics of TRPV4-mediated $[Ca^{2+}]_i$ transient in response to flow, and it also enabled this $[Ca^{2+}]_i$ transient to be negatively modulated by protein kinase G (PKG). We also found that TRPV4-TRPC1 heteromeric channel is present in native endothelial cells and it plays an important role in flow-induced endothelial $[Ca^{2+}]_i$ influx and its associated vascular relaxation.

5.2 Materials and Methods

5.2.1 Materials

Two primary antibodies anti-TRPC1 (ACC-010) and anti-TRPV4 (ACC-034) were from Alomone Labs. Another goat anti-TRPV4 antibody was from Santa Cruz Biotechnol (SC-47527). TIE3 was raised by us from rabbits. Protein A-agarose and protease inhibitor cocktail tablets were from Roche. Fura-2 and Fluo-4/acetoxymethyl ester (Fluo-4/AM) and pluronic F127 were from Molecular Probes Inc. Alexa Fluor 488 conjugated goat anti-rabbit IgG, Alexa Fluor 546 conjugated rabbit anti-goat IgG, and di-8-ANEPPS were from Invitrogen. Endothelial cell growth medium and bovine brain extract were from Lonza Inc., USA.

5.2.2 Cell culture

All animal experiments were conducted in accordance with the regulation of the U.S. National Institute of Health (NIH publication No.8523). Primary cultured MAECs were isolated from male Sprague-Dawley rats as described elsewhere (Ashley et al., 2002). Briefly, arterial branches of mesenteric bed were dissected and digested with 0.02% collagenase for 45 min at 37°C. Dispersed cells were pelleted and then cultured in endothelial cell growth medium supplemented with 1% bovine brain extract. The identity of endothelial cells was verified by immunostaining with an antibody against von Willebrand Factor. HEK293 cells were cultured in DMEM supplemented with 10% FBS, 100 μg/ml penicillin and 100 U/ml streptomycin. human umbilical vein endothelial cells (HUVECs) was cultured in EGM medium supplemented with 1% BBE, 100 μg/ml penicillin and 100 U/ml streptomycin.

5.2.3 Cloning and transfection

Mouse TRPV4 gene (NM_022017), a gift from Dr. Bernd Nilius, Belgium, was cloned into pCAGGS vector. Human TRPC1 cDNA (NM_003304) was obtained by RT-PCR from human coronary endothelial cells, and was cloned into pcDNA6 vector. Dominant negative TRPC1 construct TRPC1 Δ567-793 was a gift from Dr. Indu

Ambudkar, NIH, USA.

Transfection condition was as described elsewhere (Kwan *et al.*, 2009). Briefly, HEK293 cells were transfected with various constructs using Lipofectamine 2000 in 6-well plates. About 80% of HEK293 cells were successfully transfected by respective protocols as indicated by control transfections using a GFP-expressing pCAGGS vector. Functional studies were performed 3 days post-transfection.

5.2.4 $[Ca^{2+}]_i$ measurement

$[Ca^{2+}]_i$ was measured as described elsewhere (Kwan *et al.*, 2003;Liu *et al.*, 2006;Yao *et al.*, 2000). Briefly, cultured HEK cells were loaded with 10 μmol/L Fura-2/AM. Flow was initiated by pumping NPSS to a specially-designed parallel plate flow chamber, in which cells were adhered to the bottom. Flow shear stress was ~5 dyne/cm^2. NPSS contained in mmol/L: 140 NaCl, 5 KCl, 1 $CaCl_2$, 1 $MgCl_2$, 10 glucose, 5 Hepes, pH 7.4. Fura-2 fluorescence signals were measured with dual excitation wavelengths at 340 and 380 nm using an Olympus fluorescence imaging system. In experiments using intact artery segments, a third or fourth-order rat mesenteric artery (about 2-3 mm long) was dissected. The endothelial cell layer was intraluminally loaded with 20 μmol/L Fluo-4/AM. Flow was initiated by pumping Kreb's solution (with 1% BSA) into the lumen of artery segments. Fluo-4 fluorescence in endothelial cells was measured with FV1000 confocal system. Kreb's solution contained in mmol/L: 118 NaCl, 4.7 KCl, 2.5 $CaCl_2$, 1.2 $MgSO_4$, 1.2 KH_2PO_4, 25.2 $NaHCO_3$, 11.1 glucose, pH 7.4, and bubbled with 95% O_2-5% CO_2. Changes in $[Ca^{2+}]_i$ were displayed as change in Fura-2 ratio (for Fura-2 dye) or as a relative fluorescence intensity compared to value before flow (F1/F0, for Fluo-4 dye).

When needed, cultured cells were pretreated with T1E3 (1:100) or pre-immune IgG (1:100) at 37°C for 1 hr before experiments. Artery segments were pretreated with T1E3 (1:50) or pre-immune IgG (1:50) at 4°C overnight.

5.2.5 Preparation of T1E3 and preimmune IgG

T1E3 antibody was raised in rabbits using the strategy developed by Xu *et al* (Xu *et al.*, 2001). Briefly, a peptide corresponding to TRPC1 putative pore-region (CVGIFCEQQSNDTFHSFIGT) was synthesized and conjugated to keyhole limpet hemocyanin (KLH) at Alpha Diagnostic International (USA). The coupled T1E3 peptide was injected into the tail vein of a rabbit followed by two boost doses. T1E3 antiserum was collected four weeks after the second boost. IgG was purified from both the T1E3 antiserum and the preimmune serum using a protein G column.

In antigen preabsorption control, T1E3 was preabsorbed with excessive amount of peptides (1:16 weight ratio) for 2.5 hr at room temperature.

5.2.6 Whole-cell patch clamp

Whole cell current was measured with an EPC-9 patch clamp amplifier as described elsewhere (Voets *et al.*, 2002b). The pipette solution contained in mmol/L: 20 CsCl, 100 Cs^+-aspartate, 1 $MgCl_2$, 4 ATP, 0.08 $CaCl_2$, 10 BAPTA, 10 Hepes, pH 7.2. Bath solution contained in mmol/L: 150 NaCl, 6 CsCl, 1 $MgCl_2$, 1.5 $CaCl_2$, 10 glucose, 10 Hepes, pH 7.4.

Cells were clamped at 0 mV. Whole cell current density (pA/pF) was recorded in response to successive voltage pulses of +80 mV and -80 mV for 100 ms duration. These whole cell current values were then plotted *vs.* time. The recordings were made before and after 4α-PDD (5 μmol/L) application. If needed, cells were pretreated with T1E3 (1:100) or pre-immune IgG (1:100) at 37°C for 1 hr, or with ruthenium red (5 μM) for 5 min.

5.2.7 Pressure myography

Pressure myography studies were performed as described elsewhere (Liu *et al.*, 2006). Briefly, a third or fourth-order mesenteric artery (about 2-3 mm long) was dissected and transferred to a pressure myograph chamber (Model 110P, Danish Myotechnology) filled with oxygenated Kreb's solution at 37°C. External diameter of the artery was recorded using a CCD camera. The arteries were preconstricted with

phenylephrine. Flow was initiated by creating a pressure difference between inflow and outflow. The mean intraluminal pressure was maintained at 50 mmHg throughout flow protocol. At the end of each experiment, the dilation to acetylcholine (1 μmol/L) was used to assess the viability of the endothelium. The artery segments were pre-incubated with T1E3 (1:50) or pre-immune IgG (1:50) at 4°C overnight, or with ruthenium red (5 μmol/L) for 5 min.

5.2.8 Statistics

Student's t-test was used for statistical comparison, with probability $p<0.05$ as a significant difference. For comparison of multiple groups, One-way ANOVA with Newman-keuls was used.

5.3 Results

5.3.1 TRPC1 alters the kinetics of TRPV4-mediated $[Ca^{2+}]_i$ transient in response to flow in HEK293 cells

Consistent with the results from other groups (Gao *et al.*, 2003;Wu *et al.*, 2007), flow induced a $[Ca^{2+}]_i$ transient in TRPV4-expressing HEK293 cells (Chapter 5 Figure 1A). After $[Ca^{2+}]_i$ reached its peak, it decayed with t/1/2 at 78±7 sec (n = 6) (t/1/2 is defined as time duration for $[Ca^{2+}]_i$ to reduce to 50% of its peak value). Intriguely, co-expression of TRPC1 markedly prolonged the TRPV4-mediated $[Ca^{2+}]_i$ transient in response to flow (Chapter 5 Figure 1B). In fact, no apparent decay in $[Ca^{2+}]_i$ was observed within the time duration of experiments which lasted for ~10 min (Chapter 5 Figure 1B). TRPC1 co-expression also caused a small but statistically significant increase in the peak magnitude of flow-induced $[Ca^{2+}]_i$ transient (Chapter 5 Figure 1E). As controls, flow-induced $[Ca^{2+}]_i$ transient was absent in wild-type HEK293 cells (unpublished data), or in HEK293 cells only expressing TRPC1 (Chapter 5 Figure 1C), or in TRPV4-expressing cells that were bathed in Ca^{2+}-free medium (unpublished data). Furthermore, a TRPV antagonist ruthenium red (5 μmol/L) inhibited the $[Ca^{2+}]_i$ transient (Chapter 5 Figure 1D and E), confirming a

requirement for TRPV in flow response.

5.3.2 TRPC1 enables the PKG modulation of $[Ca^{2+}]_i$ transient in HEK cells

To study PKG regulation, HEK cells were stably transfected with PKG1α, then transiently transfected either with TRPV4 or with TRPV4 plus TRPC1. In TRPV4-expressing cells, pretreatment with a PKG activator 8-BrcGMP (2 mmol/L) for 10 min had no effect on flow-induced $[Ca^{2+}]_i$ rise (Chapter 5 Figure 2A, C). In contrast, in TRPV4-TRPC1 co-expressing cells, 8-BrcGMP (2 mmol/L) markedly reduced the magnitude of $[Ca^{2+}]_i$ rise (Chapter 5 Figure 2B, C). KT5823 (1 μmol/L), a potent and highly specific PKG inhibitor, abolished the inhibitory action of 8-BrcGMP (Chapter 5 Figure 2B, C). In cells co-transfected with TRPV4 and mutant TRPC1 that were mutated at putative PKG phosphorylation sites (TRPC1S172A or TRPC1T313A), the inhibitory action of 8-BrcGMP (2 mmol/L) was reduced (Chapter 5 Figure 2C). These data suggest that PKG does no act on TRPV4 itself. Instead it inhibits the function of TRPV4-TRPC1 complex by phosphorylating on Ser-172 and Thr-313 of TRPC1.

5.3.3 T1E3 diminish flow-induced $[Ca^{2+}]_i$ transient in TRPV4-TRPC1 co-expressing HEK293 cells

A polyclonal anti-TRPC1 antibody T1E3, which can plug the pore region of TRPC1 (Xu *et al.*, 2001), was used to study the interaction of TRPC1 with TRPV4. The results showed that pre-incubation with T1E3 (1:100) for 1 hr at 37°C diminished flow-induced $[Ca^{2+}]_i$ transient (Chapter 5 Figure 3A and B) in TRPV4-TRPC1 co-expressing HEK293 cells. The specificity of T1E3 was verified by immunoblot and patch clamp studies. In immunoblots, T1E3 recognized the expected band in TRPC1-expressing HEK293 cells (Chapter 4 Figure 8). In patch clamp study, T1E3 had no direct action on TRPV4 homomeric channels, indicated by lack of action of T1E3 on 4α-PDD-elicited cation current in TRPV4-expressing HEK293 cells (Chapter 4 Figure 8).

5.3.4 TRPC1Δ567-793 diminish flow-induced $[Ca^{2+}]_i$ transient in TRPV4-TRPC1 co-expressing HEK293 cells

Previous studies have shown that TRPC1Δ567-793, a mutant with deletion in TRPC1 pore region, is able to coassemble with wild-type TRPC1 subunits to form multimeric complex, thereafter disrupting TRPC1 function (Liu *et al.*, 2003). In the present study, co-transfection of TRPC1Δ567-793 with TRPV4 diminished flow-induced $[Ca^{2+}]_i$ rise in HEK293 cells (Chapter 5 Figure 3A and B), and it also abolished the 4α-PDD-stimulated whole cell cation current (Chapter 5 Figure 3A and B). Taken together, these data support that TRPV4 and TRPC1 coassemble to form a functional heteromultimeric channels.

5.3.5 Physical association of TRPC1 with TRPV4 in the primary cultured rat MAECs

Co-immunoprecipitation and double-labeling immunofluorescence experiments were used to study the physical association of TRPC1 and TRPV4 in the primary cultured rat MAECs. In double-labeling immunofluorescence experiments, rat MAECs were stained for TRPC1 with Alexa fluor 488 (green) and for TRPV4 with Alexa fluor 546 (red). As shown in Figure 7A and 7B, both TRPC1 and TRPV4 had significant distribution on plasma membrane, although some intracellular distribution could also be observed. On merged images, there was very strong overlapping of TRPC1 and TRPV4 fluorescence (yellow) (Chapter 5 Figure 4). In control experiments, there was no staining if the primary antibodies were preabsorbed with excessive amounts of respective antigens (Chapter 5 Figure 4). These data suggest that TRPC1 is co-localized with TRPV4 at subcellular level in rat MAECs.

In co-immunoprecipitation experiments, anti-TRPC1 antibody was able to pull-down TRPV4 (Chapter 5 Figure 5), and furthermore anti-TRPV4 antibody was also able to pull down TRPC1 (Chapter 5 Figure 5), confirming the physical interaction of TRPV4 with TRPC1 in vascular endothelial cells. Furthermore, we

investigated the possible interaction of TRPV4 with other TRP channels in the primary cultured rat MAECs using co-immunoprecipitation methods. Immunoblots showed that these endothelial cells express TRPC3, TRPC4, TRPC5 and TRPC6 (Chapter 5 Figure 6). However, the anti-TRPV4 antibody failed to pull down these TRPC isoforms (Chapter 5 Figure 6). Therefore, the interaction of TRPV4 with TRPC1 appears to be relatively specific.

5.3.6 Effect of T1E3, TRPC1Δ567-793 and TRPC1-siRNA on flow-induced $[Ca^{2+}]_i$ rise in HUVECs

HUVECs express both TRPV4 and TRPC1 (Chapter 5 Figure 7). Flow-induced $[Ca^{2+}]_i$ rise in HUVECs was inhibited by ruthenium red, T1E3 and TRPC1Δ567-793 (Chapter 5 Figure 8A, B). A TRPC1-specific siRNA was used to knock-down TRPC1 protein levels (Chapter 5 Figure 8C). Interestingly, this siRNA not only reduced the magnitude of flow-induced $[Ca^{2+}]_i$ rise, but also accelerated the decay of flow-induced $[Ca^{2+}]_i$ transient (Chapter 5 Figure 8D). These data are consistent with the notion that interaction TRPC1 with TRPV4 prolongs the flow-induced $[Ca^{2+}]_i$ transient.

5.3.7 T1E3 reduces flow-induced endothelial $[Ca^{2+}]_i$ rise in intact rat small mesenteric arteries

In experiments, flow evoked a $[Ca^{2+}]_i$ rise in endothelial cells in intact rat small mesenteric arteries (Chapter 5 Figure 9A and B). This $[Ca^{2+}]_i$ rise consisted of a transient peak followed by a relatively sustained phase, which lasted within the experimental duration of ~8-10 min (Chapter 5 Figure 9B). Both phases of the $[Ca^{2+}]_i$ response could be inhibited by ruthenium red (5 μmol/L) (Chapter 5 Figure 9D). Importantly, flow-induced endothelial $[Ca^{2+}]_i$ rise was diminished in vessels that were pretreated with T1E3 (1:50) overnight (Chapter 5 Figure 9C and D), suggesting an involvement of TRPV4-TRPC1 complex in this $[Ca^{2+}]_i$ response.

5.3.8 T1E3 reduces flow-induced endothelial vasodilation in intact rat small

mesenteric arteries

The role of TRPV4-TRPC1 complex in flow-induced dilation was explored using intact rat small mesenteric artery segments. As described in our previous report (Liu *et al.*, 2006),, flow-induced vascular dilation also consisted of an initial transient peak followed by a sustained plateau phase (Chapter 5 Figure 10A and B). The vessels rapidly contracted again as soon as the flow was stopped (Chapter 5 Figure 10B). The dilation was sensitive to ruthenium red inhibition (Chapter 5 Figure 10D), consistent with the involvement of TRPV4 (Hartmannsgruber *et al.*, 2007;Kohler *et al.*, 2006). Importantly, pretreatment of vessels with T1E3 (1:50, overnight) caused a marked reduction in flow-induced vascular dilation (Chapter 5 Figure 10C and 10D). Both the peak and sustained flow dilation were reduced in T1E3-treated vessels as compared to the controls in which the vessels were pretreated overnight with 1:50 pre-immune IgG (Chapter 5 Figure 10C and 10D). These data suggest an involvement of TRPV4-TRPC1 complex in flow dilation.

5.4 Discussion and conclusion

The major findings of this study are as follows: 1) Functional study showed that flow activated a $[Ca^{2+}]_i$ rise in TRPV4-expressing HEK cells. Co-expression of TRPC1 markedly prolonged the TRPV4-mediated $[Ca^{2+}]_i$ transient in response to flow. Furthermore, the flow-induced $[Ca^{2+}]_i$ rise in TRPV4-TRPC1 co-expressing cells was inhibited by an anti-TRPC1 blocking antibody T1E3 and by a dominant negative TRPC1 construct Δ567-793. 2) Co-expression of TRPC1 with TRPV4 enabled the flow-induced $[Ca^{2+}]_i$ transient to be negatively regulated by PKG. 3) Similar to those in TRPV4-TRPC1 co-expressing HEK cells, flow elicited a relatively prolonged Ca^{2+} transient in human umbilical vein endothelial cells. T1E3 antibody and TRPC1Δ567-793 markedly reduced flow-induced $[Ca^{2+}]_i$ rise in these cells. 4) T1E3 and ruthenium red inhibited flow-induced $[Ca^{2+}]_i$ rise in endothelial cells within intact small mesenteric artery, and they also decreased flow-induced vascular dilation. Taken together, these data strongly suggest that TRPC1 physically interacts with

TRPV4 to form heteromeric channel complex. This heteromeric channel plays an important role in flow-induced endothelial Ca^{2+} influx and subsequent vascular dilation.

Previous studies showed that TRPV4 is activated by flow shear stress in TRPV4-expressing HEK293 cells (Gao *et al.*, 2003;Wu *et al.*, 2007). Furthermore, TRPV4 is abundantly expressed in vascular endothelial cells (O'Neil and Heller, 2005;Watanabe *et al.*, 2002;Wissenbach *et al.*, 2000), and is believed to be a key component in flow-induced dilation in vascular tissues (Hartmannsgruber *et al.*, 2007;Kohler *et al.*, 2006). However, the detailed mechanism for flow-induced activation of TRPV4 remains elusive. In the present study, we found that flow activated TRPV4 in HEK cells, which is consistent with reports from others (Gao *et al.*, 2003;Watanabe *et al.*, 2003;Wu *et al.*, 2007). Intriguely, we found that TRPC1 co-expression prolonged TRPV4-mediated $[Ca^{2+}]_i$ transient in response to flow. Co-immunoprecipitation experiments demonstrated that TRPV4 and TRPC1 physically associate with each other. In functional studies, T1E3, which specifically plugs the pore of TRPC1 (Xu *et al.*, 2001), blocked TRPV4-mediated Ca^{2+} influx. Furthermore, a dominant negative construct TRPC1Δ567-793, in which the pore region of TRPC1 was deleted, also diminished the TRPV4-mediated Ca^{2+} influx. TRPC1Δ567-793 was previously shown to be assembled with wild-type TRPC1, thereby disrupting the pore region and suppressing TRPC1-mediated Ca^{2+} influx in HEK cells (Liu *et al.*, 2003). The present study showed that TRPC1Δ567-793 is also able to disrupt TRPV4-mediated Ca^{2+} influx in TRPV4-TRPC1 co-expressing HEK cells. These data strongly suggest that TRPV4 and TRPC1 may form functional heteromeric channels. The formation of such TRPV4-TRPC1 channel complex would allow TRPV4-mediated response to be modulated by signaling pathways that usually act on TRPC1.

Interestingly, with regard to the decay kinetics of flow-induced $[Ca^{2+}]_i$ transient, native endothelial cells displayed properties similar to that of TRPV4-TRPC1 co-expressing HEK cells, but unlike that of TRPV4 (alone)-expressing HEK cells.

Furthermore, T1E3 and TRPC1Δ567-793 markedly diminished flow-induced $[Ca^{2+}]_i$ rise in HUVECs. T1E3 also inhibited flow-induced endothelial $[Ca^{2+}]_i$ influx in intact artery and its subsequent vascular dilation. These data strongly suggest that TRPV4 also form complex with TRPC1 in native endothelial cells, and that such a TRPV4-TRPC1 complex plays an important role in flow-induced Ca^{2+} influx and subsequent vascular dilation.

As mentioned, the physical association of TRPC1 with TRPV4 prolonged the flow-induced $[Ca^{2+}]_i$ transient and enabled the $[Ca^{2+}]_i$ transient to be negatively regulated by PKG. This has important significance for endothelial cell function. A prolonged Ca^{2+} influx would allow endothelial cells to produce more NO, enhancing vascular dilation (Kanai *et al.*, 1995;Liu *et al.*, 2006). However, excessive $[Ca^{2+}]_i$ and NO could lead to apoptosis and cell death (Choy *et al.*, 2001). To protect from this, vascular endothelial cells possess a negative feedback mechanism, in which flow-induced Ca^{2+} influx is inhibited by $[Ca^{2+}]_i$ via Ca^{2+}-NO-cGMP-PKG pathway (Yao *et al.*, 2000). Unfortunately, the molecular identity of such flow-sensitive PKG-inhibitable Ca^{2+} influx channels is unknown. The present study strongly suggests the TRPV4-TRPC1 complex to be the candidate. This TRPV4-TRPC1 complex in endothelial cells prolongs the flow-induced Ca^{2+} influx, thus producing more NO, and at the same time, allows the $[Ca^{2+}]_i$ influx to be negatively regulated by $[Ca^{2+}]_i$ level via Ca^{2+}-NO-cGMP-PKG pathway. However, note that this negative feedback scheme cannot be applied to HEK cells, because these cells do not express NO synthases and guanylyl cyclases, which are required for the operation of Ca^{2+}-NO-cGMP-PKG pathway.

In conclusion, we demonstrated that TRPV4 forms heteromeric complex with TRPC1. Such a complex displays characteristic electrophysiological properties different from that of TRPV4 homomeric channels. In native endothelial cells, TRPV4-TRPC1 complex plays an important role in flow-induced Ca^{2+} influx and subsequent vascular dilation.

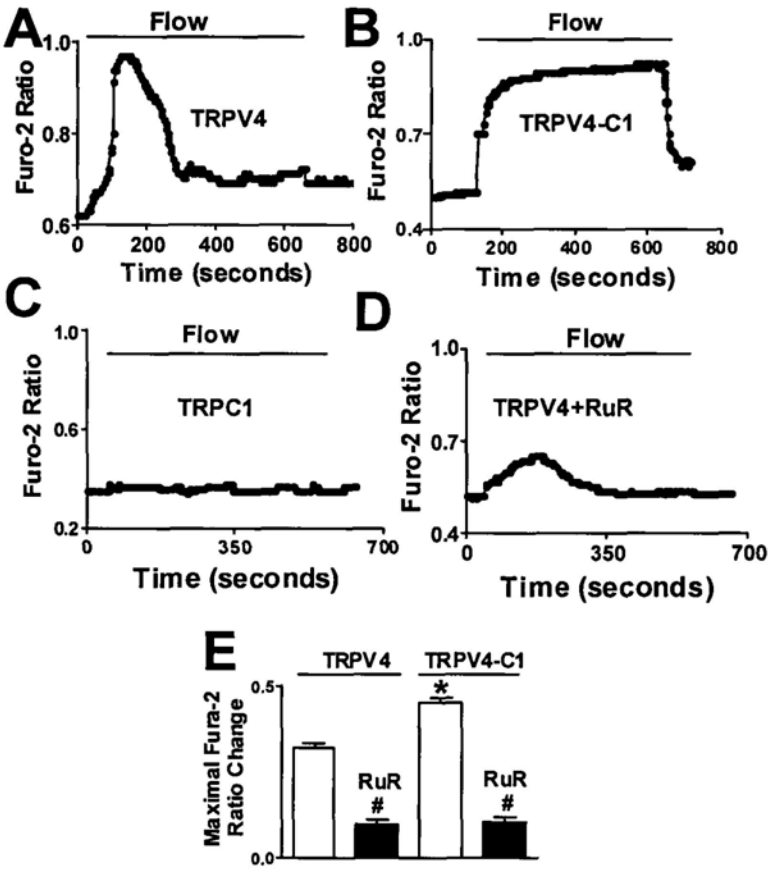

Chapter 5 Figure 1. Flow-induced $[Ca^{2+}]_i$ changes in TRPV4-expressing and TRPV4-TRPC1 co-expressing HEK cells. A-D, Representative traces illustrating the time course of flow-induced $[Ca^{2+}]_i$ changes. A and D, TRPV4-expressing HEK cells in the absence (A) or presence of 5 μmol/L ruthenium red (D); B, a TRPV4-TRPC1 co-expressing HEK cell. C, a TRPC1-expressing HEK cell. Cells were bathed in NPSS. Solid bar on top of the traces indicates the time period when laminar flow was applied. E, summary showing the amplitude of flow-induced $[Ca^{2+}]_i$ rise as expressed in maximal increase in Fura-2 ratio. RuR, ruthenium red. Mean ± SE (n = 6-8, 8 to 20 cells per experiment). #, $P<0.05$ compared to TRPV4.

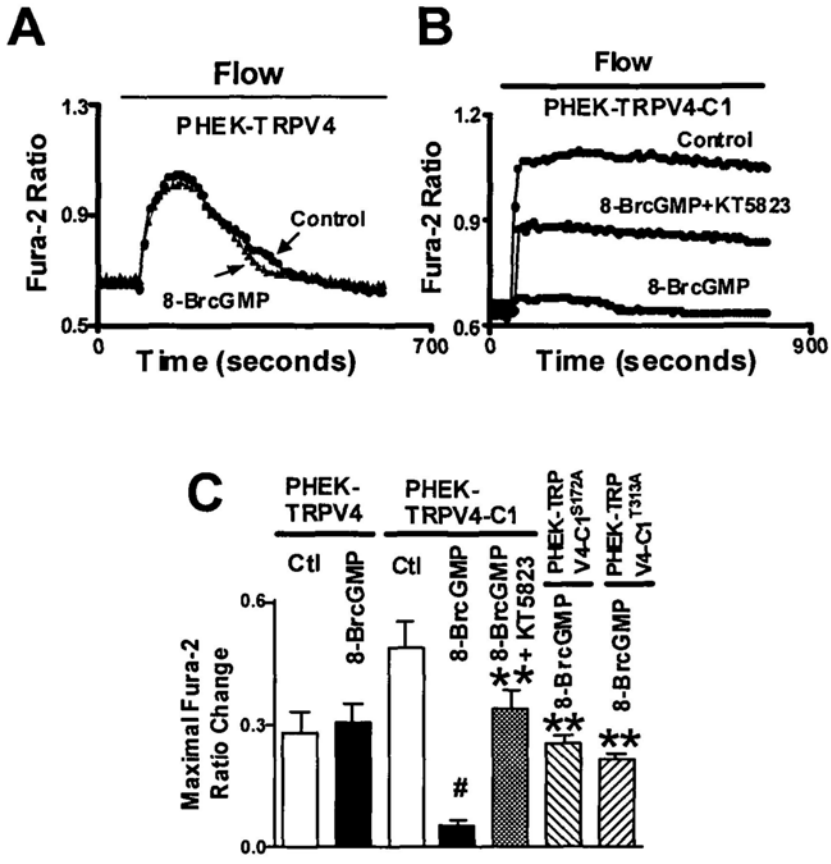

Chapter 5 Figure 2. Flow-induced $[Ca^{2+}]_i$ change in TRPV4-expressing and TRPV4-TRPC1 co-expressing PHEK cells. A and B, representative traces illustrating the time course of flow-induced $[Ca^{2+}]_i$ change. A, TRPV4-expressing PHEK, and B, TRPV4-TRPC1 co-expressing PHEK cells. Cells were stably transfected with PKG1α gene, thus labeled as PHEK. All cells were bathed in NPSS. Solid bar on top of the traces indicates the time period when laminar flow was applied. 8-BrcGMP (2 mmol/L) with/without KT5823 (1 μmol/L) was introduced 10 min before flow. Mean ± SE (n = 6-8, 8 to 20 cells per experiment). V4 stands for TRPV4, C1 for TRPC1. #, $P<0.05$ compared to the control without 8-BrcGMP (C). **, $P<0.05$ compared to those with 8-BrcGMP alone (C).

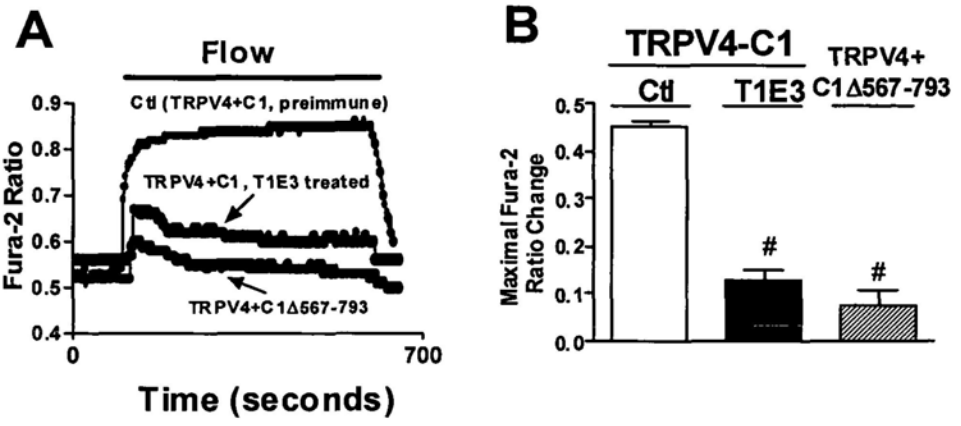

Chapter 5 Figure 3. Effect of T1E3 and TRPC1Δ567-793 on flow-induced $[Ca^{2+}]_i$ rise in HEK cells. Cells were co-transfected with TRPV4 and TRPC1. For those labeled as TRPV4+C1Δ567-793, cells were co-transfected with TRPV4 and TRPC1Δ567-793. Shown are representative traces (A) and summary of data (B) for flow-induced $[Ca^{2+}]_i$ rise. For T1E3 experiments, cells were pre-incubated with T1E3 (1:100) or preimmune IgG (1:100, as control) for 1 hr at 37°C. For antigen preabsorption, T1E3 was pre-incubated with excessive amount of TRPC1 peptide to remove T1E3. Values are Mean ± SE (n = 5-18; for $[Ca^{2+}]$i measurement, 8 to 20 cells per experiment). #, $P<0.05$ compared to control.

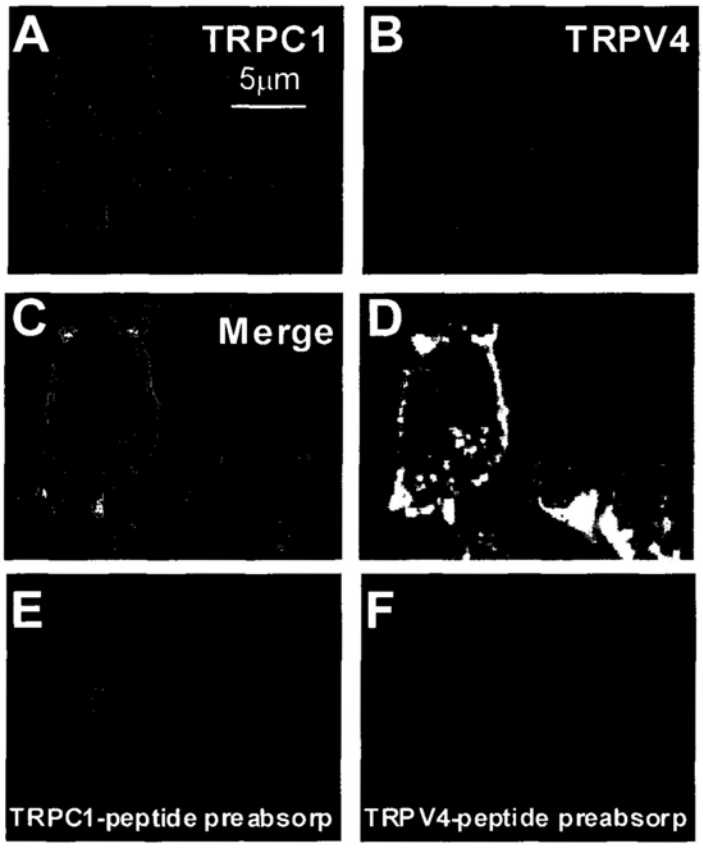

Chapter 5 Figure 4. Subcellular co-localization of TRPV4 and TRPC1 in the primary cultured rat MAECs. A and B, representative images of TRPC1 (A, green) and TRPV4 (B, red) in a MAEC; C, overlay image of A and B; D, bright field image of the same cell together with merged fluorescence; E, TRPC1 antibody was preabsorbed with excessive TRPC1 peptide; F, TRPV4 antibody was preabsorbed with excessive TRPV4 peptide. 30 cells per experiment for A-F.

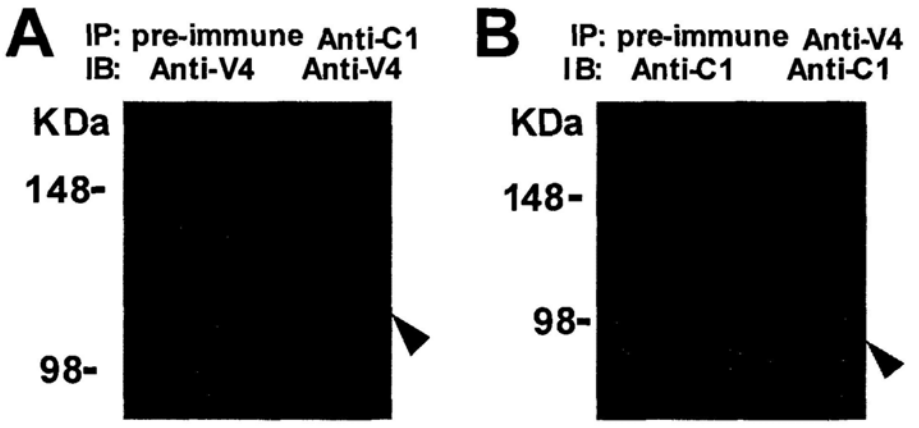

Chapter 5 Figure 5. Co-immunoprecipitation of TRPV4 and TRPC1 in the primary cultured rat mesenteric artery endothelial cells (MAECs). A and B, co-immunoprecipitation of TRPV4 with TRPC1. The pulling antibody and blotting antibody were indicated in the figure. Control immunoprecipitation was done using the preimmune IgG (labeled as pre-immune). IP, immunoprecipitation; IB, immunoblot; anti-V4, anti-TRPV4; anti-C1, anti-TRPC1. n = 3-4.

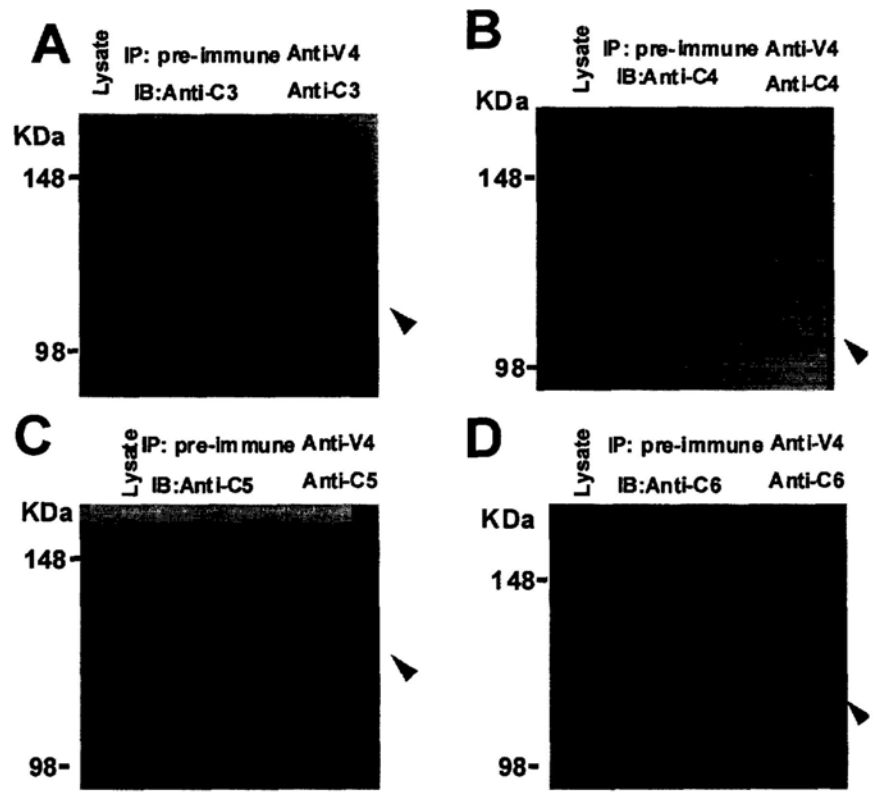

Chapter 5 Figure 6. Co-immunoprecipitation experiments of TRPV4 with TRPC isoforms in the primary cultured rat MAECs. The pulling antibody and blotting antibody were indicated in the figure. Control immunoprecipitation was done using the preimmune IgG (labeled as pre-immune). IP, immunoprecipitation; IB, immunoblot; anti-V4, anti-TRPV4; anti-C1, anti-TRPC1; anti-C3, anti-TRPC3; anti-C4, anti-TRPC4; anti-C5, anti-TRPC5; anti-C6, anti-TRPC6; n = 3-4. The right lane in each picture was loaded with the protein lysate prepared from MAECs.

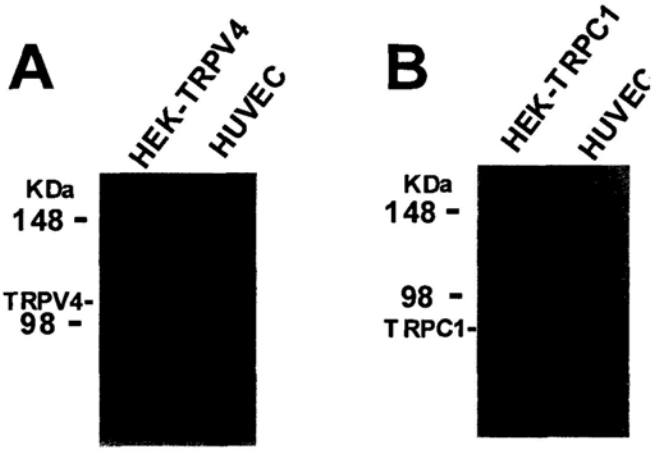

Chapter 5 Figure 7. Immunoblots showing expression of TRPV4 and TRPC1 in HUVECs. Shown are representative immunoblots with antibodies against different TRPV4 or TRPC1 (n = 3-4 for each experiment). Expressions in TRPV4- and TRPC1-overexpressing HEK cells were used as positive controls.

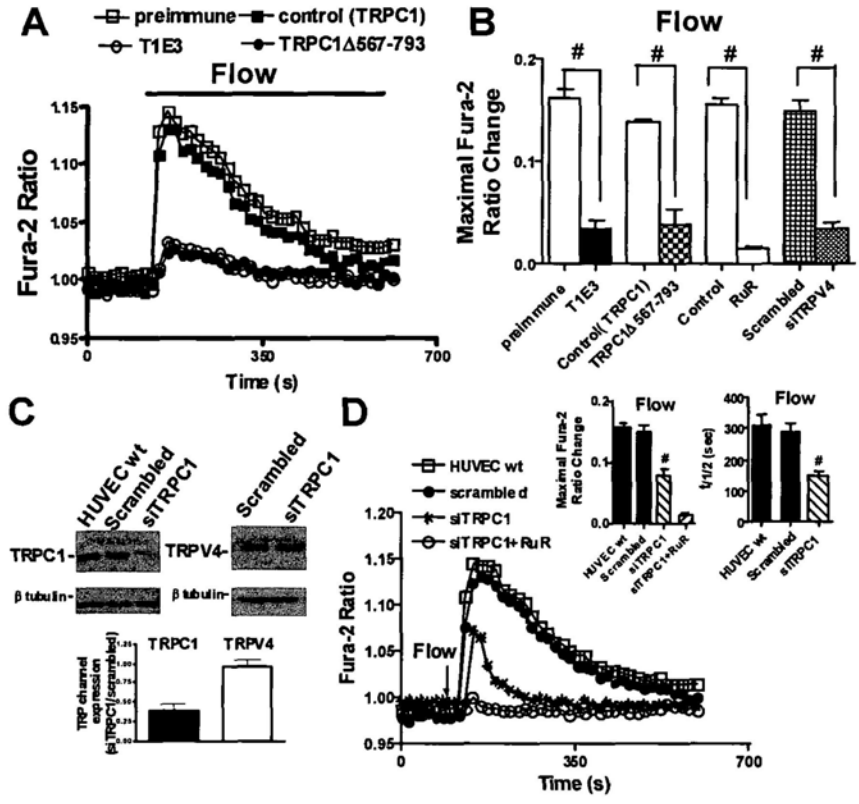

Chapter 5 Figure 8. Flow-induced $[Ca^{2+}]_i$ rise in HUVECs. A and D, Representative traces illustrating the time course of flow-induced $[Ca^{2+}]_i$ rise. For T1E3 experiments (A), cells were pre-incubated with T1E3 (1:100) or preimmune IgG (1:100, as control) for 1 hr at 37°C. For TRPC1Δ567-793 series (A), cells were transfected with wild-type TRPC1 (as control) or TRPC1Δ567-793. For TRPV4-siRNA series, cells were transfected with TRPV4-siRNA or scrambled siRNA as control. In D, cells were transfected with TRPC1-siRNA (with or without 5 μmol/L RuR pretreatment for 10 min) or scrambled siRNA as a control. B and Inset of D, summary showing the amplitude (B and the left inset in D) and the decay t/1/2 (the right inset in D) of flow-induced $[Ca^{2+}]_i$ rise. Mean ± SE (n = 4-5, 8 to 20 cells per experiment). HUVEC-wt: wild-type HUVECs. C, representative images (top) and summary (bottom) of immunoblot experiments showing the effectiveness and selectivity of TRPC1-siRNA. Mean ± SE (n = 3). #, P<0.05 compared to its respective controls.

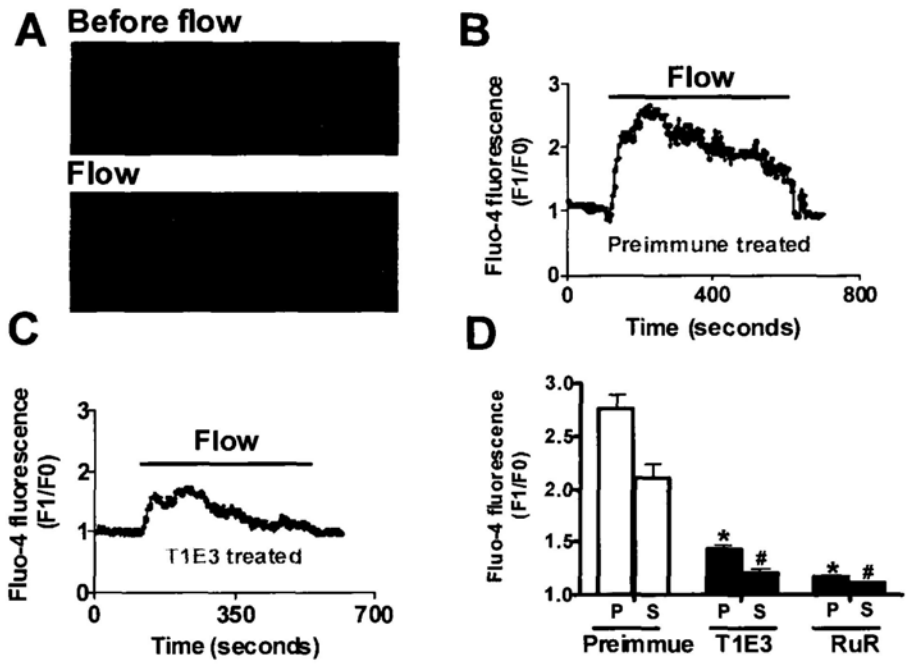

Chapter 5 Figure 9. Effect of T1E3 on flow-induced $[Ca^{2+}]_i$ rise in endothelial cells of intact small mesenteric arteries. A, Representative endothelial cell Fluo-4/AM images of an artery in Kreb's solution before and during flow. B and C, representative traces showing flow-induced $[Ca^{2+}]_i$ rise in an endothelial cell within an artery that was preincubated in pre-immune IgG (1:50; B) or T1E3 (1:50; C) overnight. Solid bar on the top of the trace indicates the time period when intraluminal flow (Kreb's solution with 1% BSA) was applied. D, summary of data showing the effect of T1E3 (1:50, overnight) and ruthenium red (RuR, 5 μmol/L) on the amplitude of peak (P) and sustained (S) $[Ca^{2+}]_i$ rise in response to flow. Control was preincubated with pre-immune IgG. Values are Mean ± SE (n = 5-6 with 8-20 cells per experiment). *, #: $P<0.05$ compared to P or S phase of the control group, respectively.

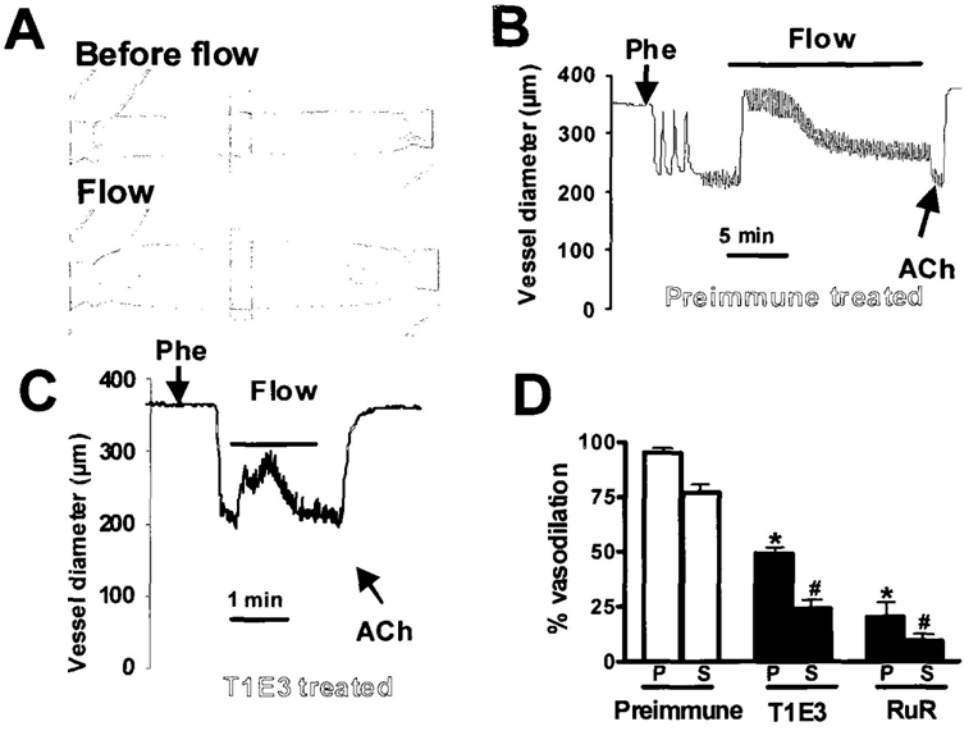

Chapter 5 Figure 10. Effect of T1E3 on flow-induced vascular dilation in small mesenteric arteries. A. Representative images of an artery in Kreb's solution before and during flow, showing changes in vessel diameter. B and C, representative traces showing dilatory responses to flow in arteries preincubated with pre-immune IgG (1:50, overnight; B) or T1E3 (1:50, overnight; C) overnight. The vessel was preconstricted with phenylephrine (Phe). D, Summary of data showing the effect of T1E3 and ruthenium red (RuR, 5 μmol/L) on the peak (P) and sustained (S) flow dilation. Control was preincubated with pre-immune IgG. Values are Mean ± SE. (n = 5 to 6 independent experiments). *, #: $P<0.05$ compared to P or S phase of the control group, respectively.

Chapter 6

Depletion of intracellular Ca^{2+} stores stimulates translocation of TRPV4-TRPC1 heteromeric channel to the plasma membrane

6.1 Introduction

TRPC1 is a Ca^{2+}-permeable cation channels that play an important function role in many cell types (Beech, 2005). Although still under debating, one condition that is suggested to activate TRPC1 channel is Ca^{2+} store depletion (Beech, 2005). The store Ca^{2+} depletion is sensed by STIM1, which serves as the Ca^{2+} sensor in endoplasmic reticulum (ER). Consequently, STIM1 forms clusters, which then translocate to the puncta immediately underneath the plasma membrane, where STIM1 gates TRPC1 to bring about the SOC (Cahalan, 2009;Huang *et al.*, 2006;Lee *et al.*, 2009). In addition to the mechanism involving STIM-TRPC interaction, SOC could be brought out by an enhanced trafficking and fusion of TRPC-containing vesicles to the plasma membrane, resulting in more channel insertion onto the plasma membrane (Cayouette and Boulay, 2007;Kim *et al.*, 2006;Yao *et al.*, 1999). However, the second mechanism that involves vesicle trafficking and fusion has received much less attention (Cayouette *et al.*, 2007;Putney, 2009). There is still a lack of general model for vesicle trafficking and TRP channel insertion in the plasma membrane in SOC (Cayouette *et al.*, 2007).

TRP channels *in vivo* are often composed of heteromeric subunits. Heteromeric assembly usually occurs between the members within the same TRP subfamily such as between TRPC1 and TRPC3 (Montell, 2005). However,

coassembly could also happen between the subunits from different TRP subfamily such as between TRPC1 and TRPP2 (Tsiokas et al., 1999), and between TRPV4 and TRPP2 (Kottgen et al., 2008). These heteromultimeric channels may display properties different from those of homomultimeric channels (Hofmann et al., 2002;Strubing et al., 2001). To our knowledge, there is almost no study about the vesicle translocation of heteromeric TRP channels. In chapter 4 and 5, I have showed that TRPC1 can co-assemble with TRPV4 to form heteromeric channels (Ma *et al.*, 2010). In the present study, we tested the hypothesis that Ca^{2+} store depletion may enhance vesicle trafficking to the plasma membrane, causing insertion of more TRPV4-TRPC1 complex into the plasma membrane. Our results show that Ca^{2+} depletion in intracellular stores triggered a rapid translocation of TRPV4-TRPC1 complex into the plasma membrane in HEK293 cells. This translocation required STIM1. Similar mechanism was also identified in native endothelial cells.

6.2 Materials and methods

6.2.1 Materials

Human embryonic kidney cell line HEK293 was from ATCC, USA. Human umbilical vein endothelial cells (HUVEC, CC-2517), endothelial cell growth medium (EGM), endothelial cell basal medium (EBM) and bovine brain extract (BBE) were from Lonza, USA. Most primary antibodies including anti-TRPC1 (ACC-010), anti-TRPV4 (ACC-034), anti-STIM1 (ACC-063) were from Alomone Labs. Fura-2/AM and pluronic F127 were from Molecular Probes Inc. Fetal bovine serum (FBS), Dulbecco's modified Eagle's medium (DMEM), Phosphate Buffered Saline (PBS), N,N,N',N'-Tetrakis-(2-pyridylmethyl)-ethylenediamine (TPEN) were from Invitrogen. (+)-Brefeldin A (BFA), 4α-phorbol 12,13-didecanoate (4α-PDD) were from Calbiochem. Nonidet P-40, trypsin, albumin bovine serum (BSA), collagenase and poly-L-lysine were from Sigma. Cell surface protein isolation kit was from Pierce.

6.2.2 Cell culture

HEK293 cells were cultured in DMEM supplemented with 10% FBS, 100 μg/ml penicillin and 100 U/ml streptomycin. human umbilical vein endothelial cells (HUVECs) was cultured in EGM medium supplemented with 1% BBE, 100 μg/ml penicillin and 100 U/ml streptomycin.

6.2.3 Total internal fluorescence reflection microscopy (TIRFM)

TIRFM generates an evanescent field that declines exponentially with increasing distance from the interface between the coverglass and the cytoplasm, illuminating only a thin section (250 nm) of the cell in contact with the coverglass, including the plasma membrane (Axelrod, 2003). Briefly, fluorescence measurements of single cells were performed using total internal fluorescence reflection microscopy (TIRFM), with a 60x 1.45 N.A. objective (Olympus, Japan), where samples were excited by using a 440nm laser for ECFP and a 513nm laser for EYFP. In this configuration, the microscope uses only a dual-band pass dichroic mirror to separate the excitation and emission light, with no excitation filters used. ECFP and EYFP emission light was simultaneously harvested using the DualView splitter (Photometrics), equipped with a filter cube containing S470/30nm and S535/30nm emission filters for ECFP and EYFP emission, respectively, and a 505nm dichroic mirror for separation of emission wavelengths. Fluorescence images were collected with a back-illuminated electron-multiplying charge-coupled device (EMCCD) camera (Photometric QuantEM 512SC). MetaMorph software was used to control the protocol of acquisition and to perform data analysis.

6.2.4 Biotinylation of surface proteins and immunoblots

Biotinylation of surface proteins was carried out using a cell surface protein isolation kit (catalog no. 89881; Pierce) as the manufacturer's instructions. In brief, prepare T75 cm^2 flasks of 90–95% confluent transfected HEK293 cells or HUVECs.

Stimulation with thapsigargin was conducted in NPSS. After stimulation, cells were washed with ice-cold phosphate buffered saline (PBS) and then Sulfo-NHS-SS linked biotin was added in PBS and incubated on ice for 10 min at 4 °C. Addition of quenching solution to quench the reaction and the cells were washed with PBS to remove free biotin. Lysates were prepared in standard lysis buffer, which contained 1.5% (vol/vol) Nonidet P-40, 150 mM NaCl, 50 mM NaF, 50 mM Tris-HCl, pH 8.0, with addition of protease inhibitor cocktail tablets (Bezzerides et al., 2004). Cell lysate was cleared by centrifugation, and then biotinylated proteins were precipitated by incubation with immobilized NeutAvidin Gel (agarose beads; Pierce) 60 min at room temperature. The beads were washed with washing buffer including protease inhibitors. The bound proteins were released by incubation with sample buffer at room temperature and then resolved by SDS-PAGE sample buffer containing 50 mM DTT for immunoblot analysis. Immunoblots were as described elsewhere (Kwan et al., 2009). Proteins from transfected HEK cells and HUVECs were then transferred to a PVDF membrane. The membrane was incubated at 4°C overnight with the primary anti-TRPV4 (1:200), anti-TRPC1 (1:200), or anti-STIM1 (1:200) in PBST buffer containing 0.1% Tween 20 and 5% nonfat dry milk. Immunodetection was accomplished using horseradish peroxidase-conjugated secondary antibody, followed by ECL detection system.

6.2.5 Cloning and transfection

Human TRPC1 cDNA (NM_003304) was obtained by RT-PCR from human coronary endothelial cells CC2585 (BioWhittaker). $TRPV4^{M680D}$ and $TRPC1^{Mut\text{-}pore}$, each has mutation at channel pore region, was described elsewhere (Liu *et al.*, 2003;Voets *et al.*, 2002b). For TIRFM, TRPV4 was tagged with CFP at its C-terminus, and TRPC1 was tagged with YFP at its N-terminus. All genes were cloned into pcDNA6 vector for expression. The nucleotide sequences of all constructs were verified with DNA sequencing. TRPC1-siRNA and scramble control were from Ambion. The sequences for human TRPC1-siRNA were

GGAUGUGCGGGAGGUGAAGtt (sense strand) and CUUCACCUCCCGCACAUCCtt (antisense strand) as described by others (Alicia et al., 2008). The sequences for human TRPV4-siRNA were GUCUUCAACCGGCCUAUCCuu (sense strand) and GGAUAGGCCGGUUGAAGACuu (antisense strand) as described by others (Pan et al., 2008). The sequences for human STIM1-siRNA were GCCUAUAUCCAGAACCGUUtt (sense strand) and AACGGUUCUGGAUAUAGGCaa (antisense strand) as described by others (Lefkimmiatis et al., 2009).

Transfection condition was as described elsewhere (Kwan et al., 2009). Briefly, HEK293 cells were transfected with various constructs using Lipofectamine 2000. Abound 6×10^4 HEK293 cells were grown in each well of the 6-well plates. Transfection was done with 4 μg plasmid and 6 μl Lipofectamine 2000 in 200 μl Opti-MEM reduced serum medium in 6-well plates. HUVECs were transfected with TRPC1-siRNA, TRPV4-siRNA, STIM1-siRNA or a scrambled-siRNA as control by electroporation using Nucleofector II following the procedure in manufacturer's instruction manual. About 80% of HEK293 cells and about 70% of HUVECs were successfully transfected by respective protocols as indicated by control transfection using a GFP-expressing pCAGGS vector. Functional studies were performed 2-3 days post-transfection.

6.2.6 $[Ca^{2+}]_i$ measurement

$[Ca^{2+}]_i$ in cultured cells was measured as described elsewhere 8. Briefly, cultured HEK cells or HUVECs were loaded with 10 μM Fura-2/AM and 0.02% pluronic F-127 for 1 hour in dark at 37°C in normal physiological saline solution (NPSS). In experiments studying the store-operated Ca^{2+} influx, Ba^{2+} was used as surrogate ion to avoid cytosolic Ca^{2+} buffering (Parekh and Putney, Jr., 2005). In these experiments, cells were pre-treated with thapsigargin (4 μM, 20 min) to deplete intracellular Ca^{2+} stores, followed by changing extracellular medium from a Ca^{2+}-free ($0Ca^{2+}$-PSS) to a

Ba^{2+}-containing solution (1 Ba^{2+}-PSS). $0Ca^{2+}$-PSS contained in mM: 140 NaCl, 5 KCl, 1 $MgCl_2$, 10 glucose, 2 EGTA and 5 Hepes, pH 7.4; 1 Ba^{2+}-PSS contained in mM: 140 NaCl, 5 KCl, 1 $BaCl_2$, 1 $MgCl_2$, 10 glucose, 5 Hepes, pH 7.4. For 4α-PDD-stimulated Ca^{2+} influx experiments, the cells were pre-treated with 4 μM thapsigargin for 20 min in NPSS. $[Ca^{2+}]_i$ change in response to 4α-PDD (5 μM) was then measured. NPSS contained in mM: 140 NaCl, 5 KCl, 1 $CaCl_2$, 1 $MgCl_2$, 10 glucose, 5 Hepes, pH 7.4. In flow experiments, flow was initiated by pumping NPSS to a specially-designed parallel plate flow chamber (Ma et al., 2010), in which the cells were adhered to the bottom. We used a flow rate with shear stress of ~5 dyne/cm2. Fura-2 fluorescence signals were measured using dual excitation wavelengths at 340 and 380 nm using an Olympus fluorescence imaging system. Changes in $[Ca^{2+}]_i$ or $[Ba^{2+}]_i$ were displayed as change in Fura-2 ratio. If needed, BFA (5 μM) was introduced 30 min before application of thapsigargin.

6.2.7 Whole-cell patch clamp

Whole cell current was measured with an EPC-9 patch clamp amplifier as described elsewhere (Voets *et al.*, 2002b). Cells were clamped at 0 mV. Whole cell current density (pA/pF) was recorded in response to successive voltage pulses of +80 mV and -80 mV for 100 ms duration. These whole cell current values were then plotted *vs.* time. The recordings were made before and after 4α-PDD (5 μM) application. For 4α-PDD-operated current, the pipette solution contained in mM: 20 CsCl, 100 Cs^+-aspartate, 1 $MgCl_2$, 4 ATP, 0.08 $CaCl_2$, 10 BAPTA, 10 Hepes, pH 7.2. Bath solution contained in mM: 150 NaCl, 6 CsCl, 1 $MgCl_2$, 1.5 $CaCl_2$, 10 glucose, 10 Hepes, pH 7.4. The store-dependent cation current was recorded with pipette solution containing in mM:140 CsCl, 2 $MgCl_2$, 1 ATP, 5 EGTA, 10 HEPES, pH 7.2, and the bath solution containing in mM: 140 NaCl, 5 KCl, 0.5 EGTA, 10 HEPES, pH 7.4. The bath solution was then was replaced by a divalent-free medium supplemented with 140 mM NMDG-Cl. If needed, BFA (5 μM) was introduced 30 min before application of thapsigargin.

6.2.8 Statistics

Student's t-test was used for statistical comparison, with probability $p<0.05$ as a significant difference. For comparison of multiple groups, One-way ANOVA with Newman-keuls was used.

6.3 Results

6.3.1 Effect of Ca^{2+} store depletion on translocation of TRPV4-TRPC1 complex to the plasma membrane in overexpression system

TIRFM utilizes evanescent wave to illuminate fluorophores within 250 nm of the plasma membrane (Steyer and Almers, 2001). It is a valuable method for observing protein movements within the periplasmic space. In these experiments, HEK293 cells were first co-transfected with CFP-tagged TRPV4 and YFP-tagged TRPC1 to allow the formation of TRPV4-TRPC1 complex (Ma *et al.*, 2010). Treatment of the cells with thapsigargin or TPEN, each of which depletes intracellular Ca^{2+} stores, induced a time-dependent increase of TRPV4 and TRPC1 fluorescence in periplasmic space. The appearance of TRPV4 and TRPC1 fluorescence matched well temporally and spatially (Chapter 6 Figure. 1A and C), which is even more evident when single vesicle fluorescence was examined (Chapter 6 Figure. 1C). The fluorescence peaked at ~2 min after TG treatment, then gradually dissipated with the average residency time of 309 ± 11 s (n = 62 cells). BFA, a blocker of protein translocation from trans-Golgi to the plasma membrane, abrogated the fluorescence increase (Chapter 6 Figure 1B). These data suggest that store depletion stimulates the translocation of vesicles containing TRPV4-TRPC1 complex close to the plasma membrane. As a control, thapsigargin treatment had no effect on the fluorescence of Pmem-YFP (Chapter 6 Figure 7), which is the fluorescent marker of the plasma membrane. This control excluded the possibility of the plasma membrane movement in the axial direction during the experiments.

TIRFM detects the protein movement within the periplasmic space, but it does not necessarily define surface expression itself. Thus cell surface biotinylation methods were used. In agreement with the results from TIRFM experiments, thapsigargin treatment increased the amount of biotinylated TRPV4 and TRPC1 by 70 ± 11% (n = 4) and 64% ± 14% (n = 3), respectively, indicating an increase in cell surface TRPV4 and TRPC1 (Chapter 6 Figure. 2A and B).

In HEK cells that were over-expressed with only one construct (TRPV4 or TRPC1 alone), thapsigargin treatment failed to significantly stimulate the trafficking of respective proteins as determined by biotinylation experiments (Chapter 6 Figure. 2C) and TIRFM (Chapter 6 Figure 2D), suggesting that TRPV4-TRPC1 complex are more favorably delivered to the plasma membrane than TRPV4 or TRPC1 homomers.

6.3.2 Functional study of TRPV4-TRPC1 complex

In whole-cell patch clamp recording, thapsigargin (4 μM) induced a large cation current in TRPV4 and TRPC1 co-expressing cells, but it only had minimal effect in cells transfected with TRPV4 (or TRPC1) alone (Chapter 6 Figure 3A). This cation current was sensitive to RuR, which is an inhibitor of TRPV4-TRPC1 complex (Ma et al., 2010). Store-operated Ba^{2+} influx was also studied. Here, the cells were pre-treated with thapsigargin (4 μM, 20 min) to deplete intracellular Ca^{2+} stores, followed by changing extracellular medium to a Ba^{2+}-containing solution (1 Ba^{2+}-PSS). The store-operated Ba^{2+} influx was much larger in cells co-transfected with TRPV4 and TRPC1 than in those transfected with TRPV4 (or TRPC1) alone (Chapter 6 Figure 3B). Furthermore, BFA inhibited the thapsigargin-stimulated cation current (Chapter 6 Figure 3A) and Ba^{2+} influx (Chapter 6 Figure 3B).

4α-PDD is synthetic phorbol ester that can activate TRPV4 homomers (Voets *et al.*, 2002b) and TRPV4-TRPC1 heteromers (Ma *et al.*, 2010). We further tested the effect of thapsigargin treatment on 4α-PDD-stimulated cation current and Ca^{2+} influx. The results show that thapsigargin treatment potentiated the 4α-PDD-stimulated cation current (Chapter 6 Figure 3C) and 4α-PDD-stimulated Ca^{2+} influx (Chapter 6

Figure 3D), the effect of which was abolished by BFA (Chapter 6 Figure 3C and D).

These data support the notion that Ca^{2+} store depletion facilitates the translocation of TRPV4-TRPC1 complex into the plasma membrane, and that the TRPV4-TRPC1 complex is delivered to the plasma membrane more favorably than TRPC1 homomer or TRPV4 homomer.

6.3.3 Participation of STIM1

To explore the role of STIM1 in TRPV4-TRPC1 complex translocation, we utilized a STIM1-specific siRNA (Lefkimmiatis et al., 2009), which could effectively "knock-down" the expression level of STIM1 proteins (Chapter 6 Figure 4A). This STIM1-siRNA markedly reduced in thapsigargin-induced translocation of TRPV4-TRPC1 complex as detected by TIRFM (Chapter 6 Figure 4B). In functional studies, the STIM1-siRNA reduced the thapsigargin-induced Ba^{2+} influx (Chapter 6 Figure 4C) as well as 4α-PDD-stimulated Ca^{2+} influx (Chapter 6 Figure 4D).

6.3.4 Effect of thapsigargin on TRPV4-TRPC1 complex translocation in native endothelial cells

TRPV4-TRPC1 heteromeric channels play important functional roles in vascular endothelial cells (Ma *et al.*, 2010). Thus we explored whether Ca^{2+} store depletion can facilitate the translocation of TRPV4-TRPC1 complex to the plasma membrane in HUVECs. Biotinylation experiments demonstrated that thapsigargin treatment (4 μM) markedly increased the TRPV4 and TRPC1 proteins in the plasma membrane (Chapter 6 Figure 5A), while it had no effect on total amount of cellular TRPV4 and TRPC1 proteins (Chapter 6 Figure 5A). TRPC1-siRNA and TRPV4-siRNA were utilized, each of which was capable of "knock-downing" the expression of its targeted genes (Chapter 6 Figure 8). Intriguedly, suppressing the TRPC1 protein expression using TRPC1-siRNA reduced the TRPV4 translocation to the plasma membrane (Chapter 6 Figure 5B), and TRPV4-siRNA reduced the TRPC1 translocation (Chapter 6 Figure 5B).

In functional studies, thapsigargin treatment potentiated the 4α-PDD-stimulated Ba^{2+} influx in HUVECs (Chapter 6 Figure 5C), the effect of which was abolished by TRPC1-siRNA, TRPV4-siRNA, STIM1-siRNA, and BFA, suggesting an involvement of TRPV4-TRPC1 complex and vesicle trafficking. 4α-PDD activates both TRPV4 homomers (Voets *et al.*, 2002b) and TRPV4-TRPC1 complex (Ma et al., 2010). However, this potentiated Ba^{2+} influx in response to 4α-PDD could only be assigned to TRPV4-TRPC1 complex, because the potentiation was inhibited by TRPC1-siRNA and a pore mutant of TRPC1 ($TRPC1^{Multi\text{-}pore}$)(Liu et al., 2003) (Chapter 6 Figure 5C). We also examined the store-operated Ba^{2+} influx, to which the TRPV4-TRPC1 complex may also contribute. This influx in HUVECs was reduced by BFA, TRPC1-siRNA, STIM1-siRNA, TRPV4-siRNA, and a pore mutant of TRPV4 ($TRPV4^{M680D}$) (Voets *et al.*, 2002b) (Chapter 6 Figure 5D), again suggesting an involvement of TRPV4-TRPC1 complex and vesicle trafficking.

These results are consistent with those obtained in TRPV4-TRPC1 co-expressing HEK cells, supporting the notion that Ca^{2+} store depletion in HUVECs stimulates the translocation of TRPV4-TRPC1 complex to the plasma membrane, and that TRPV4-TRPC1 complex are more favorably delivered to the plasma membrane than TRPV4 or TRPC1 homomers.

6.3.5 Role of TRPV4-TRPC1 complex translocation in flow-induced Ca^{2+} influx in native endothelial cells

An important function of TRPV4-TRPC1 complex is to mediate flow-induced Ca^{2+} influx in vascular endothelial cells (Ma *et al.*, 2010). Previously, it is found that Ca^{2+} store depletion potentiated the flow-induced Ca^{2+} influx in these cells (Kwan et al., 2003). We next examined whether this potentiation of Ca^{2+} influx in response to flow is related to TRPV4-TRPC1 translocation. Chapter 6 Figure 6A showed that Ca^{2+} store depletion potentiated the Ca^{2+} response to flow. This potentiation was abolished by BFA, TRPV4-siRNA, TRPC1-siRNA, $TRPV4^{M680D}$ and $TRPC1^{Mut\text{-}pore}$ (Chapter 6 Figure 6A and B), suggesting an involvement of TRPV4-TRPC1 complex and vesicle

translocation.

6.4 Discussion and conclusion

Although still under debating, a large volume of data suggests that TRPC channels contribute to SOC in many cell types at least under certain conditions (Beech, 2005;Lee et al., 2009). The major mechanism in SOC involves the gating of TRPC channels by STIM1 (Lee et al., 2009;Yuan et al., 2007). Alternatively, SOC could be due to an enhanced insertion of TRPC isoforms, such as TRPC3 (Kim et al., 2006) and TRPC6, into the plasma membrane (Cayouette et al., 2004). In addition to TRPC, a member of TRPV family TRPV6 was suggested to be a potential mediator of SOC (Yue et al., 2001). But this finding has been seriously challenged (Kahr *et al.*, 2004;Voets *et al.*, 2001). In the present study, we co-expressed the TRPV4 and TRPC1 in HEK cells to allow the formation of TRPV4-TRPC1 heteromeric channels (Ma et al., 2010), and then investigated the effect of Ca^{2+} store depletion on the trafficking of TRPV4-TRPC1 heteromeric channels to the plasma membrane. TIRFM and biotin surface labeling experiments show that Ca^{2+} store depletion by thapsigargin enhanced the plasma membrane expression of both TRPV4 and TRPC1. The increased surface expression is related to vesicle trafficking, because BFA abolished it. TIRFM experiments also demonstrated that TRPC1 and TRPV4 are inserted onto the plasma membrane as TRPV4-TRPC1 complex rather than as individual subunit, because the appearance of TRPV4 and TRPC1 fluorescence on the plasma membrane matched well temporally and spatially (Chapter 6 Figure 1). Interestingly, it appears that TRPV4-TRPC1 complex is more favorably delivered to the plasma membrane than TRPC1 homomer or TRPV4 homomer, because overexpression of one isoform (either TRPC1 or TRPV4) markedly enhanced the plasma membrane insertion of the other component.

In functional studies, the patch clamp and Ba^{2+} influx studies found that Ca^{2+} store depletion by thapsigargin caused a marked increase in cation current and Ca^{2+}

influx in TRPV4-TRPC1 co-expressing HEK cells. Ca^{2+} store depletion also enhanced 4α-PDD-stimulated cation current and Ba^{2+} influx in these cells. The increase in cation current and Ba^{2+} influx was diminished by BFA. Furthermore, the cation current and Ba^{2+} influx were much larger in TRPV4-TRPC1-coexpressing cells than in cells overexpressed with TRPC1 or TRPV4 alone. These data are consistent with TIRFM and biotinylation experiments, supporting the notion that Ca^{2+} store depletion facilitates the vesicle trafficking, resulting in the insertion of more TRPV4-TRPC1 complex into the plasma membrane, and that the TRPV4-TRPC1 complex is delivered to the plasma membrane more favorably than TRPC1 homomer or TRPV4 homomer. To our knowledge, this is the first study to demonstrate that Ca^{2+} store depletion can enhance the trafficking of a heteromeric TRP channel onto the plasma membrane.

Substantial amount of evidence indicates that STIM1 is the Ca^{2+} sensor in endoplasmic reticulum (Cahalan, 2009;Lee *et al.*, 2009). Ca^{2+} store depletion results in the formation and translocation of STIM1 clusters to the region of ER just underneath the plasma membrane. STIM1 also functions to recruit TRPC to specialized plasma membrane microdomain named lipid rafts (Alicia *et al.*, 2008;Pani *et al.*, 2008). At this ER-PM junction, STIM1 directly or indirectly gate TRPC channels (Cahalan, 2009;Lee *et al.*, 2009). In the present study, we found that knocking down of STIM1 using STIM1-siRNA markedly suppressed the delivery of TRPV4-TRPC1 heteromeric channels to the plasma membrane, suggesting that STIM1 is also important in controlling vesicle trafficking and the plasma membrane insertion of TRPV4-TRPC1 complex.

TRPV4-TRPC1 heteromeric channels are present in native vascular endothelial cells, where they mediates flow-induced endothelial $[Ca^{2+}]_i$ influx and subsequent vascular relaxation (Ma *et al.*, 2010). Flow-induced Ca^{2+} influx is subjected to a negative feedback regulation in which an elevated $[Ca^{2+}]_i$ level, through nitric oxide-cGMP-protein kinase G pathway, eventually inhibits further Ca^{2+} influx. TRPV4-TRPC1 complex is an important component in this negative feedback circuit.

This channel is activated by flow to allow Ca^{2+} influx, and at the same time serves as the target of PKG inhibition (Ma *et al.*, 2010). Because of the overall functional importance of TRPV4-TRPC1 complex, studying the membrane trafficking of this complex in native endothelial cells is of great value. In the present study, biotinylation experiments showed that depletion of intracellular Ca^{2+} stores in endothelial cells enhanced the expression of both TRPV4 and TRPC1 proteins on the plasma membrane. The enhanced surface expression of one component (either TRPV4 or TRPC1) is largely dependent on the presence of the other component. Thapsigargin treatment also enhanced two TRPV4-TRPC1 related functions: SOC and 4α-PDD-stimulated Ca^{2+} influx. The action of thapsigargin is inhibited by BFA, suggesting the involvement of vesicle trafficking. Taken together, these data suggest that store depletion enhanced the expression of TRPV4-TRPC1 complex in the plasma membrane to bring about SOC in vascular endothelial cells.

Previously, Ca^{2+} store depletion was found to enhance the flow-induced Ca^{2+} influx in vascular endothelial cells (Kwan et al., 2003). Here we explored whether an enhanced delivery of TRPV4-TRPC1 complex to the plasma membrane could be the underlying mechanism for this phenomenon. Our results showed that siRNAs or pore mutants against each TRP isoform (TRPV4 or TRPC1) could suppress the flow-induced Ca^{2+} influx in vascular endothelial cells, supporting that TRPV4-TRPC1 complex mediates the flow-induced Ca^{2+} influx. The facilitating effect of store depletion (thapsigargin) on flow-induced Ca^{2+} influx was inhibited by BFA, suggesting an involvement of vesicle trafficking. These data support the notion that Ca^{2+} store depletion enhances the vesicle trafficking, adding more TRPV4-TRPC1 channels on the plasma membrane, resulting in an increased Ca^{2+} influx in response to flow.

In conclusion, we demonstrated that depletion of intracellular Ca^{2+} stores induced a rapid incorporation of TRPV4-TRPC1 complex into the plasma membrane in both the TRPV4-TRPC1 overexpressing HEK cells and in native endothelial cells.

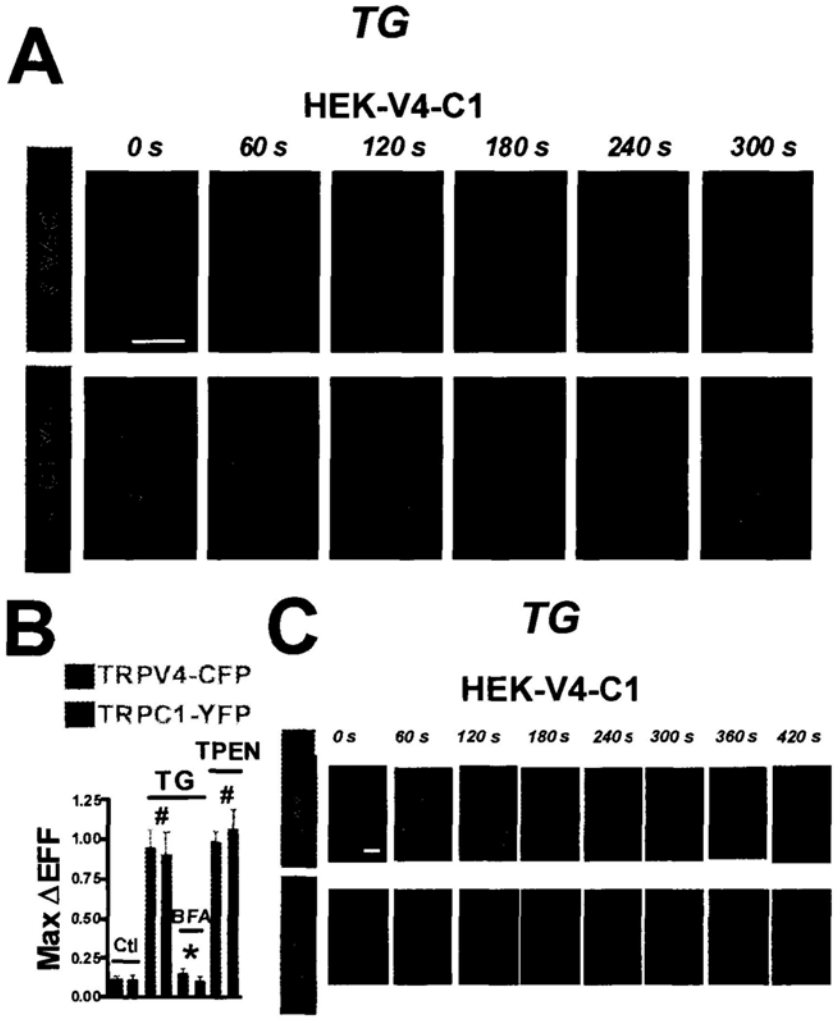

Chapter 6 Figure 1. Effect of Ca^{2+} store depletion on the translocation of TRPV4-TRPC1 complex to the plasma membrane as measured by TIRFM. A, Evanescent field fluorescent (EFF) images of a single HEK cell expressing TRPV4-CFP and TRPC1-YFP. Cells were incubated with thapsigargin (TG, 4 μM) for the indicated times. Scale bar is 5 μm. B, Summary data in experiments similar to A. Plotted was the maximum change in fluorescence in response to 4 μM TG or 1 mM TPEN. If needed, (+)-Brefeldin A (BFA, 5 μM) was introduced 30 min before application of TG. Mean ± SE (n=4-18). #, $P<0.05$ compared to the control. *, $P<0.05$ compared to the TG-treated cells stimulation without BFA. C, Consecutive EFF images of single vesicle translocation after TG stimulation. Time interval between each consecutive image is 60 s. Scale bar is 1 μm.

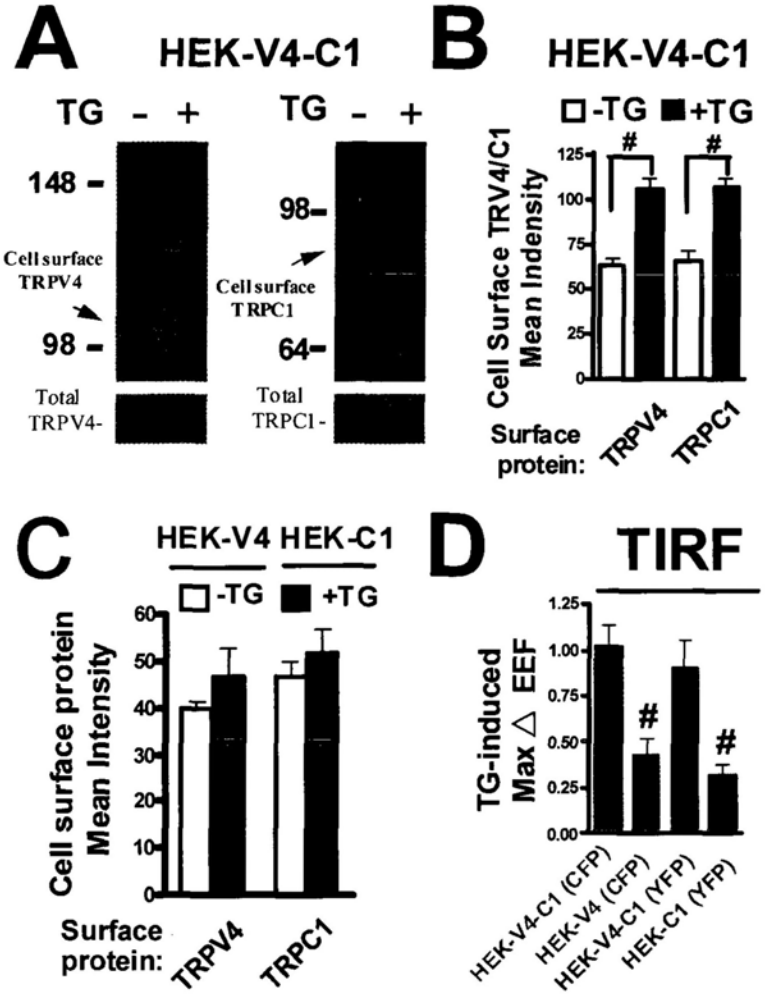

Chapter 6 Figure 2 Thapsigargin-induced translocation of TRPC1, TRPV4, and TRPV4-TRPC1 as measured by cell surface biotinylation and TIRFM. HEK cells were transfected with TRPV4, TRPC1, or TRPV4 plus TRPC1. The cells then treated with or without thapsigargin (TG, 4 μM), followed by biotinylation assay (A-C) or TIRFM (D). Shown were representative image (A) and summary data (B, C) of cell surface biotinylation experiments in cells transfected with TRPV4 (C), TRPC1 (C) or co-transfected with TRPV4 plus TRPC1 (A, B). D, Comparison of TG-induced increase of EFF intensity in cells expressed with TRPV4-CFP, TRPC1-YFP, or TRPV4-CFP plus TRPC1-YFP. Mean ± SE. (n = 3-4 experiments for A-C, or 7-18 cells for D). #, $P<0.05$ compared to the control.

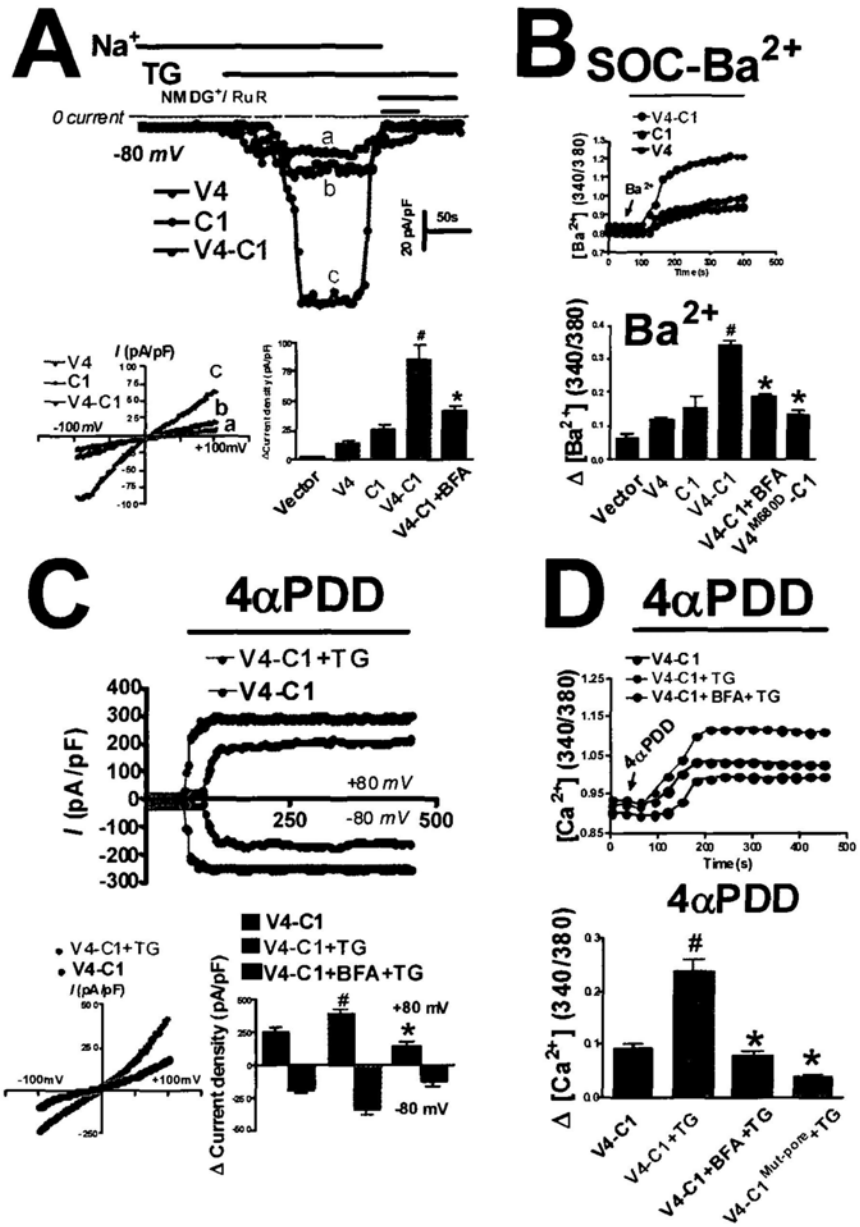

Chapter 6 Figure 3. Thapsigargin-induced cation current, store-operated Ba^{2+} influx, and 4α-PDD-stimulated responses. HEK cells were transfected with TRPV4 (A, B), TRPC1 (A, B), or TRPV4 plus TRPC1 (A-D). A and B, store-operated cation current (A) and Ba^{2+} influx (B). C and D, 4α-PDD-stimulated cation current (C) and C a^{2+} influx (D). For cation currents (A and C), shown were representative current traces at -80 mV (A, upper panel) or at ± 80 mV (C, upper

panel), corresponding I-V curves (low left panel), and summary data for the maximal change in current in response to thapsigargin (A) or 4α-PDD (C). In B (the store-operated Ba^{2+} influx and D (4α-PDD-stimulated Ca^{2+} influx), shown were representative traces (upper panel) and summary data for the maximal change in $[Ba^{2+}]_i$ (B, lower panel) and $[Ca^{2+}]_i$ (D, lower panel). $TRPV4^{M680D}$ was used to replace TRPV4 in some experiments as labeled. TG, 4 μM; 4α-PDD, 5 μM; BFA, 5 μM. Mean ± SE. (n = 3-6 experiments for B and D, or 5-8 cells for A and C). #, $P<0.05$ compared to the cells transfected with either TRPV4 or TRPC1 alone (in A and B), or the cells without TG pretreatment (in C and D). *, $P<0.05$ compared to the bar labeled with # in the same panel.

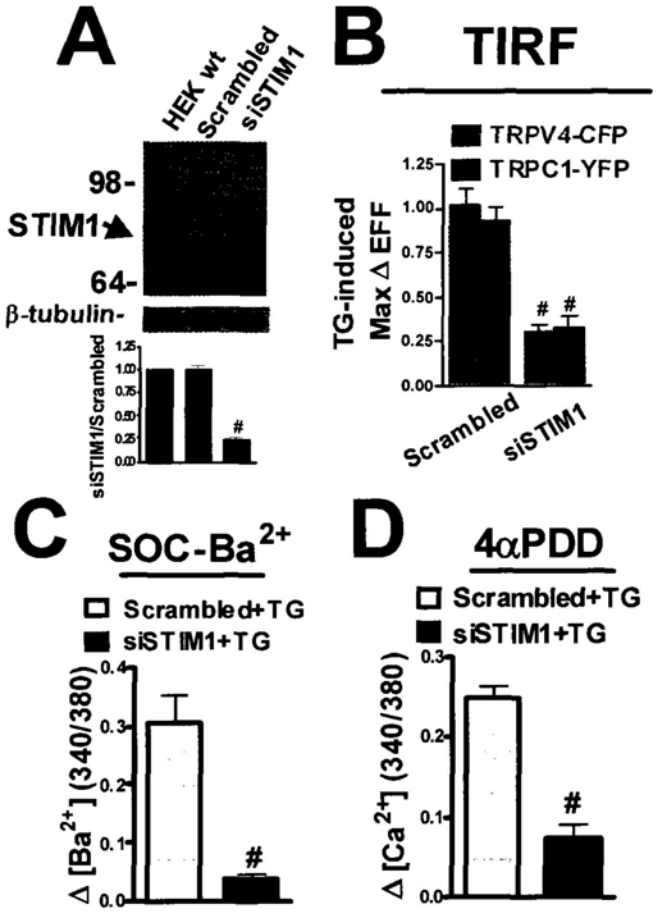

Chapter 6 Figure 4. Involvement of STIM1 in the translocation of TRPV4-TRPC1 complex in response to Ca^{2+} store depletion. A, representative images (top) and summary (bottom) of immunoblot experiments showing the effectiveness of STIM1-siRNA. In B-D, TRPV4-TRPC1-coexpressing HEK cells were treated with thapsigargin (TG, 4 μM), followed by TIRFM (B) or functional studies (C and D). STIM1-siRNA diminished the TG-induced increase in EFF intensity (B, for TRPV4-CFP and TRPC1-YFP), store-operated Ba^{2+} influx (C) and 4α-PDD-stimulated Ca^{2+} influx (D). Shown were representative image (A) and summary data (A-D). Mean ± SE. (n = 3 for A, 6-9 cells for B, 3-4 experiments for C and D). #, $P<0.05$ compared to the scrambled siRNA.

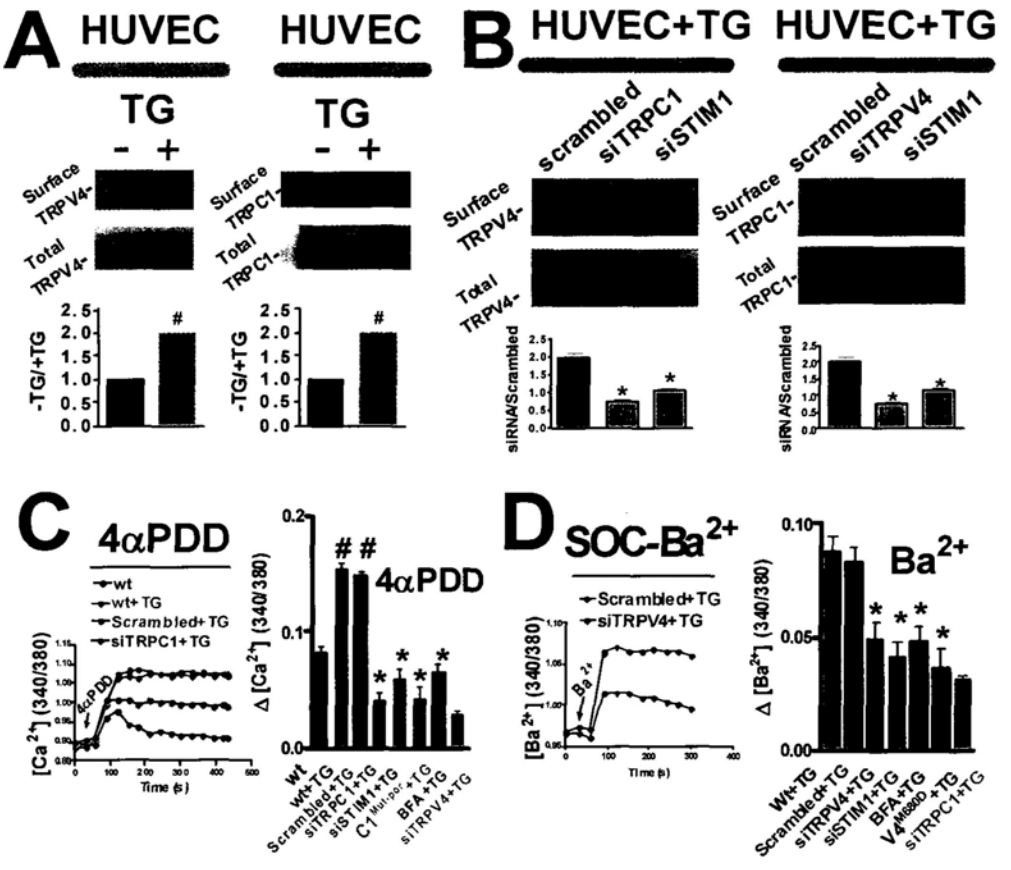

Chapter 6 Figure 5. Thapsigargin-induced change in cell surface TRPV4-TRPC1, store-operated Ba^{2+} influx, and 4α-PDD-stimulated Ca^{2+} influx in HUVECs. A, Representative images (upper) and summary (lower) of thapsigargin (TG, 4 μM)-induced increases in cell surface TRPV4 (left) and TRPC1 (right) proteins as measured by biotinylation. B, Representative images (upper) and summary (lower) of thapsigargin (TG, 4 μM)-induced increases in cell surface TRPV4 (left) and TRPC1 (right) proteins as measured by biotinylation in the presence of TRPC1-siRNA or TRPV4-siRNA or STIM1-siRNA or scrambled-siRNA. In C (4α-PDD-stimulated Ca^{2+} influx) and D (the store-operated Ba^{2+} influx), shown were representative traces (left) and summary data for the maximal change in $[Ca^{2+}]_i$ (C, right) and $[Ba^{2+}]_i$ (D, right). TG, 4 μM; 4α-PDD, 5 μM; BFA, 5 μM. Mean ± SE (n =3-6 experiments for A-D). #, P<0.05 compared to cells without TG in A and C. *, P<0.05 compared to scrambled-siRNA (for siRNA experiments), or to TG-treatment cells without BFA/pore mutant.

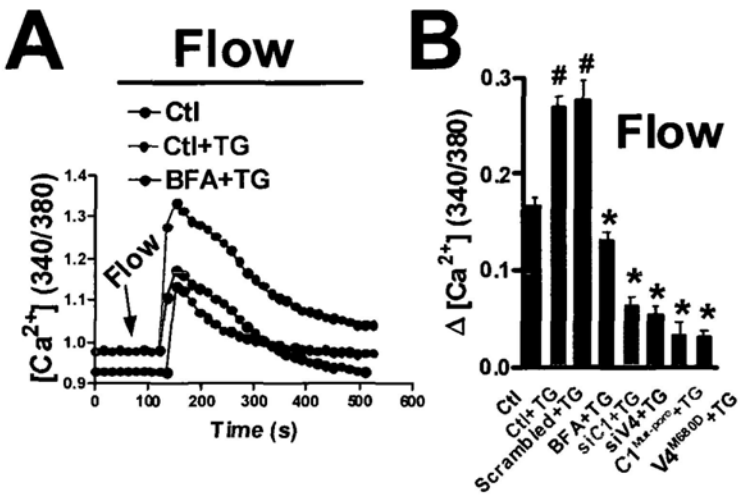

Chapter 6 Figure 6. Potentiation of flow-induced Ca^{2+} influx by thapsigargin, and the role of TRPV4-TRPC1 complex translocation in HUVECs. Shown were representative traces (left) and summary data for the maximal change in $[Ca^{2+}]_i$ (right). TG, 4 μM; BFA, 5 μM. Mean ± SE (*n* = 4-5 experiments, 8 to 20 cells per experiment). #, $P<0.05$ compared to cells without TG. *, $P<0.05$ compared to scrambled-siRNA (for siRNA experiments), or to TG-treatment cells without BFA/pore mutant.

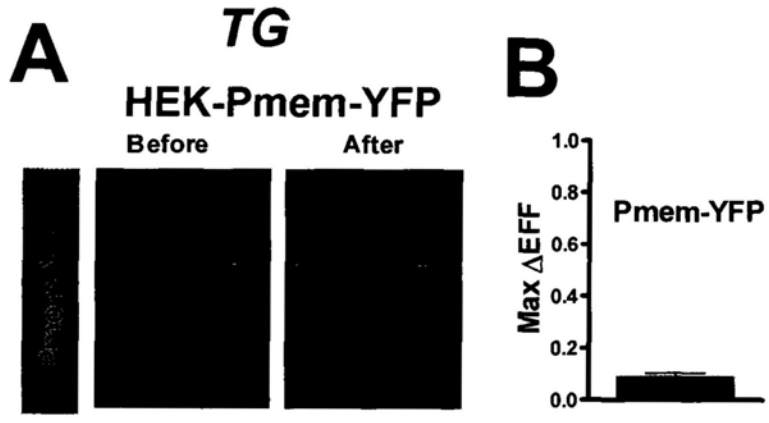

Chapter 6 Figure 7. Effect of thapsigargin on EFF of Pmem-YFP in TIRFM. A, EFF images of a single HEK cell expressing Pmem-YFP before (left) and 2.5 min after TG (right). B, Summary data as in A after stimulation with thapsigargin (TG, 4 μM). Mean ± SE (n = 11).

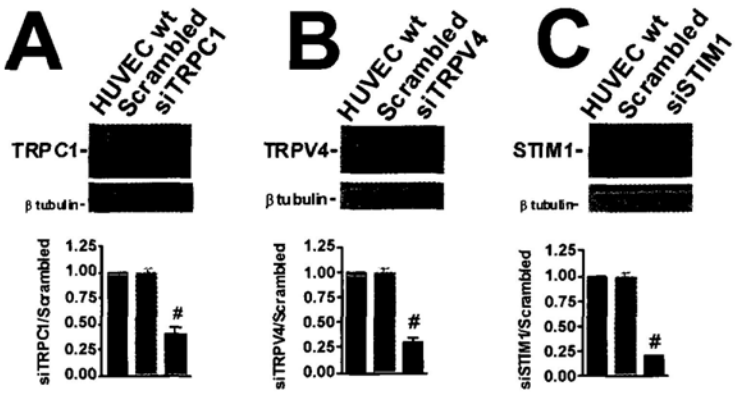

Chapter 6 Figure 8. Effectiveness of siRNAs against their respective targets in HUVECs. Shown were representative images (top) and summary (bottom) of immunoblot experiments. A, TRPC1-siRNA series; B, TRPV4-siRNA series; C, STIM1-siRNA series. Mean ± SE (3-4 experiments). #, $P<0.05$ compared to the scrambled siRNA.

Chapter 7

General discussion and conclusion

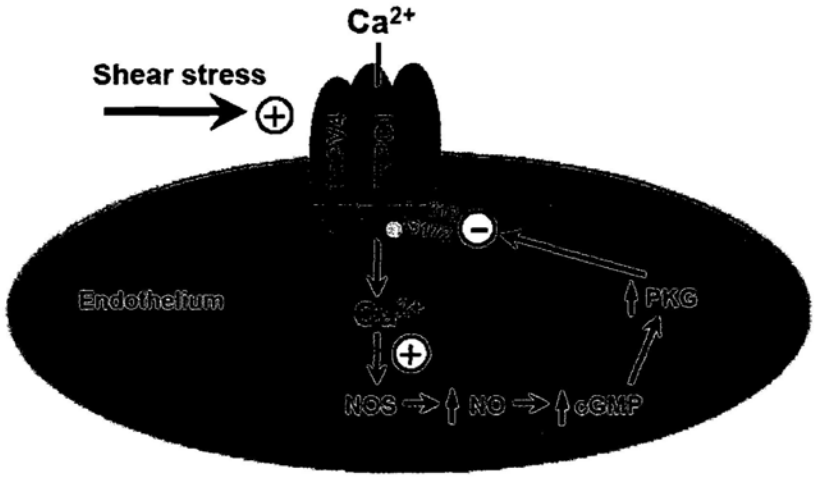

Chapter 7 Figure 1. Proposed model for flow-stimulated signal transduction involving TRPV4-TRPC1 heteromeric channels. A TRPV4-TRPC1 heteromeric channel is activated by flow stimulation. Extracellular Ca^{2+} entry activates nitric oxide synthase (NOS) to produce NO, which subsequently elevates intracellular cGMP. As a feedback regulation, the intracellular cGMP, via protein kinase G, inhibits the Ca^{2+} entry by inhibiting the TRPV4-TRPC1 heteromeric channel.

The ability of different TRP channels to interact physically and functionally is well known (Hofmann *et al.*, 2002;Strubing *et al.*, 2001). Heteromeric interaction between different TRP isoforms has been documented mostly within the same TRP subfamily such as between TRPC1 and TRPC3 and between TRPV5 and TRPV6 (Montell, 2005). Only in two cases, heteromeric assembly has been identified across different TRP subfamilies, i.e. between TRPC1 and TRPP2 (Tsiokas *et al.*, 1999), and between TRPV4 and TRPP2 (Kottgen *et al.*, 2008). In the present study, we provide the first evidence for heteromeric assembly across TRPC and TRPV subfamilies (Chapter 7 Figure 1). We demonstrated that TRPC1 interacts physically with TRPV4

to form a heteromeric functional channel complex in which C-terminal and N-terminal domains of both channels are required for heteromeric assembly. Compared to TRPV4 homomeric channels, TRPV4-TRPC1 heteromeric channels display a much slower decay of 4α-PDD-stimulated whole-cell current and a slightly larger single channel slope conductance. TRPV4-TRPC1 heteromer was slightly more permeable to Ca^{2+} but without change in relative permeability to monovalent cations. Importantly, although extracellular Ca^{2+} causes an inhibition of the current of TRPV4-TRPC1 heteromeric channel, the inhibition was significantly reduced compared with TRPV4 channel. Also, the characteristic of voltage-dependent block of TRPV4-TRPC1 channel was not quietly obvious as TRPV4 channel itself. These data indicate that heterologous expression of TRPV4 and TRPC1 can produce functionally distinct TRPV4-TRPC1 heteromeric channel different from TRPV4 homomers.

There is intense interest in searching for the molecular identity of the channels that mediate flow-induced Ca^{2+} influx. Previous studies from others suggest that TRPV4 is responsible for flow-induced Ca^{2+} influx (Gao *et al.*, 2003;Watanabe *et al.*, 2003;Wu *et al.*, 2007). In the present study, we found that TRPV4-TRPC1 heteromeric channels rather than TRPV4 are the real channels that are responsible for flow-induced Ca^{2+} influx in native endothelial cells. The physical association of TRPC1 with TRPV4 prolonged the flow-induced $[Ca^{2+}]_i$ transient and enabled the $[Ca^{2+}]_i$ transient to be negatively regulated by PKG. A prolonged Ca^{2+} influx would allow endothelial cells to produce more NO, enhancing vascular dilation. A negative regulation by PKG via Ca^{2+}-NO-cGMP-PKG pathway would prevent excessive $[Ca^{2+}]_i$ and NO, therefore protect endothelial cells from apoptosis and cell death. We also provided strong evidence that TRPV4-TRPC1 plays a crucial role in flow-induced vascular relaxation.

We also used a variety of different technology including TIRFM, cell surface biotinylation and functional studies to explore whether Ca^{2+} store depletion could affect vesicular trafficking of TRPV4-TRPC1 complex. Our results show that Ca^{2+} store depletion can stimulate the translocation of TRPV4-TRPC1 complex to the plasma membrane. Interestingly, it appears that TRPV4-TRPC1 complex is more

favorably delivered to the plasma membrane (or more efficiently) than TRPC1 homomer or TRPV4 homomer. We also found that STIM1 is important in controlling vesicle trafficking and the plasma membrane insertion of TRPV4-TRPC1 complex. Previously, Ca^{2+} store depletion was found to enhance the flow-induced Ca^{2+} influx in vascular endothelial cells (Kwan et al., 2003). Here we suggest that the underlying mechanism for this phenomenon is an enhanced insertion of TRPV4-TRPC1 channel complex into the plasma membrane under the condition of Ca^{2+} store depletion.

In further studies, we will try to explore the functional role of TRPV4-TRPC1 heteromeric channel *in vivo*. In other words, we want to further investigate the role of TRPC1 on the activities of TRPV4 channel *in vivo*. A recent report proposed that disrupting the TRPV4 gene in mice markedly reduced the sensitivity of the tail to pressure and acidic nociception (Suzuki *et al.*, 2003). Thus, similar approach such as measurement of pressure senvitivity by application of pressure on tail and acid sensation by application of 0.7% acetic acid to the abdomen will be performed in TRPC1 knockout mice *in vivo*.

Concerning the heteromeric coassembly of TRP subunits across different TRP subfamilies, three different coupling have been identified until now, that is TRPP2/TRPC1, TRPP2/TRPV4 and TRPC1/TRPV4. It is tempting to speculate that an existence of TRPC1-TRPV4-TRPP2 tri-complex or TRPC1-TRPV4-TRPP2 tri-subunit in tetramer. However, such speculation is very preliminary. For examples, these pull-down studies cannot differentiate whether it is due to the co-existence of multiple di-complex (TRPP2-TRPV4, TRPP2-TRPC1, and TRPV4-TRPC1 respectively) or an existence of TRPC1-TRPV4-TRPP2 tri-complex. Further experiments are needed for a definitive answer to the question.

In conclusion, we demonstrated that TRPV4 forms heteromeric complex with TRPC1. Such a complex displays characteristic electrophysiological properties different from that of TRPV4 homomeric channels. In native endothelial cells, TRPV4-TRPC1 complex plays an important role in flow-induced Ca^{2+} influx and subsequent vascular dilation.

REFERENCES

1. Alicia S, Angelica Z, Carlos S, Alfonso S, and Vaca L (2008) STIM1 converts TRPC1 from a receptor-operated to a store-operated channel: moving TRPC1 in and out of lipid rafts. *Cell Calcium,* **44,** 479-491.

2. Allen PB, Ouimet CC, and Greengard P (1997) Spinophilin, a novel protein phosphatase 1 binding protein localized to dendritic spines. *Proc Natl Acad Sci U S A,* **94,** 9956-9961.

3. Axelrod D (2003) Total internal reflection fluorescence microscopy in cell biology. *Methods Enzymol,* **361,** 1-33.

4. Bai CX, Giamarchi A, Rodat-Despoix L, Padilla F, Downs T, Tsiokas L, and Delmas P (2008) Formation of a new receptor-operated channel by heteromeric assembly of TRPP2 and TRPC1 subunits. *EMBO Rep,* **9,** 472-479.

5. Bao L, Rapin AM, Holmstrand EC, and Cox DH (2002) Elimination of the BK(Ca) channel's high-affinity Ca(2+) sensitivity. *J Gen Physiol,* **120,** 173-189.

6. Beech DJ (2005) TRPC1: store-operated channel and more. *Pflugers Arch,* **451,** 53-60.

7. Bevan JA (1997) Shear stress, the endothelium and the balance between flow-induced contraction and dilation in animals and man. *Int J Microcirc Clin Exp,* **17,** 248-256.

8. Bezzerides VJ, Ramsey IS, Kotecha S, Greka A, and Clapham DE (2004) Rapid vesicular translocation and insertion of TRP channels. *Nat Cell Biol,* **6,** 709-720.

9. Bichet D, Peters D, Patel AJ, Delmas P, and Honore E (2006) Cardiovascular polycystins: insights from autosomal dominant polycystic kidney disease and transgenic animal models. *Trends Cardiovasc Med,* **16,** 292-298.

10. bouAlaiwi WA, Takahashi M, Mell BR, Jones TJ, Ratnam S, Kolb RJ, and Nauli SM (2009) Ciliary polycystin-2 is a mechanosensitive calcium channel involved in nitric oxide signaling cascades. *Circ Res,* **104,** 860-869.

11. Brakeman PR, Lanahan AA, O'Brien R, Roche K, Barnes CA, Huganir RL, and Worley PF (1997) Homer: a protein that selectively binds metabotropic glutamate receptors. *Nature,* **386,** 284-288.

12. Brazer SC, Singh BB, Liu X, Swaim W, and Ambudkar IS (2003) Caveolin-1 contributes to assembly of store-operated Ca2+ influx channels by regulating plasma membrane localization of TRPC1. *J Biol Chem,* **278,** 27208-27215.

13. Bregman DB, Bhattacharyya N, and Rubin CS (1989) High affinity binding protein for the regulatory subunit of cAMP-dependent protein kinase II-B. Cloning, characterization, and expression of cDNAs for rat brain P150. *J Biol Chem,* **264,** 4648-4656.

14. Busse R and Fleming I (2003) Regulation of endothelium-derived vasoactive autacoid production by hemodynamic forces. *Trends Pharmacol Sci,* **24,** 24-29.

15. Cahalan MD (2009) STIMulating store-operated Ca(2+) entry. *Nat Cell Biol,* **11,** 669-677.

16. Caterina MJ, Rosen TA, Tominaga M, Brake AJ, and Julius D (1999) A capsaicin-receptor homologue with a high threshold for noxious heat. *Nature,* **398,** 436-441.

17. Caterina MJ, Schumacher MA, Tominaga M, Rosen TA, Levine JD, and Julius D (1997) The capsaicin receptor: a heat-activated ion channel in the pain pathway. *Nature,* **389,** 816-824.

18. Cayouette S and Boulay G (2007) Intracellular trafficking of TRP channels. *Cell Calcium,* **42,** 225-232.

19. Cayouette S, Lussier MP, Mathieu EL, Bousquet SM, and Boulay G (2004) Exocytotic insertion of TRPC6 channel into the plasma membrane upon Gq protein-coupled receptor activation. *J Biol Chem,* **279,** 7241-7246.

20. Cha SK, Wu T, and Huang CL (2008) Protein kinase C inhibits caveolae-mediated endocytosis of TRPV5. *Am J Physiol Renal Physiol,* **294,** F1212-F1221.

21. Chen J, Crossland RF, Noorani MM, and Marrelli SP (2009) Inhibition of TRPC1/TRPC3 by PKG contributes to NO-mediated vasorelaxation. *Am J Physiol Heart Circ Physiol,* **297,** H417-H424.

22. Cheng W, Yang F, Takanishi CL, and Zheng J (2007) Thermosensitive TRPV channel subunits coassemble into heteromeric channels with intermediate conductance and gating properties. *J Gen Physiol,* **129,** 191-207.

23. Chevesich J, Kreuz AJ, and Montell C (1997) Requirement for the PDZ domain protein, INAD, for localization of the TRP store-operated channel to a signaling complex. *Neuron,* **18,** 95-105.

24. Choy JC, Granville DJ, Hunt DW, and McManus BM (2001) Endothelial cell apoptosis: biochemical characteristics and potential implications for atherosclerosis. *J Mol Cell Cardiol,* **33,** 1673-1690.

25. Chubanov V, Waldegger S, Schnitzler M, Vitzthum H, Sassen MC, Seyberth HW, Konrad M, and Gudermann T (2004) Disruption of TRPM6/TRPM7 complex formation by a mutation in the TRPM6 gene causes hypomagnesemia with secondary hypocalcemia. *Proc Natl Acad Sci U S A,* **101,** 2894-2899.

26. Clapham DE, Julius D, Montell C, and Schultz G (2005) International Union of Pharmacology. XLIX. Nomenclature and structure-function relationships of transient receptor potential channels. *Pharmacol Rev,* **57,** 427-450.

27. Cohen AW, Hnasko R, Schubert W, and Lisanti MP (2004) Role of caveolae and caveolins in health and disease. *Physiol Rev,* **84,** 1341-1379.

28. Cooke JP, Rossitch E Jr, Andon NA, Loscalzo J, and Dzau VJ (1991) Flow activates an endothelial potassium channel to release an endogenous nitrovasodilator. *J Clin Invest,* **88,** 1663-1671.

29. Davies PF (1995) Flow-mediated endothelial mechanotransduction. *Physiol Rev,* **75,** 519-560.

30. Delmas P (2004) Polycystins: from mechanosensation to gene regulation. *Cell,* **118,** 145-148.

31. Dohke Y, Oh YS, Ambudkar IS, and Turner RJ (2004) Biogenesis and topology of the transient receptor potential Ca2+ channel TRPC1. *J Biol Chem,* **279,** 12242-12248.

32. Earley S, Gonzales AL, and Crnich R (2009) Endothelium-dependent cerebral artery dilation mediated by TRPA1 and Ca2+-Activated K+ channels. *Circ Res,* **104,** 987-994.

33. Earley S, Heppner TJ, Nelson MT, and Brayden JE (2005) TRPV4 forms a novel Ca2+ signaling complex with ryanodine receptors and BKCa channels. *Circ Res,* **97,** 1270-1279.

34. Embark HM, Setiawan I, Poppendieck S, van de Graaf SF, Boehmer C, Palmada M, Wieder T, Gerstberger R, Cohen P, Yun CC, Bindels RJ, and Lang F (2004) Regulation of the epithelial Ca2+ channel TRPV5 by the NHE regulating factor NHERF2 and the serum and glucocorticoid inducible kinase isoforms SGK1 and SGK3 expressed in Xenopus oocytes. *Cell Physiol Biochem,* **14,** 203-212.

35. Fagni L, Worley PF, and Ango F (2002) Homer as both a scaffold and transduction molecule. *Sci STKE,* **2002,** re8.

36. Falcone JC, Kuo L, and Meininger GA (1993) Endothelial cell calcium increases during flow-induced dilation in isolated arterioles. *Am J Physiol,* **264,** H653-H659.

37. Fanger CM, Ghanshani S, Logsdon NJ, Rauer H, Kalman K, Zhou J, Beckingham K, Chandy KG, Cahalan MD, and Aiyar J (1999) Calmodulin mediates calcium-dependent activation of the intermediate conductance KCa channel, IKCa1. *J Biol Chem,* **274,** 5746-5754.

38. Gao X, Wu L, and O'Neil RG (2003) Temperature-modulated diversity of TRPV4 channel gating: activation by physical stresses and phorbol ester derivatives through protein kinase C-dependent and -independent pathways. *J Biol Chem,* **278,** 27129-27137.

39. Goel M, Sinkins W, Keightley A, Kinter M, and Schilling WP (2005) Proteomic analysis of T. *Pflugers Arch,* **451,** 87-98.

40. Goel M, Sinkins WG, and Schilling WP (2002) Selective association of TRPC channel

subunits in rat brain synaptosomes. *J Biol Chem,* **277,** 48303-48310.

41. Greffrath W, Binzen U, Schwarz ST, Saaler-Reinhardt S, and Treede RD (2003) Co-expression of heat sensitive vanilloid receptor subtypes in rat dorsal root ganglion neurons. *Neuroreport,* **14,** 2251-2255.

42. Hanaoka K, Qian F, Boletta A, Bhunia AK, Piontek K, Tsiokas L, Sukhatme VP, Guggino WB, and Germino GG (2000) Co-assembly of polycystin-1 and -2 produces unique cation-permeable currents. *Nature,* **408,** 990-994.

43. Hartmannsgruber V, Heyken WT, Kacik M, Kaistha A, Grgic I, Harteneck C, Liedtke W, Hoyer J, and Kohler R (2007) Arterial response to shear stress critically depends on endothelial TRPV4 expression. *PLoS One,* **2,** e827.

44. Hellwig N, Albrecht N, Harteneck C, Schultz G, and Schaefer M (2005) Homo- and heteromeric assembly of TRPV channel subunits. *J Cell Sci,* **118,** 917-928.

45. Hoenderop JG, Voets T, Hoefs S, Weidema F, Prenen J, Nilius B, and Bindels RJ (2003) Homo- and heterotetrameric architecture of the epithelial Ca2+ channels TRPV5 and TRPV6. *EMBO J,* **22,** 776-785.

46. Hofmann T, Schaefer M, Schultz G, and Gudermann T (2002) Subunit composition of mammalian transient receptor potential channels in living cells. *Proc Natl Acad Sci U S A,* **99,** 7461-7466.

47. Huang GN, Zeng W, Kim JY, Yuan JP, Han L, Muallem S, and Worley PF (2006) STIM1 carboxyl-terminus activates native SOC, I(crac) and TRPC1 channels. *Nat Cell Biol,* **8,** 1003-1010.

48. Hughes J, Ward CJ, Peral B, Aspinwall R, Clark K, San Millan JL, Gamble V, and Harris PC (1995) The polycystic kidney disease 1 (PKD1) gene encodes a novel protein with multiple cell recognition domains. *Nat Genet,* **10,** 151-160.

49. Jiang Y, Lee A, Chen J, Cadene M, Chait BT, and MacKinnon R (2002) Crystal structure and mechanism of a calcium-gated potassium channel. *Nature,* **417,** 515-522.

50. Ju M, Stevens L, Leadbitter E, and Wray D (2003) The Roles of N- and C-terminal determinants in the activation of the Kv2.1 potassium channel. *J Biol Chem,* **278,** 12769-12778.

51. Kahr H, Schindl R, Fritsch R, Heinze B, Hofbauer M, Hack ME, Mortelmaier MA, Groschner K, Peng JB, Takanaga H, Hediger MA, and Romanin C (2004) CaT1 knock-down strategies fail to affect CRAC channels in mucosal-type mast cells. *J Physiol,* **557,** 121-132.

52. Kanai AJ, Strauss HC, Truskey GA, Crews AL, Grunfeld S, and Malinski T (1995) Shear stress induces ATP-independent transient nitric oxide release from vascular endothelial cells,

measured directly with a porphyrinic microsensor. *Circ Res,* **77,** 284-293.

53. Kim EY, varez-Baron CP, and Dryer SE (2009) Canonical transient receptor potential channel (TRPC)3 and TRPC6 associate with large-conductance Ca2+-activated K+ (BKCa) channels: role in BKCa trafficking to the surface of cultured podocytes. *Mol Pharmacol,* **75,** 466-477.

54. Kim JY, Zeng W, Kiselyov K, Yuan JP, Dehoff MH, Mikoshiba K, Worley PF, and Muallem S (2006) Homer 1 mediates store- and inositol 1,4,5-trisphosphate receptor-dependent translocation and retrieval of TRPC3 to the plasma membrane. *J Biol Chem,* **281,** 32540-32549.

55. Kiselyov K, Shin DM, Kim JY, Yuan JP, and Muallem S (2007) TRPC channels: interacting proteins. *Handb Exp Pharmacol,* 559-574.

56. Kobori T, Smith GD, Sandford R, and Edwardson JM (2009) The transient receptor potential channels TRPP2 and TRPC1 form a heterotetramer with a 2:2 stoichiometry and an alternating subunit arrangement. *J Biol Chem,* **284,** 35507-35513.

57. Kohler R, Heyken WT, Heinau P, Schubert R, Si H, Kacik M, Busch C, Grgic I, Maier T, and Hoyer J (2006) Evidence for a functional role of endothelial transient receptor potential V4 in shear stress-induced vasodilatation. *Arterioscler Thromb Vasc Biol,* **26,** 1495-1502.

58. Kottgen M, Buchholz B, Garcia-Gonzalez MA, Kotsis F, Fu X, Doerken M, Boehlke C, Steffl D, Tauber R, Wegierski T, Nitschke R, Suzuki M, Kramer-Zucker A, Germino GG, Watnick T, Prenen J, Nilius B, Kuehn EW, and Walz G (2008) TRPP2 and TRPV4 form a polymodal sensory channel complex. *J Cell Biol,* **182,** 437-447.

59. Kwan HY, Leung PC, Huang Y, and Yao X (2003) Depletion of intracellular Ca2+ stores sensitizes the flow-induced Ca2+ influx in rat endothelial cells. *Circ Res,* **92,** 286-292.

60. Kwan HY, Shen B, Ma X, Kwok YC, Huang Y, Man YB, Yu S, and Yao X (2009) TRPC1 associates with BK(Ca) channel to form a signal complex in vascular smooth muscle cells. *Circ Res,* **104,** 670-678.

61. Lambers TT, Weidema AF, Nilius B, Hoenderop JG, and Bindels RJ (2004) Regulation of the mouse epithelial Ca2(+) channel TRPV6 by the Ca(2+)-sensor calmodulin. *J Biol Chem,* **279,** 28855-28861.

62. Lee KP, Yuan JP, Hong JH, So I, Worley PF, and Muallem S (2009) An endoplasmic reticulum/plasma membrane junction: STIM1/Orai1/TRPCs. *FEBS Lett.*

63. Lefkimmiatis K, Srikanthan M, Maiellaro I, Moyer MP, Curci S, and Hofer AM (2009) Store-operated cyclic AMP signalling mediated by STIM1. *Nat Cell Biol,* **11,** 433-442.

64. Leiser M, Rubin CS, and Erlichman J (1986) Differential binding of the regulatory subunits (RII) of cAMP-dependent protein kinase II from bovine brain and muscle to RII-binding

proteins. *J Biol Chem,* **261,** 1904-1908.

65. Lepage PK and Boulay G (2007) Molecular determinants of TRP channel assembly. *Biochem Soc Trans,* **35,** 81-83.

66. Lepage PK, Lussier MP, Barajas-Martinez H, Bousquet SM, Blanchard AP, Francoeur N, Dumaine R, and Boulay G (2006) Identification of two domains involved in the assembly of transient receptor potential canonical channels. *J Biol Chem,* **281,** 30356-30364.

67. Levitan IB (1999) It is calmodulin after all! Mediator of the calcium modulation of multiple ion channels. *Neuron,* **22,** 645-648.

68. Liedtke W, Choe Y, Marti-Renom MA, Bell AM, Denis CS, Sali A, Hudspeth AJ, Friedman JM, and Heller S (2000) Vanilloid receptor-related osmotically activated channel (VR-OAC), a candidate vertebrate osmoreceptor. *Cell,* **103,** 525-535.

69. Liu C, Ngai CY, Huang Y, Ko WH, Wu M, He GW, Garland CJ, Dora KA, and Yao X (2006) Depletion of intracellular Ca2+ stores enhances flow-induced vascular dilatation in rat small mesenteric artery. *Br J Pharmacol,* **147,** 506-515.

70. Liu X, Bandyopadhyay BC, Singh BB, Groschner K, and Ambudkar IS (2005) Molecular analysis of a store-operated and 2-acetyl-sn-glycerol-sensitive non-selective cation channel. Heteromeric assembly of TRPC1-TRPC3. *J Biol Chem,* **280,** 21600-21606.

71. Liu X, Singh BB, and Ambudkar IS (2003) TRPC1 is required for functional store-operated Ca2+ channels. Role of acidic amino acid residues in the S5-S6 region. *J Biol Chem,* **278,** 11337-11343.

72. Long SB, Campbell EB, and Mackinnon R (2005) Crystal structure of a mammalian voltage-dependent Shaker family K+ channel. *Science,* **309,** 897-903.

73. Lu M, Branstrom R, Berglund E, Hoog A, Bjorklund P, Westin G, Larsson C, Farnebo LO, and Forsberg L (2010) Expression and association of TRPC subtypes with Orai1 and STIM1 in human parathyroid. *J Mol Endocrinol.*

74. Lussier MP, Cayouette S, Lepage PK, Bernier CL, Francoeur N, St-Hilaire M, Pinard M, and Boulay G (2005) MxA, a member of the dynamin superfamily, interacts with the ankyrin-like repeat domain of TRPC. *J Biol Chem,* **280,** 19393-19400.

75. Ma X, Qiu S, Luo J, Ma Y, Ngai CY, Shen B, Wong CO, Huang Y, and Yao X (2010) Functional Role of TRPV4-TRPC1 Complex in Flow-Induced Ca2+ Influx. *Arterioscler Thromb Vasc Biol.*

76. Maroto R, Raso A, Wood TG, Kurosky A, Martinac B, and Hamill OP (2005) TRPC1 forms the stretch-activated cation channel in vertebrate cells. *Nat Cell Biol,* **7,** 179-185.

77. Maruyama Y, Nakanishi Y, Walsh EJ, Wilson DP, Welsh DG, and Cole WC (2006)

Heteromultimeric TRPC6-TRPC7 channels contribute to arginine vasopressin-induced cation current of A7r5 vascular smooth muscle cells. *Circ Res,* **98,** 1520-1527.

78. McAvoy T, Allen PB, Obaishi H, Nakanishi H, Takai Y, Greengard P, Nairn AC, and Hemmings HC, Jr. (1999) Regulation of neurabin I interaction with protein phosphatase 1 by phosphorylation. *Biochemistry,* **38,** 12943-12949.

79. Mery L, Strauss B, Dufour JF, Krause KH, and Hoth M (2002) The PDZ-interacting domain of TRPC4 controls its localization and surface expression in HEK293 cells. *J Cell Sci,* **115,** 3497-3508.

80. Miyawaki A, Llopis J, Heim R, McCaffery JM, Adams JA, Ikura M, and Tsien RY (1997) Fluorescent indicators for Ca2+ based on green fluorescent proteins and calmodulin. *Nature,* **388,** 882-887.

81. Montell C (2005) The TRP superfamily of cation channels. *Sci STKE,* **2005,** re3.

82. Moran MM, Xu H, and Clapham DE (2004) TRP ion channels in the nervous system. *Curr Opin Neurobiol,* **14,** 362-369.

83. Morenilla-Palao C, Planells-Cases R, Garcia-Sanz N, and Ferrer-Montiel A (2004) Regulated exocytosis contributes to protein kinase C potentiation of vanilloid receptor activity. *J Biol Chem,* **279,** 25665-25672.

84. Nakanishi H, Obaishi H, Satoh A, Wada M, Mandai K, Satoh K, Nishioka H, Matsuura Y, Mizoguchi A, and Takai Y (1997) Neurabin: a novel neural tissue-specific actin filament-binding protein involved in neurite formation. *J Cell Biol,* **139,** 951-961.

85. Nauli SM, Alenghat FJ, Luo Y, Williams E, Vassilev P, Li X, Elia AE, Lu W, Brown EM, Quinn SJ, Ingber DE, and Zhou J (2003) Polycystins 1 and 2 mediate mechanosensation in the primary cilium of kidney cells. *Nat Genet,* **33,** 129-137.

86. Nauli SM, Kawanabe Y, Kaminski JJ, Pearce WJ, Ingber DE, and Zhou J (2008) Endothelial cilia are fluid shear sensors that regulate calcium signaling and nitric oxide production through polycystin-1. *Circulation,* **117,** 1161-1171.

87. Niemeyer BA, Bergs C, Wissenbach U, Flockerzi V, and Trost C (2001) Competitive regulation of CaT-like-mediated Ca2+ entry by protein kinase C and calmodulin. *Proc Natl Acad Sci U S A,* **98,** 3600-3605.

88. Nilius B, Prenen J, Wissenbach U, Bodding M, and Droogmans G (2001) Differential activation of the volume-sensitive cation channel TRP12 (OTRPC4) and volume-regulated anion currents in HEK-293 cells. *Pflugers Arch,* **443,** 227-233.

89. Nilius B, Vriens J, Prenen J, Droogmans G, and Voets T (2004) TRPV4 calcium entry channel: a paradigm for gating diversity. *Am J Physiol Cell Physiol,* **286,** C195-C205.

90. O'Neil RG and Heller S (2005) The mechanosensitive nature of TRPV channels. *Pflugers Arch,* **451,** 193-203.

91. Obukhov AG and Nowycky MC (2004) TRPC5 activation kinetics are modulated by the scaffolding protein ezrin/radixin/moesin-binding phosphoprotein-50 (EBP50). *J Cell Physiol,* **201,** 227-235.

92. Olson PA, Tkatch T, Hernandez-Lopez S, Ulrich S, Ilijic E, Mugnaini E, Zhang H, Bezprozvanny I, and Surmeier DJ (2005) G-protein-coupled receptor modulation of striatal CaV1.3 L-type Ca2+ channels is dependent on a Shank-binding domain. *J Neurosci,* **25,** 1050-1062.

93. Palmada M, Poppendieck S, Embark HM, van de Graaf SF, Boehmer C, Bindels RJ, and Lang F (2005) Requirement of PDZ domains for the stimulation of the epithelial Ca2+ channel TRPV5 by the NHE regulating factor NHERF2 and the serum and glucocorticoid inducible kinase SGK1. *Cell Physiol Biochem,* **15,** 175-182.

94. Pan Z, Yang H, Mergler S, Liu H, Tachado SD, Zhang F, Kao WW, Koziel H, Pleyer U, and Reinach PS (2008) Dependence of regulatory volume decrease on transient receptor potential vanilloid 4 (TRPV4) expression in human corneal epithelial cells. *Cell Calcium,* **44,** 374-385.

95. Pani B, Ong HL, Brazer SC, Liu X, Rauser K, Singh BB, and Ambudkar IS (2009) Activation of TRPC1 by STIM1 in ER-PM microdomains involves release of the channel from its scaffold caveolin-1. *Proc Natl Acad Sci U S A,* **106,** 20087-20092.

96. Pani B, Ong HL, Liu X, Rauser K, Ambudkar IS, and Singh BB (2008) Lipid rafts determine clustering of STIM1 in endoplasmic reticulum-plasma membrane junctions and regulation of store-operated Ca2+ entry (SOCE). *J Biol Chem,* **283,** 17333-17340.

97. Parekh AB and Putney JW, Jr. (2005) Store-operated calcium channels. *Physiol Rev,* **85,** 757-810.

98. Patterson GH, Piston DW, and Barisas BG (2000) Forster distances between green fluorescent protein pairs. *Anal Biochem,* **284,** 438-440.

99. Patterson RL, van Rossum DB, Ford DL, Hurt KJ, Bae SS, Suh PG, Kurosaki T, Snyder SH, and Gill DL (2002) Phospholipase C-gamma is required for agonist-induced Ca2+ entry. *Cell,* **111,** 529-541.

100. Pedersen SF, Owsianik G, and Nilius B (2005) TRP channels: an overview. *Cell Calcium,* **38,** 233-252.

101. Peier AM, Reeve AJ, Andersson DA, Moqrich A, Earley TJ, Hergarden AC, Story GM, Colley S, Hogenesch JB, McIntyre P, Bevan S, and Patapoutian A (2002) A heat-sensitive TRP channel expressed in keratinocytes. *Science,* **296,** 2046-2049.

102. Plant TD and Strotmann R (2007a) TRPV4. *Handb Exp Pharmacol,* 189-205.

103. Plant TD and Strotmann R (2007b) TRPV4. *Handb Exp Pharmacol,* 189-205.

104. Putney JW (2009) Capacitative calcium entry: from concept to molecules. *Immunol Rev,* **231,** 10-22.

105. Qiu S, Hua YL, Yang F, Chen YZ, and Luo JH (2005) Subunit assembly of N-methyl-d-aspartate receptors analyzed by fluorescence resonance energy transfer. *J Biol Chem,* **280,** 24923-24930.

106. Sala C, Roussignol G, Meldolesi J, and Fagni L (2005) Key role of the postsynaptic density scaffold proteins Shank and Homer in the functional architecture of Ca2+ homeostasis at dendritic spines in hippocampal neurons. *J Neurosci,* **25,** 4587-4592.

107. Satoh A, Nakanishi H, Obaishi H, Wada M, Takahashi K, Satoh K, Hirao K, Nishioka H, Hata Y, Mizoguchi A, and Takai Y (1998) Neurabin-II/spinophilin. An actin filament-binding protein with one pdz domain localized at cadherin-based cell-cell adhesion sites. *J Biol Chem,* **273,** 3470-3475.

108. Schreiber M and Salkoff L (1997) A novel calcium-sensing domain in the BK channel. *Biophys J,* **73,** 1355-1363.

109. Schulteis CT, Nagaya N, and Papazian DM (1996) Intersubunit interaction between amino- and carboxyl-terminal cysteine residues in tetrameric shaker K+ channels. *Biochemistry,* **35,** 12133-12140.

110. Schumacher MA, Rivard AF, Bachinger HP, and Adelman JP (2001) Structure of the gating domain of a Ca2+-activated K+ channel complexed with Ca2+/calmodulin. *Nature,* **410,** 1120-1124.

111. Shi J, Krishnamoorthy G, Yang Y, Hu L, Chaturvedi N, Harilal D, Qin J, and Cui J (2002) Mechanism of magnesium activation of calcium-activated potassium channels. *Nature,* **418,** 876-880.

112. Singh BB, Liu X, Tang J, Zhu MX, and Ambudkar IS (2002) Calmodulin regulates Ca(2+)-dependent feedback inhibition of store-operated Ca(2+) influx by interaction with a site in the C terminus of TrpC1. *Mol Cell,* **9,** 739-750.

113. Singh BB, Lockwich TP, Bandyopadhyay BC, Liu X, Bollimuntha S, Brazer SC, Combs C, Das S, Leenders AG, Sheng ZH, Knepper MA, Ambudkar SV, and Ambudkar IS (2004) VAMP2-dependent exocytosis regulates plasma membrane insertion of TRPC3 channels and contributes to agonist-stimulated Ca2+ influx. *Mol Cell,* **15,** 635-646.

114. Spassova MA, Soboloff J, He LP, Xu W, Dziadek MA, and Gill DL (2006) STIM1 has a plasma membrane role in the activation of store-operated Ca(2+) channels. *Proc Natl Acad Sci U S A,* **103,** 4040-4045.

115. Stamboulian S, Moutin MJ, Treves S, Pochon N, Grunwald D, Zorzato F, De WM, Ronjat M, and Arnoult C (2005) Junctate, an inositol 1,4,5-triphosphate receptor associated protein, is present in rodent sperm and binds TRPC2 and TRPC5 but not TRPC1 channels. *Dev Biol,* **286,** 326-337.

116. Steyer JA and Almers W (2001) A real-time view of life within 100 nm of the plasma membrane. *Nat Rev Mol Cell Biol,* **2,** 268-275.

117. Stiber JA, Tabatabaei N, Hawkins AF, Hawke T, Worley PF, Williams RS, and Rosenberg P (2005) Homer modulates NFAT-dependent signaling during muscle differentiation. *Dev Biol,* **287,** 213-224.

118. Strotmann R, Harteneck C, Nunnenmacher K, Schultz G, and Plant TD (2000) OTRPC4, a nonselective cation channel that confers sensitivity to extracellular osmolarity. *Nat Cell Biol,* **2,** 695-702.

119. Strubing C, Krapivinsky G, Krapivinsky L, and Clapham DE (2001) TRPC1 and TRPC5 form a novel cation channel in mammalian brain. *Neuron,* **29,** 645-655.

120. Sutton KA, Jungnickel MK, Wang Y, Cullen K, Lambert S, and Florman HM (2004) Enkurin is a novel calmodulin and TRPC channel binding protein in sperm. *Dev Biol,* **274,** 426-435.

121. Suzuki M, Mizuno A, Kodaira K, and Imai M (2003) Impaired pressure sensation in mice lacking TRPV4. *J Biol Chem,* **278,** 22664-22668.

122. Tang J, Lin Y, Zhang Z, Tikunova S, Birnbaumer L, and Zhu MX (2001) Identification of common binding sites for calmodulin and inositol 1,4,5-trisphosphate receptors on the carboxyl termini of trp channels. *J Biol Chem,* **276,** 21303-21310.

123. Tang Y, Tang J, Chen Z, Trost C, Flockerzi V, Li M, Ramesh V, and Zhu MX (2000) Association of mammalian trp4 and phospholipase C isozymes with a PDZ domain-containing protein, NHERF. *J Biol Chem,* **275,** 37559-37564.

124. Treves S, Feriotto G, Moccagatta L, Gambari R, and Zorzato F (2000) Molecular cloning, expression, functional characterization, chromosomal localization, and gene structure of junctate, a novel integral calcium binding protein of sarco(endo)plasmic reticulum membrane. *J Biol Chem,* **275,** 39555-39568.

125. Treves S, Franzini-Armstrong C, Moccagatta L, Arnoult C, Grasso C, Schrum A, Ducreux S, Zhu MX, Mikoshiba K, Girard T, Smida-Rezgui S, Ronjat M, and Zorzato F (2004) Junctate is a key element in calcium entry induced by activation of InsP3 receptors and/or calcium store depletion. *J Cell Biol,* **166,** 537-548.

126. Tsiokas L, Arnould T, Zhu C, Kim E, Walz G, and Sukhatme VP (1999) Specific association of the gene product of PKD2 with the TRPC1 channel. *Proc Natl Acad Sci U S A,* **96,** 3934-3939.

127. Tsunoda S, Sierralta J, Sun Y, Bodner R, Suzuki E, Becker A, Socolich M, and Zuker CS (1997) A multivalent PDZ-domain protein assembles signalling complexes in a G-protein-coupled cascade. *Nature,* **388,** 243-249.

128. Tu JC, Xiao B, Yuan JP, Lanahan AA, Leoffert K, Li M, Linden DJ, and Worley PF (1998) Homer binds a novel proline-rich motif and links group 1 metabotropic glutamate receptors with IP3 receptors. *Neuron,* **21,** 717-726.

129. Van Buren JJ, Bhat S, Rotello R, Pauza ME, and Premkumar LS (2005) Sensitization and translocation of TRPV1 by insulin and IGF-I. *Mol Pain,* **1,** 17.

130. van Rossum DB, Patterson RL, Sharma S, Barrow RK, Kornberg M, Gill DL, and Snyder SH (2005) Phospholipase Cgamma1 controls surface expression of TRPC3 through an intermolecular PH domain. *Nature,* **434,** 99-104.

131. van AM, Hoenderop JG, and Bindels RJ (2005) The epithelial calcium channels TRPV5 and TRPV6: regulation and implications for disease. *Naunyn Schmiedebergs Arch Pharmacol,* **371,** 295-306.

132. Voets T, Prenen J, Fleig A, Vennekens R, Watanabe H, Hoenderop JG, Bindels RJ, Droogmans G, Penner R, and Nilius B (2001) CaT1 and the calcium release-activated calcium channel manifest distinct pore properties. *J Biol Chem,* **276,** 47767-47770.

133. Voets T, Prenen J, Vriens J, Watanabe H, Janssens A, Wissenbach U, Bodding M, Droogmans G, and Nilius B (2002a) Molecular determinants of permeation through the cation channel TRPV4. *J Biol Chem,* **277,** 33704-33710.

134. Voets T, Prenen J, Vriens J, Watanabe H, Janssens A, Wissenbach U, Bodding M, Droogmans G, and Nilius B (2002b) Molecular determinants of permeation through the cation channel TRPV4. *J Biol Chem,* **277,** 33704-33710.

135. Wang X, Zeng W, Soyombo AA, Tang W, Ross EM, Barnes AP, Milgram SL, Penninger JM, Allen PB, Greengard P, and Muallem S (2005) Spinophilin regulates Ca2+ signalling by binding the N-terminal domain of RGS2 and the third intracellular loop of G-protein-coupled receptors. *Nat Cell Biol,* **7,** 405-411.

136. Watanabe H, Davis JB, Smart D, Jerman JC, Smith GD, Hayes P, Vriens J, Cairns W, Wissenbach U, Prenen J, Flockerzi V, Droogmans G, Benham CD, and Nilius B (2002) Activation of TRPV4 channels (hVRL-2/mTRP12) by phorbol derivatives. *J Biol Chem,* **277,** 13569-13577.

137. Watanabe H, Vriens J, Prenen J, Droogmans G, Voets T, and Nilius B (2003) Anandamide and arachidonic acid use epoxyeicosatrienoic acids to activate TRPV4 channels. *Nature,* **424,** 434-438.

138. Wissenbach U, Bodding M, Freichel M, and Flockerzi V (2000) Trp12, a novel Trp related protein from kidney. *FEBS Lett,* **485,** 127-134.

139. Wu L, Gao X, Brown RC, Heller S, and O'Neil RG (2007) Dual role of the TRPV4 channel as a sensor of flow and osmolality in renal epithelial cells. *Am J Physiol Renal Physiol,* **293,** F1699-F1713.

140. Xia XM, Fakler B, Rivard A, Wayman G, Johnson-Pais T, Keen JE, Ishii T, Hirschberg B, Bond CT, Lutsenko S, Maylie J, and Adelman JP (1998) Mechanism of calcium gating in small-conductance calcium-activated potassium channels. *Nature,* **395,** 503-507.

141. Xia XM, Zeng X, and Lingle CJ (2002) Multiple regulatory sites in large-conductance calcium-activated potassium channels. *Nature,* **418,** 880-884.

142. Xiao B, Tu JC, Petralia RS, Yuan JP, Doan A, Breder CD, Ruggiero A, Lanahan AA, Wenthold RJ, and Worley PF (1998) Homer regulates the association of group 1 metabotropic glutamate receptors with multivalent complexes of homer-related, synaptic proteins. *Neuron,* **21,** 707-716.

143. Xiao B, Tu JC, and Worley PF (2000) Homer: a link between neural activity and glutamate receptor function. *Curr Opin Neurobiol,* **10,** 370-374.

144. Xu SZ and Beech DJ (2001) TrpC1 is a membrane-spanning subunit of store-operated Ca(2+) channels in native vascular smooth muscle cells. *Circ Res,* **88,** 84-87.

145. Yamaguchi H, Matsushita M, Nairn AC, and Kuriyan J (2001) Crystal structure of the atypical protein kinase domain of a TRP channel with phosphotransferase activity. *Mol Cell,* **7,** 1047-1057.

146. Yamamoto K, Korenaga R, Kamiya A, and Ando J (2000) Fluid shear stress activates Ca(2+) influx into human endothelial cells via P2X4 purinoceptors. *Circ Res,* **87,** 385-391.

147. Yamamoto K, Sakagami Y, Sugiura S, Inokuchi K, Shimohama S, and Kato N (2005) Homer 1a enhances spike-induced calcium influx via L-type calcium channels in neocortex pyramidal cells. *Eur J Neurosci,* **22,** 1338-1348.

148. Yamamoto K, Sokabe T, Matsumoto T, Yoshimura K, Shibata M, Ohura N, Fukuda T, Sato T, Sekine K, Kato S, Isshiki M, Fujita T, Kobayashi M, Kawamura K, Masuda H, Kamiya A, and Ando J (2006) Impaired flow-dependent control of vascular tone and remodeling in P2X4-deficient mice. *Nat Med,* **12,** 133-137.

149. Yang XR, Lin MJ, McIntosh LS, and Sham JS (2006) Functional expression of transient receptor potential melastatin- and vanilloid-related channels in pulmonary arterial and aortic smooth muscle. *Am J Physiol Lung Cell Mol Physiol,* **290,** L1267-L1276.

150. Yao X, Kwan HY, Chan FL, Chan NW, and Huang Y (2000) A protein kinase G-sensitive channel mediates flow-induced Ca(2+) entry into vascular endothelial cells. *FASEB J,* **14,** 932-938.

151. Yao Y, Ferrer-Montiel AV, Montal M, and Tsien RY (1999) Activation of store-operated

Ca2+ current in Xenopus oocytes requires SNAP-25 but not a diffusible messenger. *Cell,* **98,** 475-485.

152. Yuan JP, Kiselyov K, Shin DM, Chen J, Shcheynikov N, Kang SH, Dehoff MH, Schwarz MK, Seeburg PH, Muallem S, and Worley PF (2003) Homer binds TRPC family channels and is required for gating of TRPC1 by IP3 receptors. *Cell,* **114,** 777-789.

153. Yuan JP, Zeng W, Huang GN, Worley PF, and Muallem S (2007) STIM1 heteromultimerizes TRPC channels to determine their function as store-operated channels. *Nat Cell Biol,* **9,** 636-645.

154. Yue L, Peng JB, Hediger MA, and Clapham DE (2001) CaT1 manifests the pore properties of the calcium-release-activated calcium channel. *Nature,* **410,** 705-709.

155. Zhang P, Luo Y, Chasan B, Gonzalez-Perrett S, Montalbetti N, Timpanaro GA, Cantero MR, Ramos AJ, Goldmann WH, Zhou J, and Cantiello HF (2009) The multimeric structure of polycystin-2 (TRPP2): structural-functional correlates of homo- and hetero-multimers with TRPC1. *Hum Mol Genet,* **18,** 1238-1251.

156. Zhang SL, Yu Y, Roos J, Kozak JA, Deerinck TJ, Ellisman MH, Stauderman KA, and Cahalan MD (2005) STIM1 is a Ca2+ sensor that activates CRAC channels and migrates from the Ca2+ store to the plasma membrane. *Nature,* **437,** 902-905.

157. Zhang X, Li L, and McNaughton PA (2008) Proinflammatory mediators modulate the heat-activated ion channel TRPV1 via the scaffolding protein AKAP79/150. *Neuron,* **59,** 450-461.

158. Zhang Z, Tang J, Tikunova S, Johnson JD, Chen Z, Qin N, Dietrich A, Stefani E, Birnbaumer L, and Zhu MX (2001) Activation of Trp3 by inositol 1,4,5-trisphosphate receptors through displacement of inhibitory calmodulin from a common binding domain. *Proc Natl Acad Sci U S A,* **98,** 3168-3173.

159. Zheng J, Trudeau MC, and Zagotta WN (2002) Rod cyclic nucleotide-gated channels have a stoichiometry of three CNGA1 subunits and one CNGB1 subunit. *Neuron,* **36,** 891-896.

160. Zhu MX (2005) Multiple roles of calmodulin and other Ca(2+)-binding proteins in the functional regulation of TRP channels. *Pflugers Arch,* **451,** 105-115.